The role of fatty acids on dicarbonyl-induced protein glycation, receptor expression and inflammatory biomarkers

Brock Peake
Bachelor of Medical and Pharmaceutical Biotechnology

A Thesis submitted for the degree of Masters by Research

Clinical and Health Sciences

University of South Australia
Adelaide

On this day

24th November 2022



Table of Contents

List of Figures ..... **v**
List of Tables ..... **vii**
Abbreviations ..... **viii**
Acknowledgements ..... **x**
Declaration ..... **xii**
Abstract ..... **xiii**
Publications arising ..... **xv**
Introductory contextual statement ..... **xvi**
Author Statement ..... **xvii**
Chapter 1 - Literature Review **1**
1.1 – Introduction **2**
1.2 – Chemistry of AGE formation **4**
1.2.1 – Maillard reaction and history 5
1.2.2 – Glucose Autoxidation 7
1.2.3 – Lipid peroxidation and advanced lipoxidation endproducts (ALEs) 8
1.2.4 – Glycolysis 9
1.2.5 – Polyol pathway 10
1.3 – Fluorescent and non-fluorescent AGEs **11**
1.3.1 – Pentosidine 13
1.3.2 – Nε-Carboxymethyllysine (CML) 13
1.3.3 – Carboxyethyllysine (CEL) 14
1.3.4 – Methylglyoxal derived hydroimidazolone (MG-H1) 14
1.3.5 – Quantification of AGEs in biological samples 16
1.4 – α-Dicarbonyl compounds **18**
1.4.1 – Dicarbonyl Stress 20
1.5 – The receptor for advanced glycation end products (RAGE) **22**
1.6 – AGEs and disease implications **27**
1.6.1 – Diabetes Mellitus and its association with AGES 27
1.6.2 – Cardiovascular disease and its association with AGEs 30
1.6.3 – Relationship between AGEs and neurodegenerative diseases 31
1.6.4 – AGEs and their association with cancer 31

1.6.5 – AGEs and Cytotoxicity 32
1.6.6 – Reactive Oxygen Species (ROS) and oxidative stress (OS) 33
1.6.8 – Cytokines and AGEs 34
1.7 – Fatty Acids 37
1.7 – Nomenclature 37
1.7.2 – Chain length and saturation 37
1.7.3 – Sources 38
1.7.4 – Biological effects and inflammation 38
1.7.5 – Fatty acids and AGEs 40
1.8 – Study aims and objectives 44
1.8.1 – Hypothesis 44
1.8.2 – Aims of this study 44
1.8.2.1 – Objectives: 44
Chapter 2 - The Role of saturated and unsaturated fatty acids on dicarbonyl derived advanced glycation end products in vitro 46
2.1 – Introduction 47
2.2 – Materials and Methods. 50
2.2.1 – Materials 50
2.2.2 – Time and concentration-dependent AGE formation 50
2.2.3 – Saturated and unsaturated fatty acid treatment 51
2.2.4 – Determination of protein-bound fluorescent AGEs 51
2.2.5 – Preparation of samples for LC-MS/MS 52
2.2.6 – Solid Phase Extraction (SPE) 53
2.2.7 – Liquid chromatography-mass spectrometry 53
2.2.8 - Statistical Analysis 55
2.3 – Results 55
2.3.1 – Kinetics of protein-bound fluorescent AGE formation 55
2.3.2 – Kinetics of CML, CEL and MG-H1 levels. 57
2.3.3 – The effect of fatty acids on AGE formation. 59
2.4 – Discussion 63
2.5 – Conclusion 68
Chapter 3 – The role of fatty acids on dicarbonyl-albumin induced expression of the receptor for advanced glycation end products (RAGE) and inflammatory markers in human endothelial cells 69
3.1– Introduction 70
3.2 – Materials 72

3.2.1 – Chemicals 72
3.2.2 – Fatty Acids 72
3.2.3 – Cell culture 72
3.2.4 – Western Blotting 73
3.2.5 – PCR 73
3.2.6 – ELISA 73
3.3 - Methods 74
3.3.1 – Preparation of dicarbonyl derived AGEs for cell culture treatment 74
3.3.2 – Ultrafiltration extraction of protein bound AGEs for cell culture experiments 74
3.3.3 – Protein concentration determination of glycated models using the BCA method 75
3.3.4 – HUVEC culture maintenance 76
3.3.5 – MTT trials to assess the effect of dicarbonyl induced AGE treatment on HUVEC proliferation 76
3.2.6 – MTT assay to assess the effect of fatty acids on HUVEC proliferation 77
3.3.7 – Cell Treatments. 78
3.3.8 – Cell lysis and protein extraction for western blot analysis 79
3.3.9 – RNA extraction 79
3.3.10 – gDNA digestion and cDNA synthesis 81
3.3.11 – Sodium dodecyl sulfate (SDS) Polyacrylamide gel electrophoresis (PAGE) and western blotting. 83
3.3.12 – Quantitative real-time polymerase chain reaction (qPCR) 84
3.3.13 – Quantification of cytokine levels by enzyme linked immunosorbent assay (ELISA) 86
3.3.14 – Statistical analysis 87
3.4 - Results 88
3.4.1 – Quantification of AGEs in glycated proteins used for cell culture treatment 88
3.4.2 – 3-(4,5-Dimethylthiazol-2-yl)-2,5-diphenyltetrazolium bromide (MTT) assay 91
3.4.2.1 – HUVECs treated with the BSA-dicarbonyl model 91
3.4.2.2 – Effect of fatty acid treatment on HUVEC viability 94
3.4.3 – qPCR analysis for RAGE/NF-κB expression 96
3.4.3.1 – The effect of MGO-BSA and GO-BSA derived AGEs on RAGE and NF-κB mRNA expression. 96
3.4.3.2 – The effect of FA pretreatment on AGE induced RAGE and NF-κB mRNA expression in HUVECs 98
3.4.4 – Western Blotting for RAGE expression 100

3.4.4.1 – Time and concentration-dependent studies to establish RAGE expression in HUVECs 100
3.4.4.2 – The effect of FA pretreatment on AGE induced RAGE protein expression in HUVECs. 102
3.4.5 – Inflammatory cytokine production in HUVECs treated with dicarbonyl-BSA derived AGEs with or without fatty acid pre-treatment. 104
3.5 – Discussion 108
3.6 – Conclusion 116
Chapter 4 – General discussion and future directions 117
4.1 – Introduction 118
4.2 – The role of saturated and unsaturated fatty acids on dicarbonyl derived advanced glycation end products in vitro 118
4.2.1 – Develop and optimise a dicarbonyl-BSA model system 118
4.2.2 – The role of fatty acids on dicarbonyl induced AGE production 120
4.3 – The role of fatty acids on dicarbonyl-albumin induced expression of the receptor for advanced glycation end products and inflammatory markers in human endothelial cells 121
4.3.1 – Development and optimisation of an endothelial cell model 121
4.3.2 – The effect of fatty acids on RAGE expression and inflammatory cytokines. 122
4.4 – Conclusion 125
References 126
Chapter 5 – Appendix and supplementary information 151
5.1 – supplementary information for chapter 2 152
5.1.1 – Comparison of 20μM, 50μM and 100μM fatty acid models 152
5.1.2 – Concentration dependent quantitation of CML/CEL and MG-H1 production in a BSA-dicarbonyl model using LC-MS/MS. 153
5.2 – Supplementary information for chapter 3 157
5.2.1 – MTT Trials using TCA 157

List of Figures

Figure 1.1 - Formation of a Schiff base and Amadori rearrangement product (ARP). 3
Figure 1.2 - Overview of the pathways that lead to advanced glycation endproduct formation. 5
Figure 1.3 - The structure of commonly glycated amino acids lysine and arginine 6
Figure 1.4 - Formation of *N*ε-Carboxymethyllysine, -(CML) from glucose. 7
Figure 1.5 - Structure of common fluorescent and non-fluorescent AGEs. 12
Figure 1.6 - Formation of 5-hydro-5-methyl-imidazol-4-one (methylglyoxal hydroimidazolidine-1 (MG-H1)). 15
.... 22
Figure 1.7 - Backbone and ribbon diagram of the crystal structure of human RAGE extracellular domain (V-C1-C2 domains). 22
Figure 1.8 - The structure of the receptor for advanced glycation endproducts and its binding domains. 23
Figure 1.9 - An example of an AGE binding to the multi-ligand receptor for AGEs 26
(RAGE) and triggering an intracellular signal cascade 26
Figure 1.10 - Activation of nuclear factor (NF)- κB signalling pathway 35
Figure 1.11 - Chemical structure of common fatty acids investigated. 41
Figure 2.1 - Kinetics of time dependent protein bound fluorescent AGEs quantification 56
Figure 2.2 - Kinetics of concentration dependent protein bound fluorescent AGEs quantification 57
Figure 2.3 - Species specific AGE generation – time dependent study 58
Figure 2.4 - Species-specific AGEs generated in a concentration-dependent study 59
Figure 2.5 - The role of fatty acids on dicarbonyl induced protein-bound fluorescent AGE production. 60
Figure 2.6 - The role of dicarbonyls on CML, CEL and MG-H1 production 62
Figure 3.1 - Effect of ultra-filtrated dicarbonyl derived protein-bound AGEs on cell viability in a HUVEC model. 93
.... 95
Figure 3.2 - Effect of fatty acids on HUVEC viability. 95
Figure 3.3 - The effect of dicarbonyl derived AGEs on RAGE mRNA expression (A) and NF- κB (B) in HUVECs. 97

Figure 3.4 - The effect of fatty acid pre-treatment on AGE induced RAGE mRNA expression (A.) and NF- κB mRNA expression (B.) in HUVECs 99
Figure 3.5 - Time and concentration-dependent effect on RAGE expression in HUVECs treated with dicarbonyl-derived AGEs 101
Figure 3.6 - The effect of fatty acids on dicarbonyl derived AGEs on RAGE expression in HUVECs 103
Figure 3.7 - Production of extracellular IL-6 by HUVECs treated with dicarbonyl derived AGEs 106
Figure 3.8 - Production of extracellular IL-8 by HUVECs treated with dicarbonyl derived AGEs 107
Figure 3.9 - Production of extracellular MCP-1 in HUVECs treated with dicarbonyl derived AGEs 107
Figure 5.1 - The effect of different concentration of fatty acids on the production of protein-bound fluorescent AGEs. 153
Figure 5.2 - Concentration dependent quantitation of protein bound non-fluorescent AGE production 155
Figure 5.3 - TCA protein precipitation trials on cell culture model system 157
Figure 5.4 - TCA precipitation vs Media only testing for optimisation of protein extraction. 158

List of Tables

Table 1.1 - Examples and characteristics of major advanced glycation/lipoxidation end products. 16
Table 1.2 – Advantages and disadvantages of common methods for AGE detection and quantitation 17
Table 1.3 - Levels of endogenous AGEs in human plasma samples determined using different analytical methods. 28
Table 1.4 - Examples of common saturated fatty acids, structure and formula 42
Table 1.5 – Examples of common polyunsaturated fatty acids, structure, and formula. 43
Table 2.1 - Multiple reaction monitoring (MRM) conditions of LC-MS/MS analysis 54
Table 3.1 - DNAse reaction protocol and conditions 82
Table 3.2 - cDNA synthesis reaction table and conditions 82
Table 3.3 - Primer sequences used in qPCR and accession number 86
Table 3.4 - Quantitation of protein-bound fluorescent AGE production used in cell culture treatments. 90
Table 3.5 - Quantitation of species-specific protein-bound AGEs used in cell culture treatments 91
Table 5.1 – Limit of quantitation for liquid chromatography mass spectrometry analysis of AGEs 156
Table 5.2 – limit of detection for liquid chromatography mass spectrometry analysis of AGEs 156

Abbreviations

AA	Arachidonic acid
Ab	Antibody
AD	Alzheimer's Disease
AGE	Advanced glycation end product
AGER1	Advanced glycation end product receptor 1
ALA	Alpha linoleic acid
ALE	Advanced Lipoxidation end product
AP-1	Activating protein - 1
ARP	Amadori rearrangement product
AU	Arbitrary units
BSA	Bovine serum albumin
BCA	Bicinchoninic acid
cDNA	Complimentary DNA
CEL	Carboxyethyllysine
CML	Carboxymethyllysine
CVDs	Cardiovascular diseases
DHA	Docosahexaenoic acid
DM	Diabetes Mellitus
DNL	*De novo* lipogenesis
DTT	Dithiothreitol
ELISA	Enzyme linked immunosorbent assay
EPA	Eicosapentaenoic acid
EtOH	Ethanol
FAs	Fatty acids
FBS	Fetal bovine serum
gDNA	Genomic DNA
GO	Glyoxal
GOLD	Glyoxal lysine dimer
HBSS	Hanks Balanced Salt solution
HNE	4-hydroxynonenal
HL-CML	D_2-CML (Heavy labelled CML)
HL-CEL	D_2-CEL (Heavy labelled CEL)
HL-Lys	D_4-lysine (Heavy labelled lysine)
HL-MG-H1	*D3*-MG-H1 (Heavy labelled MG-H1)
HPLC	High-performance liquid chromatography
HSA	Human serum albumin
HUVEC	Human umbilical vein endothelial cells
ICAM-1	Intercellular adhesion molecule-1
IL-1β	Interleukin 1-β
IL-6	Interleukin-6
IL-8	Interleukin-8
JNK	c-Jun N terminal kinase
LA	Linoleic acid
LC-MS/MS	Liquid chromatography-mass spectrometry/mass spectrometry
LDL	Low density lipoproteins
LOD	Limit of detection
LLOQ	Lower limit of quantitation

LYS	Lysine
MAPK	Mitogen-activating protein kinase
MCP-1	Monocyte chemoattractant protein-1
MDA	Malondialdehyde
MeOH	Methanol
MG-H1	Methylglyoxal derived hydroimidazolone isomer 1
MGO	Methylglyoxal
MOLD	Methylglyoxal lysine dimer
mRNA	Messenger RNA
NF-κB	Nuclear factor kappa B
OS	Oxidative Stress
PBS	Phosphate buffered saline
PD	Parkinson's Disease
PRR	Pattern recognition receptor
PMSF	Phenylmethylsulphonyl fluoride
PUFAs	Polyunsaturated fatty acids
qPCR	Quantitative real-time polymerase chain reaction
RAGE	Receptor for advanced glycation endproducts
ROS	Reactive oxygen species
RT	Room temperature
SDS	Sodium dodecyl sulphate
SDS-PAGE	Sodium dodecyl sulphate polyacrylamide gel electrophoresis
TCA	Trichloroacetic acid.
TFA	Trifluoracetic acid
TGF-β	Transforming growth factor-β
TNF-α	Tumour necrosis factor-α
VCAM-1	Vascular cell adhesion molecule-1
3-DG	3-deoxyglucosone

Acknowledgements

Firstly, in no particular order, I would like to acknowledge my supervisors who firstly provided me with an opportunity to undertake a project, and also all generously gave me their time and support throughout my candidature. Permal, thank you for being open to the idea of taking on a part-time student, to begin with and for allowing me to take on a project within your field. Thanks to you for your encouragement and assistance throughout my studies and for your continued encouragement even when I thought I would never get to the finish line.

Maurizio I really appreciate your guidance and most of all your patience with me, thank you for our many quick chats whether it be in your office or during Biochemistry practicals, and keeping me focused and on track in the times when you could see I really needed it. There were many times when I thought all was lost, but you always helped me see the positive and kept pushing me, I really appreciated that.

Cobus, thank you for joining as a supervisor along the way. I am so appreciative for you agreeing to take my project on even knowing how busy you were with your research/teaching commitments and other HDR students. Your contribution and many thoughtful discussions and ideas arising from seeing the project from a different angle have been a great part in my success.

I would like to acknowledge the financial support received from the Commonwealth Government Research Training Program (RTP) through an Australian Government Research Training Program Scholarship.

Many thanks to my lab mates Emma and Leigh, who shared both the highs and lows of experimental work. You have both always been there for a quick chat or a long chat, always offering advice and helping me to pick myself up and keep going, and always happy to share any advice. You both have helped me out more than you know. I couldn't have done it without you both.

To my Masters partner in crime Shaun, well it was you in the first place who inspired me to even think about enrolling in Masters. There have been many times throughout I have cursed you for this, but ultimately going through it with you has been an amazing experience, sharing all the ups and downs, keeping each other motivated and ultimately helping each other reach the end goal.

My thanks also to Maulik Ghetia for the assistance with LC-MS/MS method development. I could not have asked for a more patient and helpful LC-MS/MS mentor.

Last but certainly not least, I would like to thank my beautiful wife, Melissa. Thank you supporting me and helping me in achieving this goal. Many times, throughout this journey you were there to point me back in the right direction and encouraged me to push through. Thank you for the patience and encouragement that you gave to me that enabled me to achieve this goal.

Declaration

I declare that:

This thesis presents work carried out by myself and does not incorporate without acknowledgment any material previously submitted for a degree or diploma in any university.

To the best of my knowledge, it does not contain any materials previously published or written by another person except where due reference is made in the text and all substantive contributions by others to the work presented, including jointly authored publications, is clearly acknowledged.



Brock Peake

24th November 2022

Abstract

Glycation is a non-enzymatic reaction that occurs between the free amino group of proteins and reducing sugars and/or lipids, leading to the formation of advanced glycation end-products (AGEs). The reaction also produces reactive oxygen species that have detrimental effects on intracellular and extracellular proteins. Aminoguanidine is a known inhibitor of AGE formations, while some fatty acids have been shown to have beneficial *in vivo* activities by reducing inflammation and oxidative stress. However, the role of fatty acids on AGE formation has not been thoroughly reported.

This thesis investigated the role of a range of fatty acids in the formation of AGEs and their reactive intermediates using an *in vitro* BSA-dicarbonyl model. The model assessed a time-dependent (0-72 h) and dicarbonyl concentration (0-2 mM) dependent studies to identify the optimal formation of AGEs. A 72 h time point was found to be optimal for the reaction of BSA with either methylglyoxal (MGO) or glyoxal (GO) to generate AGE-BSA complexes. When arachidonic (20:4 n-6), eicosapentaenoic (20:5 n-3) or docosahexaenoic (22:6 n-3) acids were included in the reaction, a significant decrease in protein-bound fluorescent AGEs was seen compared to BSA alone. In contrast, saturated and 18 carbon polyunsaturated fatty acids showed no significant inhibitory activity.

Liquid chromatography-mass spectrometry (LC-MS/MS) analysis showed that saturated fatty acids significantly decreased the production of N^{ϵ}-carboxymethyllysine (CML) and N^{ϵ}-carboxyethyllysine (CEL) from GO and MGO models, respectively while increasing methylglyoxal derived hydroimidazolone (MG-H1). In contrast, arachidonic (20:4 n-6), eicosapentaenoic (20:5 n-3) and docosahexaenoic acid (22:6 n-3) did not significantly change either CEL or MG-H1 while significantly reducing CML levels compared to no treatment controls.

To investigate whether fatty acids could attenuate the up-regulation of the receptor for AGEs (RAGE), a dicarbonyl-BSA model was used to explore RAGE expression and related inflammatory biomarkers in a human endothelial cell line. Human umbilical vein endothelial cells (HUVECs) were exposed to dicarbonyl-BSA derived AGEs. Quantification of RAGE expression in HUVECs was optimised in time and

concentrations studies. Cells were then pre-treated with fatty acids to determine what effect if any they had on RAGE expression. It was confirmed for the first time that arachidonic acid (20:4 n-6), eicosapentaenoic (20:5 n-3) and docosahexaenoic acid (22:6 n-3) were able to significantly inhibit AGE induced RAGE expression in HUVECs. The role of fatty acids on IL-1β, IL-6, IL-8 and MCP-1 as markers of BSA-dicarbonyl induced inflammation was also investigated, however no effect was observed.

This study shows that pre-treatment of HUVECs with fatty acids warrants further investigation into the potential of fatty acids as a therapeutic agent aimed a mitigating RAGE expression and inflammation induced by AGEs *in vitro*. The studies reported in this thesis provide evidence of significant advancement towards a more physiologically relevant model to investigate AGEs and the study of potential therapeutics aimed at alleviating AGE-induced receptor expression and the upregulation of inflammatory and oxidative stress biomarkers.

Publications arising

Publications included in this thesis:

Peake, B., Ghetia, M., Gerber, C., Costabile, M., Deo P, **(2021).** Role of saturated and unsaturated fatty acids on dicarbonyl–albumin derived advanced glycation endproducts in vitro. *Amino Acids* https://doi.org/10.1007/s00726-021-03069-6

Peake, B., Jaunay, E., Gerber, C., Costabile, M., Deo P, **(2022).** Unsaturated fatty acids downregulate dicarbonyl-derived advanced glycation end product induced receptor expression in HUVECs
In preparation: *Amino Acids*

Co-authored articles not included in this thesis:

Deo, P., Dhillon, V. S., Lim, W. M., Jaunay, E. L., Donnellan, L., **Peake, B.,** McCullough, C. L. and Fenech, M. **(2020)** Advanced glycation end-products (AGEs) accelerate telomere attrition and increase pro-inflammatory mediators in human WIL2-NS cells. *Mutagenesis*, 35 (3), pp. 291-297.

Deo, P, Chern, C, **Peake, B,** Tan, S **(2020)** Non-nutritive sweeteners are in concomitant with the formation of endogenous and exogenous advanced glycation end-products, *International Journal of Food Sciences and Nutrition*, 71:6, 706-714, DOI: 10.1080/09637486.2020.1712683

Introductory contextual statement

This thesis is submitted as a Thesis Containing Published Research in accordance with UniSA Academic Policy for Research Degrees AB-58 AD2.

The overall aim of this project was to develop a robust and physiologically relevant model system that enables the *in vitro* investigation of AGE induced receptor expression and inflammatory biomarkers. A robust model system would enable the examination of the effects of saturated and unsaturated fatty acids on dicarbonyl-derived AGE induced expression of the receptor for AGEs (RAGE). Furthermore, the model system would allow for the testing of fatty acids for activities against inflammatory markers resulting from dicarbonyl-derived AGE treatment in human endothelial cells. A series of objectives were developed to assist with addressing this aim

- To develop and optimize a BSA-dicarbonyl model system to generate and quantify AGE production.
- To determine the effect of saturated and unsaturated fatty acids on dicarbonyl induced AGE production *in vitro.*
- To determine if the receptor for AGEs (RAGE) expression and markers of inflammation are increased in human umbilical vein endothelial cells HUVEC) treated with dicarbonyl-BSA derived AGEs.
- To determine the effect of polyunsaturated fatty acids on RAGE expression and inflammatory biomarkers in human umbilical vein endothelial cells (HUVEC) treated with dicarbonyl-BSA derived AGE treatment.

This thesis is submitted as a Thesis Containing Published Research in accordance with UniSA Academic Policy for Research Degrees AB-58 Appendix AD2 presented in a traditional chapter format. The manuscript published during candidature (Chapter 2) arose from experimental data relating to **Chapter 2**. The contents of the manuscript has been reformatted to ensure consistency and clarity throughout the thesis. The incorporation of this manuscript is critical to the overall narrative of the thesis and the chapter includes additional data obtained to satisfy the objectives stipulated above.

Author Statement

As the first author of the published work contained in **Chapter 2,** I conducted the experimental work, data analysis and constructed the manuscript drafts. Co-authors and supervisors Permal Deo, Maurizio Costabile and Cobus Gerber each provided oversight in the conception and experimental work and provided editing on all manuscripts submitted or accepted for publication and this thesis. Maulik Ghetia assisted with LC-MS/MS work and method editing.

Their individual specific involvement in this thesis is further described in the following:

Permal Deo provided the initial conceptualisation of the glycation model systems used throughout the experimental **Chapters 2 and 3**

Maurizio Costabile provided input across all aspects of the experimental work and critical advice regarding the appropriate use of fatty acids, protein, and cytokine investigation in **Chapter 3**

Cobus Gerber provided advice on the experiments that were undertaken in all chapters in particular **Chapter 2** and assistance in LC-MS/MS experimentation and optimisation.

Maulik Ghetia developed the LC-MS/MS method that was used to quantify the levels of protein-bound AGEs in the dicarbonyl-albumin model systems.

Emma Jaunay assisted in the establishment of the Western blot and qPCR methods used in **Chapter 3**.

Chapter 1 - Literature Review

1.1 – Introduction

Glycation is a series of non-enzymatic reactions that occurs between the free amino group of proteins, lipids and nucleic acids and reducing sugars, such as glucose and fructose [1-3]. In the early stages of glycation an unstable Schiff base is generated from the initial reaction between a reducing sugar and amine whereby, the aldehydic carbon-oxygen double bond of the reducing sugar is converted to a carbon-nitrogen double bond with the amine, and elimination of water (H_2O). This generates a glycosylamine intermediate (Schiff base) which is unstable, and its rearrangement produces an enaminol intermediate. Additional spontaneous rearrangement forms a ketoamine (Amadori rearrangement product (ARP)), such as fructoselysine when glucose is the reducing sugar.

Amadori products further undergo complex reactions (rearrangement, dehydration and condensation) becoming the irreversibly crosslinked heterogenous group known as advanced glycation endproducts [4] (Figure 1.1).

Methylglyoxal (MGO), Glyoxal (GO) and 3-deoxyglucosone (3-DG) are highly reactive endogenous α-dicarbonyl compounds present in most mammalian cells. They are generated both endogenously and exogenously by cell metabolism, glucose oxidation and lipid peroxidation [5].

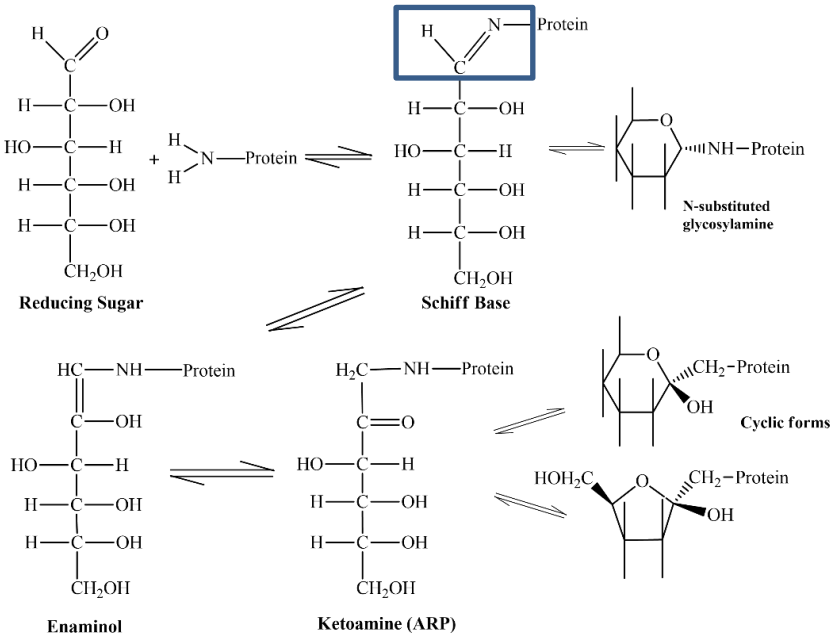


Figure 1.1 - Formation of a Schiff base and Amadori rearrangement product (ARP).

The formation of a Schiff base and Amadori rearrangement product following the reaction between a reducing sugar and a protein. Adapted from [6]

Advanced glycation endproducts (AGEs) have been demonstrated to have detrimental effects on both intracellular and extracellular proteins [7, 8]. AGEs can be produced both endogenously and exogenously. Endogenous AGEs form spontaneously and accumulate in all cells in the body under normal physiological conditions such as aging, however conditions such as hyperglycaemia, hyperlipemia, increased inflammation and oxidative stress accelerates AGE production [9, 10].The major source of exogenous AGEs are derived from diets high in carbohydrates [11], and highly processed foods [12, 13]. Glycated proteins have the potential to lose their ability to bind substrates, becoming recognised as misfolded and directed to the proteasome for degradation. These protein post-translational modifications can alter tertiary structure resulting in functional loss [14-16]. AGEs such as pentosidine can induce protein crosslinking which has been shown to result in subsequent protein aggregation during protein glycation, leading to the inhibition

of the glycated protein being degraded by proteasome [17, 18]. Crosslinking can also occur in extracellular matrix proteins such as collagen and elastin, resulting in stiffness of connective tissue [19]. These changes can have clinical implications such as retinopathy, nephropathy, neuropathy and coronary heart disease as a consequence of the increased inflammation and oxidative stress (OS) levels within the cell resultant from AGEs [15, 20]. Increases in inflammation and OS occur due to the overexpression of the receptor for advanced glycation endproducts (RAGE) [14, 21, 22]. Binding of AGEs to RAGE is known to increase the inflammatory responses in cells, by activating various signalling pathways including mitogen-activated protein (MAP) kinase, Nuclear factor KappaB (NF-κB), and the AGE-RAGE binding cascade leading to cellular dysfunction [7].

Of the 20 naturally occurring amino acids, the R-group side chains of arginine and lysine are most susceptible to glycation due to their positive charge at physiological pH and free amino group making them primary targets for post-translational modifications. Reactive intermediates produced during this process are α-oxoaldehydes, in particularly MGO and GO, which are approximately 20,000 fold more reactive than glucose in glycation reactions [23]. Lipids (specifically polyunsaturated fatty acids), can also undergo peroxidation and form advanced lipoxidation endproducts (ALEs) having similar effects on proteins as noted for AGEs [24].

1.2 – Chemistry of AGE formation

AGEs are generated by five main pathways; 1, Maillard reaction; 2, glucose oxidation, 3, lipid oxidation; 4, glycolysis and 5, polyol pathway (Figure 1.2) [25]. Aside from the Maillard pathway, all other pathways lead to the production of reactive dicarbonyls MGO

and GO, which are formed as intermediates of glycation and have detrimental effects on cellular homeostasis, including activating apoptotic pathways [23, 26].

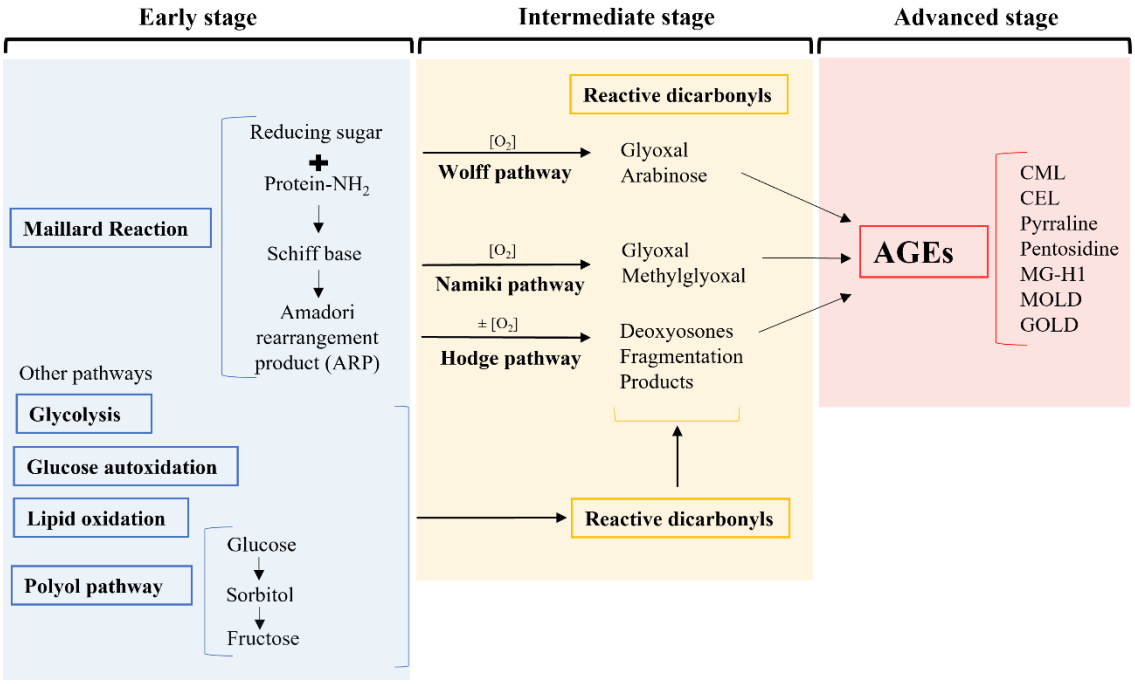


Figure 1.2 - Overview of the pathways that lead to advanced glycation endproduct formation.

Pathways that can occur during the early stage of glycation are the Maillard reaction, glycolysis, glucose autoxidation, lipid oxidation and the polyol pathway. They form reactive dicarbonyls which are rearranged to form advanced glycation end products (AGEs). CEL: *N*ε-carboxyethyllysine, CML: *N*ε-carboxymethyllysine, GOLD: glyoxal-lysine dimer, MG-H1: methylglyoxal-derived hydroimidazolone, MOLD: methylglyoxal-lysine dimer. Adapted from [6, 27].

1.2.1 – Maillard reaction and history

The Maillard reaction was first documented in the early 1900's when French chemist L.C Maillard pioneered work on heating amino acids in the presence of sugars producing a yellow/brown colour [1, 28]. In the early 1900's Robert Ling studied similar reactions in both food and physiological chemistry, producing both flavoured and coloured

compounds from heat drying proteins with glucose and maltose, making them some of the earliest recorded adducts formed between sugars and amines [29]. In the 1960's the degradation of fructosamine to 3-deoxyglucosone and its importance was reported along with the discovery of glucose-derived Amadori products of haemoglobin in diabetic blood samples (HbA1c) [30, 31]. It was not until 1986 that the term advanced glycation endproduct was used to refer to the brown fluorescent pigments which irreversibly crosslink proteins [31].

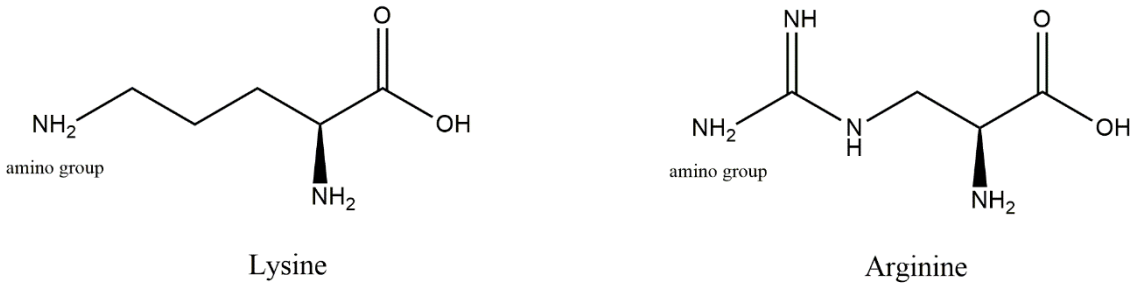


Figure 1.3 - The structure of commonly glycated amino acids lysine and arginine

The functional structure of Lysine and Arginine which are the most commonly glycated amino acids due to due to their positive charge at physiological pH and free amino group making them primary targets for post-translational modifications Adapted from [32]

The Maillard reaction is the most studied AGE pathway [27] and can be further subdivided into 3 stages: early, advanced and final stage. In the early stages the carbonyl group of a reducing sugar (glucose, fructose) attaches to the free amino group of arginine and/or lysine residues to form a Schiff base (Figure 1.) [33]. This adduct then undergoes rearrangement to form the more stable Amadori Product (AP), also known as an early glycation adduct. APs irreversibly form both fluorescent AGEs (e.g. pentosidine), and non-fluorescent AGEs (e.g. carboxymethyllysine, carboxyethyllysine and methylglyoxal derived hydroimidazolone) via the Hodge pathway [27]. Schiff bases can also lead to the

generation of α-dicarbonyl compounds, including methylglyoxal, glyoxal and 3-deoxyglucosone via the Namiki pathway [34].

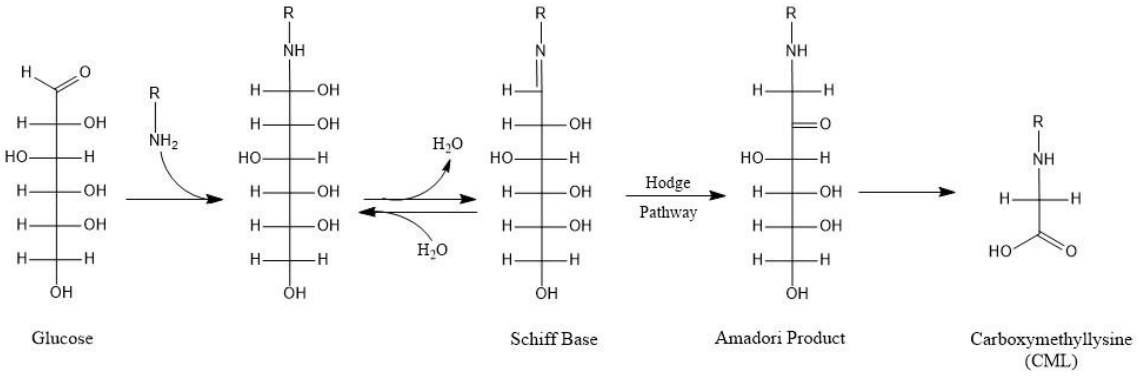


Figure 1.4 - Formation of *N*ε-Carboxymethyllysine, -(CML) from glucose.

A reducing sugar, typically glucose or fructose reacts with lysine residues to form a Schiff base in a reversible reaction. The Schiff base can then undergo rearrangement to form the more stable Amadori product which is cleaved to irreversibly form CML and the homologue CEL. Adapted from [35].

1.2.2 – Glucose Autoxidation

Autoxidation of monosaccharides is a process catalysed by transition metals and contributes to the *in vitro* modification of proteins by the generation of α-ketoaldehydes (MGO/GO), hydrogen peroxide (H_2O_2) and free radical intermediates [36, 37] leading to functional and conformational changes to the protein. Ketoaldehydes can bind to the side chains of lysine residues and lead to the generation of reactive intermediates, ultimately irreversibly forming AGEs [37].

1.2.3 – Lipid peroxidation and advanced lipoxidation endproducts (ALEs)

Proteins can also undergo modification by reacting with lipids [38] forming advanced lipoxidation endproducts (ALEs). ALEs refers to a variety of covalent adducts that are non-enzymatically produced by reactive carbonyl species such as GO and MGO, which can be generated by lipid oxidation and metabolism [39]. Peroxidation of fatty acids leads to the generation of dicarbonyls such as malondialdehyde (MDA) and aldehyde 4-hydroxynonenal (HNE) [40]. Glyoxal, the smallest dialdehyde, can be formed from both sugars and lipids [41] via lipid peroxidation, for example linoleic acid which generates peroxide intermediates that degrade and form glyoxal [42]. Oxidative modification of lipids plays an important role in atherogenesis along with contributing to vascular abnormalities in people with diabetes and also normal ageing [43]. Arachidonic acid and other poly unsaturated fatty acids (PUFAs) generate hydroperoxides as a result of being cleaved in the presence of metal ions (Mg^{2+}, Mn^{2+}, Fe^{2+}, Ca^{2+}) forming radicals, leading to the perception they are involved in the generation of chronic diseases [44]. It has been theorised that lipids may suppress or promote the Maillard reaction as some lipid oxidation products are able to react with Maillard products, however, the literature surrounding the interaction between lipids and Amadori products is limited, with few studies investigating the link between peroxidation products changes and subsequent amino acid modifications [40, 45].

1.2.4 – Glycolysis

Glycolysis plays an important role in the rapid production of AGEs by generating reactive intermediate metabolites (MGO/GO/3-DG). This occurs rapidly when glycolysis is interrupted by reactive oxygen species (ROS) [46]. MGO can be formed as a by-product of glycolysis, resulting from the nonenzymatic degradation of glyceraldehyde 3-phosphate (G3P) and dihydroxyacetone phosphate (DHAP) [47]. Excess MGO can also be formed as a result if the abnormal buildup of glycolytic intermediates, resulting from excess superoxide's preventing the normal progression of glycolysis hence associated with the AGE pathway (Figure 1.5). It is of particular relevance in diabetes which induces hyperglycemia along with many metabolic alterations in glycolytic metabolism [48]. These changes in levels of intermediate metabolites are involved in an increase in glycation in diabetic tissues by non-enzymatically modifying proteins [48].

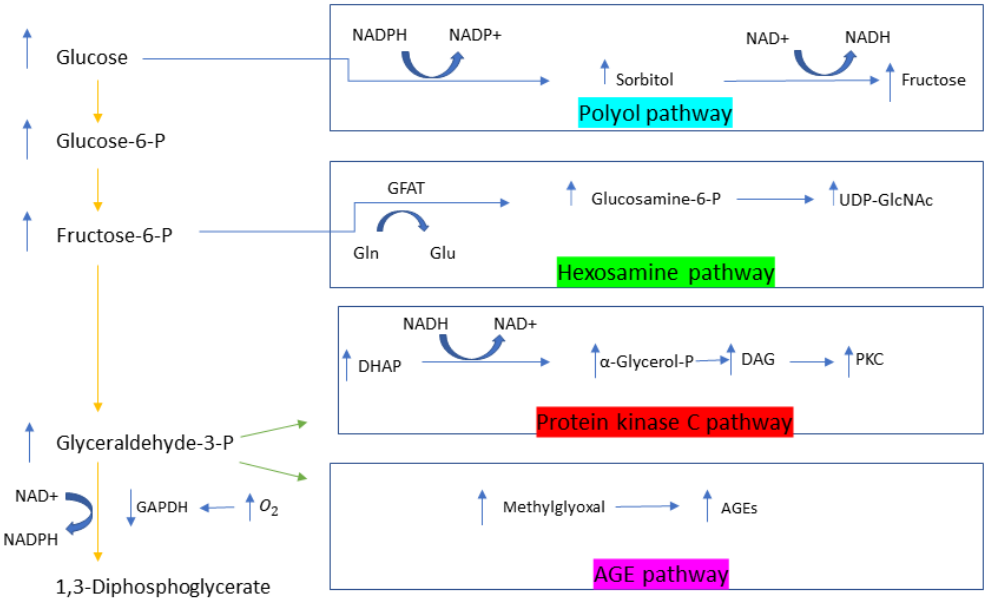


Figure 1.5 – The activation of four pathways of hyperglycemic damage by hyperglycemia-induced mitochondrial superoxide overproduction, a potential Mechanism.

Excess superoxide partly inhibits the glycolytic enzyme GAPDH, thus diverting upstream metabolites from glycolysis into pathways of glucose overutilization. This results in amplified flux of dihydroxyacetone phosphate (DHAP) to DAG, an activator of PKC, and of triose phosphates to methylglyoxal, the main intracellular AGE precursor. Increased flux of fructose-6-phosphate to UDP-N-acetylglucosamine increases modification of proteins by O-linked N-acetylglucosamine (GlcNAc) and increased glucose flux through the polyol pathway consumes NADPH and depletes GSH. Adapted from [49]

1.2.5 – Polyol pathway

The polyol pathway comprises aldose reductase which reduces glucose to sorbitol via NADPH and sorbitol dehydrogenase, which converts sorbitol to fructose via NAD^+ [50]. This pathway has long been implicated in the pathogenesis of diabetic symptoms. It has

been shown that inhibitors of aldose reductase (Epalrestat), can reduce diabetic complications [51]. Aldose reductase inhibitors exist in many classes, for example carboxylic acid derivatives (e.g.Epalrestat, Alrestatin, Zopalrestat), spirohydantoins and related cyclic amides (e.g. Sorbinil, Minalrestat) and phenolic derivatives (e.g. Chalcone) [52].

However a review article by Chalk et at 2007, demonstrated a meta-analysis of controlled aldose reductase inhibitors showed no significant difference in the treatment of people with diabetes as compared to no treatment controls, thus making it difficult to make definitive conclusions about their efficacy [53]. While fructose and glucose are responsible for the involvement of the polyol pathway in glycation, their metabolites fructose-3-phosphate and sorbitol-3-phosphate are more potent in terms of glycation capability [54]. Fructose and its metabolites however undergo glycation to form AGEs much faster than glucose due to its open-chain structure and ketone group. This further increases levels of cellular OS contributing to the generation of ROS and increases cellular dysfunction [51]. It is important to note that both sorbitol and fructose have been positively correlated with CML levels, inferring the pathway and associated polyol metabolites are involved in the formation of AGEs [55].

1.3 – Fluorescent and non-fluorescent AGEs

AGEs are heterogeneous compounds that can be categorized into 3 main categories: fluorescent cross-linking AGEs (e.g., pentosidine), non-fluorescent cross-linking AGEs (e.g. methylglyoxal lysine dimer - MOLD), and non-fluorescent non-crosslinking AGEs

(e.g. CML, CEL, MG-H1) (Figure 1.6). CML is the most extensively investigated AGE and is formed by GO reacting with lysine residues in proteins [56]. In the presence of proteins and lipids, MGO can react with lysine residues to form N^{ε}-carboxyethyllysine (CEL) a homologue of CML [57]. MOLD is similarly formed by reactions of MGO with lysine residues [58]. MGO can also react with arginine residues forming hydroimidazolones, primarily methylglyoxal derived hydroimidazolone or MG-H1[59, 60]. MG-H1 has recently emerged as an important marker due to its cellular abundance and elevated serum levels implicating it in disease [61, 62].

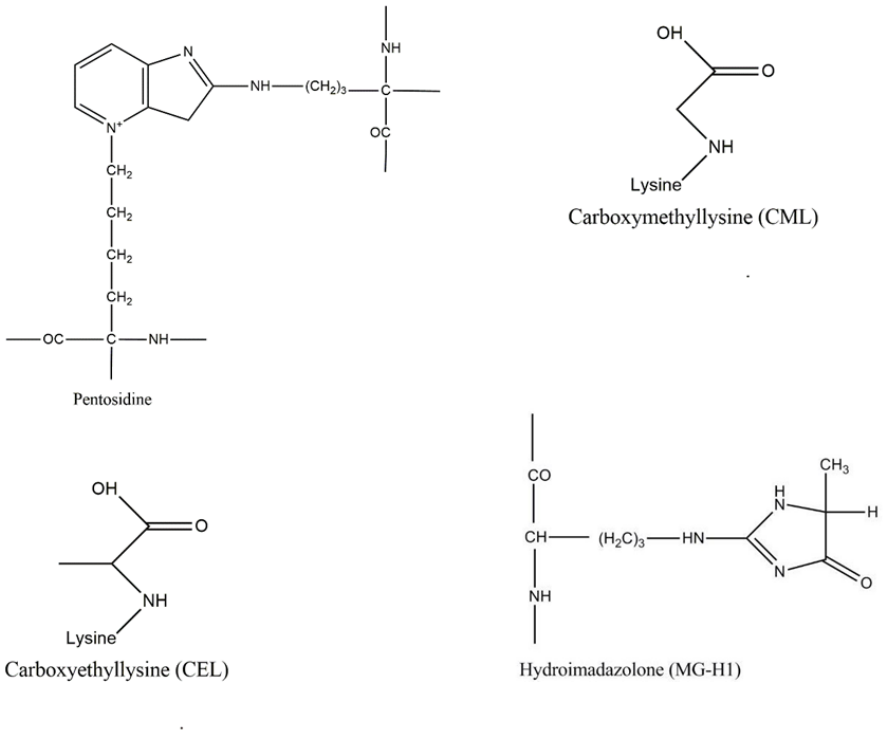


Figure 1.6 - Structure of common fluorescent and non-fluorescent AGEs.

Non-fluorescent AGEs; Nε-Carboxymethyllysine (CML), Nε-Carboxyethyllysine (CEL), Methylglyoxal hydroimidazolone -1 (MG-H1), and Pentosidine a fluorescent AGE. Adapted from [63]

1.3.1 – Pentosidine

Pentosidine is a fluorescent AGE that forms protein crosslinks in the extracellular matrix by interacting with both highly reactive lysine and arginine residues [64, 65]. It is a reliable and well-characterized marker of glycation that accumulates with normal ageing in tissue collagen. It is formed when pentose reacts with lysine residues to form an Amadori product which then reacts with an arginine residue to form pentosidine [65]

1.3.2 – Nε-Carboxymethyllysine (CML)

CML, first discovered in human urine in 1975 [66], is an AGE formed from proteins as a result of glycation or oxidative fragmentation of Amadori products from glucose. [67, 68]. It is derived from both food and biological systems. CML can also be formed as a product of the metal-catalysed oxidation of lipids in the presence of proteins and is thus classified as both an AGE and an ALE [67]. CML is the most extensively studied AGE, and considered to be the most abundant AGE *in vivo*, and it is used as a maker for glycoxidative, lipoxidative, oxidative and carbonyl stress [69]. Elevated levels of CML have also been linked to the development of diseases such as Diabetes and Alzheimer's disease (AD) [70, 71]. In Diabetes, CML levels are a marker of disease progression, where glycation of proteins leads to an increase in OS increasing AGE formation [67]. CML is a late-stage oxidative product, and there is extensive evidence that it is a biomarker of both glycation and oxidation reactions [72]. Diabetic rat models have shown that CML binds to RAGE resulting in changes to cellular protein structure and hence function [73]. CML levels in plasma in healthy and people with diabetes differs

depending on the method of quantification and whether free or protein-bound CML is the target [3]. Once formed, CML is a stable irreversible final product of glycation.

1.3.3 – Carboxyethyllysine (CEL)

CEL much like its homologue CML is a stable final glycation product formed during the non-enzymatic glycation of lysine residues of proteins [3]. It has been detected in human plasma at similar levels to CML [74]. Concentrations of CEL in tissue proteins can be an important biomarker for OS [74]. Much like CML, plasma levels of CEL in in healthy individuals and people with diabetes can vary depending on the method of quantification, Typical ranges for healthy controls is 44 (36-55) nmol/L, while people with diabetes are 49 (39-64) nmol/L [3, 75, 76].

1.3.4 – Methylglyoxal derived hydroimidazolone (MG-H1)

As a potent reactive glycating agent, MGO reacts primarily with arginine residues and modifies proteins leading to the formation of AGEs and generating hydroimidazolones (Figure 1.7). Hydroimidazolones and their adducts have been detected in all forms of biological life [77]. The main AGE formed when MGO reacts with arginine residues is N_{δ}-(5-hydro-5-methyl-4-imidazolon-2-yl)-ornithine or MG-H1 [77], which is also quantitatively abundant *in vivo* [78] .There are also the structural isomers MG-H2 and MG-H3, however ,MG-H3 is unstable and rarely quantified. [79-81]. This reaction leads to cellular and protein dysfunction as arginine is found in abundance at the functional site of proteins. MG-H1 accounts for >90% of glycation adducts *in vitro* and *in vivo* and is

said to be the most physiologically relevant MGO-derived AGE [82]. MG-H1 has a relatively long half-life (12 days) compared to the majority of cellular proteins (46 h) [59] resulting in irreversible modification. Proteins which have been modified by MGO to form MG-H1 have a net loss of their positive charge, as compared to glycation by glucose where the positive charge on the N-terminal is retained [59]. This difference is thought to contribute to the damaging effect of MGO based glycation.

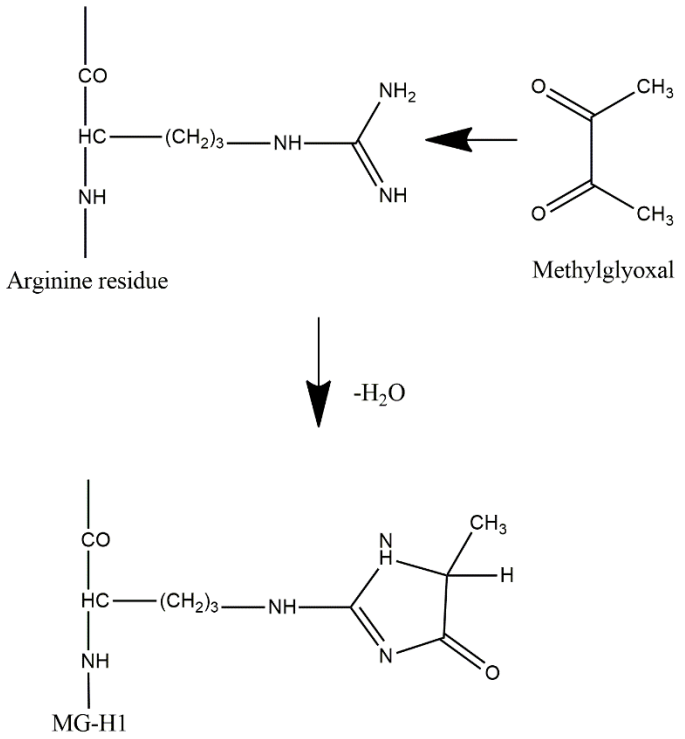


Figure 1.7 - Formation of 5-hydro-5-methyl-imidazol-4-one (methylglyoxal hydroimidazolidine-1 (MG-H1)).

MGO reacting with arginine residues to form MG-H1. Adapted from [83]

Table 1.1 - Examples and characteristics of major advanced glycation/lipoxidation end products.

AGE compound	Mechanism of formation	Quantitation	Reference/s
CML	Isomerisation	Various tissues, plasma, blood cells, urine, lens	[84, 85]
CEL	Isomerisation	Plasma, blood cells, urine, lens	[86-88]
MG-H1	Isomerisation	Plasma, blood cells, urine, lens	[80, 81, 89]
Pyrraline	Cyclisation	Plasma, serum, urine, lens	[90-92]
Pentosidine	Cyclisation	Plasma, serum, urine, blood cells, lens	[91, 93, 94]

Common AGEs that are relevant *in the body* – adapted from **[68]**. CML - N^{ε}-carboxymethyllysine, CEL - N^{ε}-carboxyethyllysine, MG-H1 - Methylglyoxal hydroimidazolone-1

1.3.5 – Quantification of AGEs in biological samples

The heterogenous nature of AGEs generated during glycation has resulted in difficulties developing accepted standardised method to quantify all types of AGEs in a sample. Commonly used methods are summarised in Table 1.2 with a brief description of the advantages and disadvantages of each method. Quantification of AGEs using ELISA techniques are quick and inexpensive however reliability and repeatability is questionable [95]. The most accepted method of AGE quantification currently is LC-MS/MS techniques, as this can quantify a variety of reactive dicarbonyl species and a variety of characterised AGEs [96, 97]. Using LC-MS/MS to quantify AGEs in biological samples is preferred due to its sensitivity, accuracy and rapid analysis of multiple samples and target analytes. The method separates target analytes through liquid chromatography,

which are then ionized allowing filtering and detection based on the mass/charge ratio of the ionized chemical species [97]. The purification technique for processing samples before LC-MS/MS analysis typically involves the isolation and acid hydrolysis of the glycated protein and subsequent solid phase extraction to yield isolated AGE residues [98]

Table 1.2 – Advantages and disadvantages of common methods for AGE detection and quantitation

Detection method	Marker	Location	Advantage	Disadvantage	Reference/s
Fluorescence	Fluorescent AGEs (pentosidine)	Skin serum, urine saliva	Simple, quick	Nonfluorescent AGEs are not detected, no units for expression apart from arbitrary units	[99, 100]
HPLC	Pentosidine, CML, CEL MG-H1	Plasma, tissue	Appropriate for AGE monitoring	More costly, only useful for AGEs of known structure and mass	[101]
GC-MS	CML, CEL MG-H1	Urine	Highly sensitive, valid data	Expensive, specialist training required	[102]

LC-MS/MS	CML, CEL MG-H1	Plasma, urine, model systems	No derivatisation is required, highly sensitive, valid data	Expensive, training is required, isotopic labelled standards required	[103, 104]
UHPLC	CML, CEL MG-H1	Plasma, tissue	Rapid, good resolution	Expensive, training is required isotopic labelled standards required	[105]
ELISA	AGEs, Pentosidine, CML, CEL	Skin, serum, urine, tissue	Simple, inexpensive no need for expensive equipment	Lack of specificity, interference from free adducts	[106]
Immunoblotting	Antibodies against different molecules	Skin. Any tissue	Highly specific, cheap	Accuracy, timely procedure, sensitivity of antibodies.	[107, 108]

A summary of advantages and disadvantages of methods for quantitation of AGEs in various samples. Adapted from [109]

1.4 – α-Dicarbonyl compounds

MGO, GO and 3-DG are highly reactive endogenous α-dicarbonyl compounds present in most mammalian cells. Both MGO and GO are metabolic intermediates and are known to be major precursors for AGEs formed during protein, glucose and fatty acid metabolism [110]. They are generated endogenously by cell metabolism, glucose oxidation and lipid peroxidation; however, they can also be formed by the degradation of carbohydrates in both food and beverages [5]. Dicarbonyl compounds can accumulate in many cell types, most notably endothelial cells experiencing hyperglycaemic conditions

[111]. *In vivo* the majority of MGO formed is from the enzymatic and spontaneous breakdown of triose phosphates glyceraldehyde-3-phosphate and dihydroxyacetone phosphate accompanied by the metabolism of ketone bodies. In contrast GO is largely formed by lipid peroxidation. [67, 68, 77]. Both MGO and GO are primarily detoxified by the glyoxalase system [112]. MGO principally reacts in a reversible reaction with arginine, lysine and cysteine residues generating both fluorescent AGEs such as pentosidine and non-fluorescent AGEs such as MG-H1 and CEL [110, 113, 114]. MGO binds to the amino group of arginine and lysine residues in the late stages of protein glycation. MGO can also bind to guanidine and is thought to be an important factor relating to oxidative DNA damage and cell cytotoxicity [113]. However MGO mainly affects arginine residues and results in the loss of positive charge via the formation of hydroimidazolones [115]. The majority of GO is formed from the degradation of glucose and fructosyl-lysine under physiological conditions [14]. GO, itself reacts primarily with lysine residues forming CML.

Elevated levels of MGO in the plasma have been associated with diabetes with plasma MGO levels two to four-fold higher compared to healthy individuals [5, 113]. Elevated levels of MGO leads to an increase in ROS production which can increase OS and alter cellular structure and protein function all while leading to dicarbonyl stress [110, 116]. For example, in late-stage diabetes, vascular tissue is abundant in MGO derived AGEs, which contribute to vasculopathies [117]. MGO has also been shown to cause endothelial dysfunction which can lead to atherosclerosis and diabetic vascular disease [118]. It is suggested that MGO can covalently modify the 20S proteasome, which decreases the ability of the kidney to remove damaged proteins [117, 119]. Braun et al (2019) showed MGO down-regulates the expression of cell cycle genes, leading to the activation of the p53 pathway, cell cycle arrest, apoptosis, or senescence [120]. GO levels are elevated in

people with diabetes however the link to diabetic complications remains unclear. This is largely in part due to the majority of studies surrounding dicarbonyl and dicarbonyl derived AGEs focussing on MGO [40].

1.4.1 – Dicarbonyl Stress

Dicarbonyl stress is defined as the imbalance between reactive dicarbonyl compounds (MGO/GO) and detoxifying enzymes (GLO 1 and GLO 2) resulting in an increase in protein glycation [79, 121]. The increase in glycation contributes to post-translational modifications of proteins and DNA damage, causing cell and tissue dysfunction prominent in ageing and diseases including Diabetes and AD [122]. Although it remains unclear how dicarbonyl stress induces an inflammatory response, it is hypothesized that proteins that have been modified by GO and MGO are identified as misfolded leading to the unfolded protein response and being sent to the proteasome for proteolysis [121, 122]. Dicarbonyls in foods are metabolised and react with proteins before they are absorbed in the gastro intestinal tract, thus imposing dicarbonyl stress largely in the gastrointestinal lumen [123].

Physiological levels of MGO and 3-DG in the cell are low, typically 1-4 µM, when the levels rise, dicarbonyl stress occurs and contributes to a deterioration of health, leading to disease [122]. Recent studies surrounding dicarbonyl stress have provided a greater understanding of its impact surrounding ageing and disease progression and have enabled the design of new pharmaceuticals to be trialled [124] including GLO-1 inducers for the treatment of obesity, diabetes and cardiovascular disease. On the other hand, GLO-1 inhibitors have been trialled for multidrug-resistant tumours [124]. Indeed, increasing

numbers of studies are investigating the role dicarbonyl derived AGEs play in age-related tissue dysfunction revealing a previously underestimated role of dicarbonyl stress [26]. Masania et al (2016) found that dicarbonyl stress may be a mediator of obesity and also insulin resistance, thus a possible risk factor in the development of T2DM [125].

1.5 – The receptor for advanced glycation end products (RAGE)

The receptor for advanced glycation endproducts (RAGE) was first identified and described by Neeper et al in 1992 [126] (Figure 1.8). RAGE is a multiligand receptor and a member of the immunoglobulin superfamily of cell surface molecules [127, 128]. It is a pattern recognition receptor (PRR) and a central mediator of the innate immune response [129]. RAGE consists of 404 amino acids with a molecular weight of 45-55 kDa, however this can also be dependent upon differential states of glycation [130].

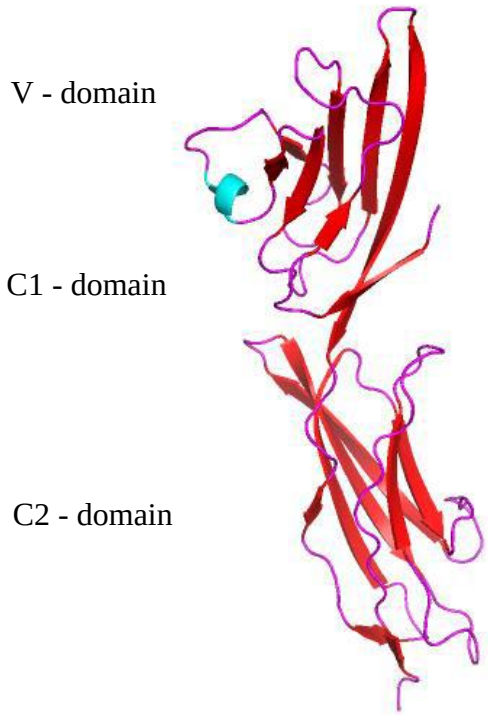


Figure 1.8 - Backbone and ribbon diagram of the crystal structure of human RAGE extracellular domain (V-C1-C2 domains).

Protein data bank structure coordinates: 4LP5 from primary publication [131]; Diagram drawn using The PyMOL Molecular Graphics System, Version 2.0 Schrödinger, LLC [132] (126); red flat arrows show β-strands, magenta smooth ribbon shows backbone, blue spring shaped ribbon show helices.

RAGE is expressed in several cell types including, microglia, smooth muscle cells, lymphocytes, platelets and endothelial cells. Its transcription is regulated by nuclear factor κB (NF-κB) [129, 133]. RAGE was first thought to be a specific receptor for AGE products, however it has since been shown to bind multiple ligands including S100, amphoterin/high mobility group box-1, amyloid-β and Mac-1 [130]. RAGE is comprised of 3 extracellular domains (V, C1 and C2), a transmembrane helix and a highly charged intracellular domain which facilitates interactions with OS-related molecules such as MAP kinase and NF-κB [128] **(**Figure 1.8**)**, AGEs however, will only bind to the V domain [134].

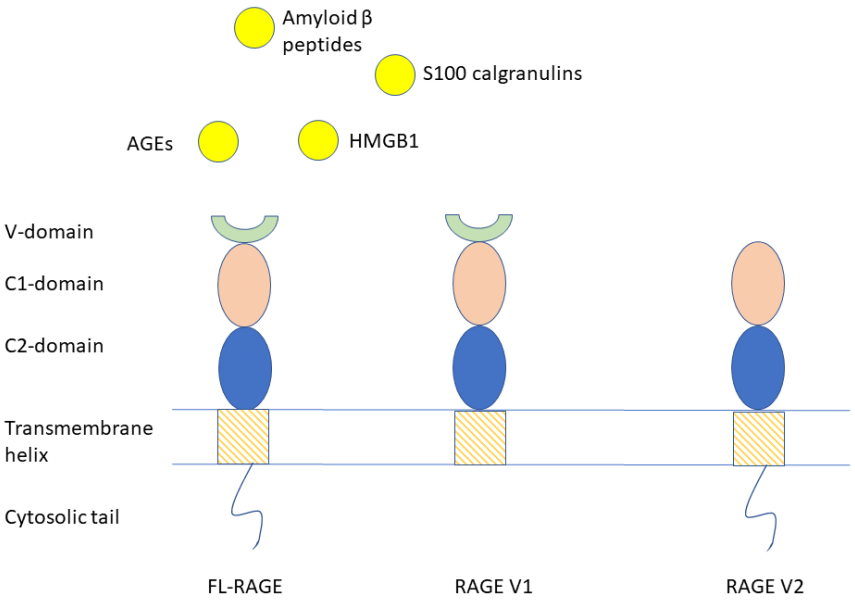


Figure 1.9 - The structure of the receptor for advanced glycation endproducts and its binding domains.

RAGE structure domains and the three most prevalent isoforms. RAGE has multiple ligands including AGEs, S100/calgranulins, HMGB1 and amyloid-b. RAGE-V1- represents a spliced version which can act as a decoy receptor, preventing ligand interaction with full-length RAGE adapted from [135]

RAGE is located on chromosome 6 close to the major histocompatibility complex III, indicative of its involvement in immune responses [136]. The binding of AGEs to RAGE **(**Figure 1.10) results in the phosphorylation of various protein kinases (MAPKs/JAK) and initiates an intracellular signalling cascade resulting in the activation of transcription factors such as NF-κB. Upon activation NF-κB translocates to the nucleus initiating the upregulation of defence and signalling proteins [137] and the release of pro-inflammatory cytokines including tumour necrosis factor-alpha (TNF-α) and interleukin-6 (IL-6) [21]. The activation of NF-κB in the nucleus also upregulates nuclear transcription of RAGE, in turn increasers the concentration of RAGE at the cell surface (Figure 1.10). In vitro binding of AGE-RAGE results in activation of NF-κB for approximately 1 week, while in vivo (mice) AGE-RAGE binding activates NF-κB for approximately 1 month [138]. The consequences of this sustained activation increases the formation of ROS, along with upregulation of pro inflammatory cytokines, leading to cellular dysfunction and the pathogenies of chronic conditions such as CVD, neurodegenerative disorders, stroke, arthritis, cancer and diabetic complications .[7, 95, 139-141].

There is evidence that RAGE is vital for maintaining protein homeostasis in the central nervous system, and if the expression is increased it may contribute to neuroinflammation [142]. Conditions such as diabetes disturbed homeostasis, can increase RAGE expression along with increased production of AGEs and induce the release of intracellular calcium-binding molecules known as S100 calgranulins [111]. Increased RAGE expression can also lead to the increased production of collagen, laminin and fibronectin. This occurs as collagen is exposed to glucose in vascular and extra vascular fluids, where glycation induced cross-linking decreases vascular elasticity [143] resulting in tissue fibrosis [144]. It is the activation of RAGE that is believed to be mainly responsible for the pathogenicity

associated with AGEs [134]. RAGE is constitutively expressed during embryonic development but decreases in adulthood [21]. Under physiological conditions, RAGE expression is relatively low in most tissues, however, is upregulated in pathophysiological states (chronic inflammation, neurodegenerative disorders or diabetes [126, 145]. The AGE-RAGE interaction is thought to activate glial cells and stimulate cytokine release, in particular IL-6, interleukin 1 alpha (IL-1α), TNF-α [146] and the generation ROS [15, 147].

Soluble RAGE (sRAGE) consists of the extracellular domains of RAGE; however, both the transmembrane and cytosolic domains are missing. sRAGE is produced either by proteolytic cleavage of RAGE, or alternate mRNA splicing [148, 149]. By lacking the cytosolic tail domain sRAGE does not transmit any cellular signals and does not contribute to the inflammatory response. sRAGE is also known to be a decoy receptor, due to its ability to inhibit full-length RAGE ligand binding [150, 151].

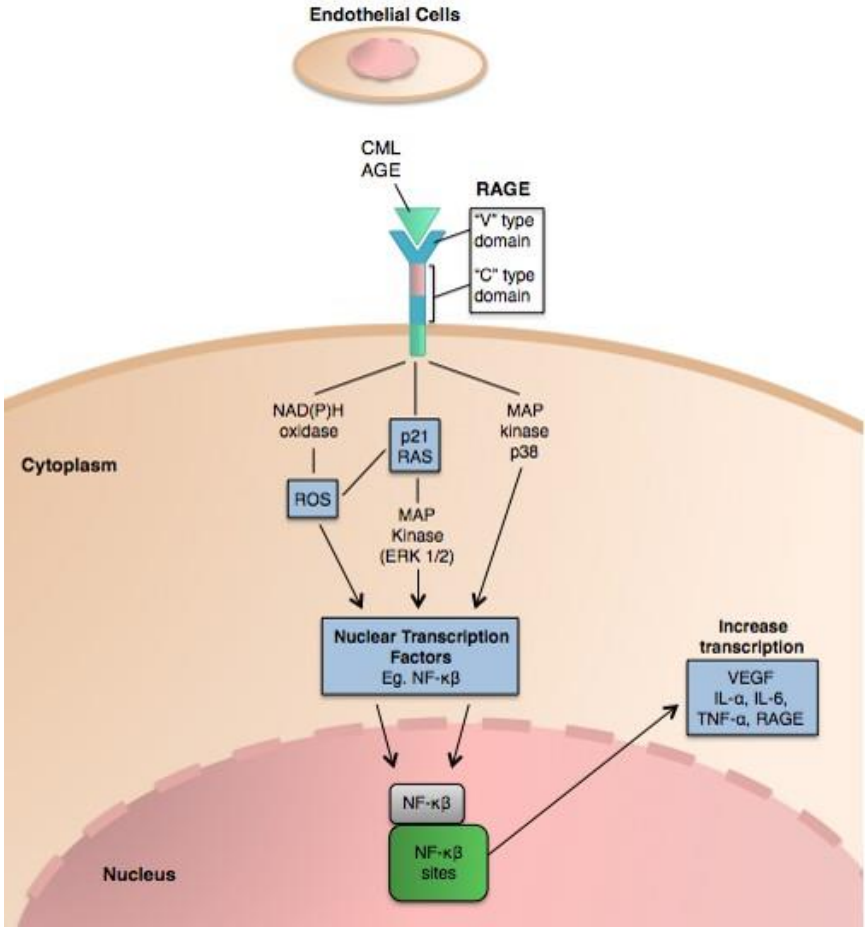


Figure 1.10 - An example of an AGE binding to the multi-ligand receptor for AGEs (RAGE) and triggering an intracellular signal cascade

Once a protein-bound AGE binds to the receptor a variety of signal pathways are triggered. These can include NAD(P)H oxidase and p21 pathways which increase reactive oxygen species (ROS), mitogen-activated protein kinases (MAPK), c-Jun N-terminal kinases (JNK) and extracellular signal-regulated kinase 1/2 (ERK 1/2). The MAPK p38 pathway can also be stimulated from AGE-RAGE binding. The activation of these pathways can lead to the translocation of nuclear factor- kappa B (NF-κB) into the nucleus. There is increased transcription of genes such as vascular cell adhesion molecule-1 (VCAM-1), intercellular adhesion molecule-1 (ICAM-1), E-selectin, vascular endothelial growth factor (VEGF), tumour necrosis factor-α (TNF- α) and pro-inflammatory cytokine genes, interleukin-6 (IL-6) and interleukin-1β (IL-1β). Adapted from [33]

1.6 – AGEs and disease implications

It is well established that AGEs can have a major impact on protein structure and resulting function, which stems from the interaction of AGEs with cell surface receptors. This AGE-RAGE interaction has been linked to the progression of pathophysiological conditions associated with Diabetes, cardiovascular disease, neurodegeneration, and more recently cancer [71, 152, 153]. The majority of these investigations quantify the level of either or both AGEs and RAGE in tissues/serum/model systems relating to specific diseases of interest to determine the impact of AGE-induced effects within the body, including inflammation, ROS, dicarbonyl stress and OS [13].

1.6.1 – Diabetes Mellitus and its association with AGES

Diabetes mellitus (DM) is a general term for a group of disorders that are characterized by elevated levels of blood glucose along with reduced insulin sensitivity [154]. AGE mediated pathologies occurring during hyperglycaemic conditions can be attributed to the increased substrate (glucose) available to generate AGEs and also to the interaction of AGEs with RAGE, triggering a raft of signalling pathways (p38, MAPK's, JNK) [133]. In addition, the consequences of diabetes results in extracellular changes, as a result of AGE induced crosslinking of long-lived proteins such as extracellular matrix proteins and basement membrane proteins, resulting in damage to the kidney glomeruli [155, 156]. Diabetes predisposes patients to chronic health complications that affect the kidneys, eyes, blood vessels and nerves [127, 146]. It develops when insulin, a hormone that regulates blood glucose, is not produced in sufficient amounts, resulting in hyperglycaemia which is associated with type 2 diabetes mellitus (T2DM). T2DM is characterised by a combination of insulin resistance, hyperglycaemia and obesity [157].

People with the disease have a higher risk of morbidity and mortality compared to healthy individuals [154].

Table 1.3 - Levels of endogenous AGEs in human plasma samples determined using different analytical methods.

Marker	Level	Method	Reference
CML			
Control T1DM	92.5 ± 15.7 nmol/mmol Lys 104.6 ± 19.4 nmol/mmol Lys*	UPLC-MS/MS	[88]
Control (Free CML) Impaired GT (Free CML) T2DM (Free CML) Control (P-b CML) Impaired GT (P-b CML) T2DM (P-b CML)	78 (61-100) nmol/L^ 77 (58-96) nmol/L^ 80 (64-98) nmol/L^ 34 (30-41) nmol/mmol Lys^ 33 (28-37) nmol/mmol Lys^ 31 (26-37) nmol/mmol Lys^	UPLC-MS/MS	[158]
Control (Free CML) CVD (Free CML) Control (P-b CML) CVD (P-b CML)	77 (60-96) nmol/L^ 83 (66-101) nmol/L^ 34 (29-39) nmol/mmol Lys^ 33 (27-38) nmol/mmol Lys^	UPLC-MS/MS	[158]
Control Diabetic	10.1-32.6 ng/mL 13.0-44.4 ng/mL	LC-MS/MS	[75]
CEL			
Control T1DM	14.5± 3.2 nmol/mmol Lys 15.1 ± 3.7 nmol/mmol Lys	UPLC-MS/MS	[88]
Control (Free CEL) Impaired GT (Free CEL) T2DM (Free CEL) Control (P-b CEL) Impaired GT (P-b CEL) T2DM (P-b CEL)	44 (36-55) nmol/L^ 44 (36-56) nmol/L^ 49 (39-64) nmol/L^ 28 (23-35) nmol/mmol Lys^ 31 (23-38) nmol/mmol Lys^ 31 (22-39) nmol/mmol Lys^	UPLC-MS/MS	[158]

Control (Free CEL) CVD (Free CEL) Control (P-b CEL) CVD (P-b CEL)	45 (36-56) nmol/L^ 48 (39-62) nmol/L^* 28 (22-35) nmol/mmol Lys^ 32 (25-40) nmol/mmol Lys^*	UPLC-MS/MS	[158]
MG-H1			
Control (Free MG-H1) Impaired GT (Free MG-H1) T2DM (Free MG-H1)	127 (91-169) nmol/L^ 115 (84-173) nmol/L^ 121 (84-183) nmol/L^	UPLC-MS/MS	[158]
Control (Free MG-H1) CVD (Free MG-H1)	116 (84-165) nmol/L^ 141 (96-209) nmol/L ^*	UPLC-MS/MS	[158]

Values expressed as mean ± SD; values with ^ are expressed as median (interquartile range); * indicates that the AGE level was significantly higher than the respective control from each study. CML: *N*ε-carboxymethyllysine, CVD: cardiovascular disease, GT: glucose tolerance, LC-MS/MS: liquid chromatography tandem mass spectrometry, P-b: protein-bound, T1DM: Type 1 diabetes mellitus, T2DM: Type 2 diabetes mellitus, UPLC-MS/MS: ultra-performance liquid chromatography tandem mass spectrometry.

Although type 1 DM is an autoimmune disease it has been shown that a link between high sugar diets, AGE's, genetic and environmental factors exists [56]. Increased levels of AGEs in people with diabetes are mostly attributed to elevated precursor levels (glucose and dicarbonyls) and are thought to contribute to the pathogenesis of diabetic retinopathy [40, 78]. Non-enzymatic glycation of macromolecules, notably proteins, is elevated in people with diabetes as a result of hyperglycaemia and is known to worsen the complications associated with the disease [20, 40]. Non-enzymatic glycation occurs naturally under normal physiological conditions however, human serum albumin (HSA) is approximately 2-3 times more likely to be glycated in hyper glycaemic conditions [159]. This phenomenon results in people with diabetes having higher serum concentrations of CML [7]. Hyperglycaemia associated with diabetes promotes multiple damage pathways and increases the concentration of MGO, which is 2-4 times higher in the plasma of people with diabetes [5]. Fosmark *et al* (2006), investigated 89 patients

with non-proliferative diabetic retinopathy and 52 patients with proliferative diabetic retinopathy along with 86 healthy controls and found serum levels of MG-H1 were significantly increased (p<0.08 and 0.02 respectively) in both proliferative and non-proliferative patients compared to healthy controls [78].

1.6.2 – Cardiovascular disease and its association with AGEs

Cardiovascular diseases (CVDs) are the leading cause of death globally [160]. CVDs are a group of disorders of the heart and blood vessels including but not limited to, coronary heart disease, hypertension, stroke, thrombosis, and cerebrovascular disease. Risk factors include physical inactivity, unhealthy diet, diabetes, obesity and elevated levels of low-density lipoproteins (LDL) in the blood. Atherosclerosis is common in patients with CVD accompanied by endothelial cell dysfunction and has been more recently identified as an inflammatory disease [161]. In recent years the activation and expression of RAGE have been linked with the generation and development of cardiovascular disease, due in part to ROS generation and an increase in the secretion of pro-inflammatory cytokines [162].

An increase in plasma glucose levels in people with diabetes induces endothelial cell dysfunction ultimately leading to the development of vascular complications which can also lead to atherosclerosis [121]. Martinez *et al* (2019), demonstrated a 7-8% increase in glycated albumin in patients suffering cardio vascular failure as compared to healthy controls, however interestingly CML levels were not significantly different [159]. It has been reported that AGEs can have a direct effect on the myocardium, via cross-linking of extracellular cardiac proteins and the interaction with RAGE expressed on the myocardium [163, 164].

1.6.3 – Relationship between AGEs and neurodegenerative diseases

AGEs trigger the accumulation and aggregation of key neuronal proteins contributing to the pathological impact of neuro degenerative disorders (NDDs) [165]. It has been demonstrated that glycated proteins are present in the substantia nigra, cerebral cortex and amygdala of healthy persons and these levels are increased in patients with Parkinson's disease (PD) [166]. OS and ROS both generated by AGEs are known to be contributing factors to NDDs. Glycated proteins have been detected in Lewy bodies in the brains of patients with PD and in tau proteins in AD [165]. Sharma *et al* (2020) found plasma levels of CML to be significantly higher in both PD and AD patients as compared to healthy age-matched controls (males $p<0.0001$ and females $p<0.002$ respectively) [165]. Crosslinking has been observed on plaques in different areas of the brain in patients with AD and the polymerisation of β-amyloid is significantly increased by AGE induced crosslinking [167, 168]. Amyloid precursor protein is upregulated by AGEs both *in vitro* and *in vivo*, and treatment of a neuroblastoma cell line with a ROS inhibitor blocked the effects of AGEs [169].

1.6.4 – AGEs and their association with cancer

In general, cancer cells demonstrate increased metabolism and elevated glycation rates, thus enhancing the formation of AGEs. An increasing number of studies are investigating the relationship between AGEs and cancer. Shiraf *et al* (2015) showed that MGO-BSA derived AGEs increased proliferation, migration and invasion of the breast cancer cell line MDA-MB-231, suggesting that AGEs may contribute to the progression of invasive breast cancer [152]. A study in 2020 investigating the link between dietary AGEs and

cancer found a positive correlation between increased AGE-CML levels and breast cancer risk [153]. Increased levels of circulating sRAGE have been correlated with higher levels of RAGE binding and expression on the cell surface, and increased risk of colorectal cancer in patients with T2DM [170]. The link between cancer progression and involvement of AGEs/RAGE are still preliminary and more research is required to strengthen this association.

1.6.5 – AGEs and Cytotoxicity

The formation of AGEs and dicarbonyls affect numerous biological responses due to their pro-inflammatory and pro-oxidant nature, leading to the activation of various signaling pathways, mediated by cell surface receptors [162]. The accumulation of AGEs can lead to apoptosis. This apoptotic effect has been reproduced in various cultured tissues including retinal pericytes, corneal endothelial cells, neuronal cells and renal mesangial cells and is demonstrated by an increased expression of pro-inflammatory cytokines [171-173] . Hung *et al*, (2010) showed that treatment of T cells with AGEs resulted in apoptosis with the effects involving increased production of ROS along with the involvement of caspase and mitochondrial dependent pathways [174]. AGE induced cell death was confirmed as apoptotic rather than necrotic based on annexin V and propidium iodide (PI) staining [174].

Loske *et al* (1998) showed that the addition of BSA-AGE to BHK 21 and SH-SY5Y cells led to a dose-dependent cell death, measured using an MTT assay and confirmed by measuring lactate dehydrogenase release [175]. Loske *et al* (1998) also demonstrated that the cytotoxicity of glycated proteins increases linearly with the degree of AGE modification until it reaches a protein-specific maximum [175]. Sublethal concentrations

of AGEs can exert OS on the cell, leading to cell damage and ultimately cell death [175]. MGO can cause cytotoxicity through the induction of apoptosis, it can attenuate this through the production of ROS, induction of oxidative DNA damage and also via the accrual of MGO derived AGEs [176]. Ghosh *et al* (2011) recently demonstrated that MGO can also induce apoptosis by inhibiting both glycolysis and mitochondrial respiration [177]. Our group has previously shown a positive correlation between AGES and accelerated telomere attrition and inflammatory biomarkers [178]. More recently we have demonstrated an associated between AGEs and an increase in DNA damage markers [179]

1.6.6 – Reactive Oxygen Species (ROS) and oxidative stress (OS)

Reactive oxygen species (ROS) are highly reactive metabolites of molecular oxygen containing an unpaired electron, which can generate new free radicals [180]. The most abundant free radicals for example, hydrogen peroxide (H_2O_2), superoxide anion (O_2-), and reactive hydroxyl radical (.OH) originate from molecular oxygen [181]. During the glycation reaction superoxides and hydroxyl radicals are generated [162]. Within physiological conditions, ROS levels remain low due to anti-oxidative mechanisms, however under hyperglycaemic conditions, there is an increase in mitochondrial ROS production, which can lead to strand breaks in nuclear DNA [111]. These strand breaks activate poly(ADP-ribose) polymerase (PARP) which modifies GADPH, reducing its activity and activating the polyol pathway, thereby increasing intracellular AGE formation [49, 182]. The interaction of AGEs with RAGE upregulates NADPH oxidase expression which in turn generates more ROS, further promoting the activation of NF-κB leading to an increase in pro-inflammatory cytokine production [183].

OS results from the imbalance between the formation and removal of free radicals and is often associated with vascular tissue damage in diabetes, atherosclerosis, and ageing [181, 184, 185]. Generally, OS develops when excess free radicals are formed, while antioxidants and other free radical scavenging mechanisms (e.g. scavenging enzymes) fail to neutralise the free radicals [186]. OS can directly modify proteins via ROS and indirectly from the generation of MGO and GO formed from the auto-oxidation of carbohydrates, lipids and amino acids [120]. AGEs elicit OS in a variety of cells types and ultimately cause inflammatory reactions via the interaction with RAGE [187].

1.6.8 – Cytokines and AGEs

Cytokines are small, secreted soluble proteins, that have a specific action on interactions and communication between cells. More specifically they can be monokines (produced by monocytes), chemokines (cytokines with chemotactic properties), and interleukins (made by one leukocyte, which then act on other leukocytes) [188]. Cytokines can act in 4 main ways; by acting on the very cells that secrete them (autocrine), by acting on nearby cells (paracrine) by acting on distant cells (endocrine) and also by causing a cascade effect where one cytokine stimulates the production of another and then another and so on. They are broadly classified as either pro or anti-inflammatory in nature [163, 189, 190]. Hence the balance in cytokine production can alter the physiological state of a biological system

Some cytokines have very short half-lives, resulting from their secretion being dependent on new protein synthesis. Consequently their amplification in response to inflammatory stimuli is regulated by the transcription rates of cytokinetic genes, in particular NF-κB

[191] (Figure 1.11). AGE induced RAGE stimulation is known to increase both NF-κB transcription along with production on inflammatory cytokines [192]

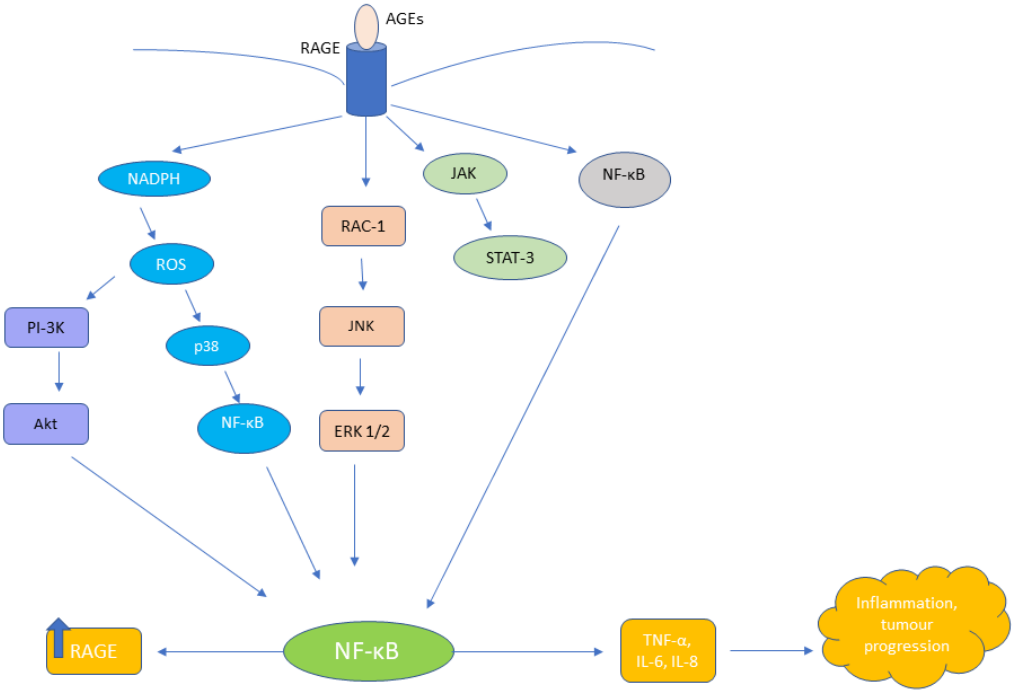


Figure 1.11 - Activation of nuclear factor (NF)- κB signalling pathway

The binding of AGEs with RAGE activates various signaling cascades including NF-κB and Janus kinase and promotes ROS production ultimately responsible for NF-κB activation in the nucleus, secretion of pro-inflammatory cytokines and upregulated RAGE expression. Adapted from [193] PI-3K - Phosphoinositide 3-kinase, Akt – Protein kinase b, NADPH – nicotinamide adenine dinucleotide phosphate, ROS -reactive oxygen species, P38 MAPK, (NF)- κB – nuclear factor kappa B, RAC-1 – Ras-related C3botulinum toxin substrate 1, JNK- c-Jun N-terminal kinase, ERK1/2 – extracellular signal related kinas 1/2, JAK- Janus kinase, STAT-3 -signal transducer and activator of transcription 3.

MGO has been shown to stimulate cytokine production the neutrophils of health patients [194] as well as increase IL-1β and TNF-α expression in endothelial cells [195]. Simm *et al* (1997) showed that tubular cells incubated with AGE modified albumin stimulated the expression of MAPK, activating protein-1 (AP-1) and transforming growth factor (TGF-β) [196]. MGO has been shown to induce apoptosis in Jurkat cells via activation of the c-Jun N-terminal kinase (JNK) pathway, leading to a reduction in mitochondrial membrane potential and caspase-3 activation [197, 198]. Wu *et al* (2002), demonstrated that vascular smooth muscle cells taken from rats with hypertension showed elevated levels of both MGO and AGEs paired with data showing MGO results in an increase in OS, activation of NF-κB and increased intracellular adhesion molecule 1 (ICAM-1) expression [199]. Fan *et al* 2003 found that RAW 264.7 cells treated with MGO-BSA demonstrated a significant increase in TNF-α secretion in a dose-dependent manner over 4-5 h [197]. AGEs have been shown to upregulate expression levels of IL-6 and ICAM-1 via MAPK and NF-κB pathways in human gingival fibroblasts [200]. Matsui *et al* 2016 [4] found that sulforaphane, a naturally occurring antioxidant found in broccoli, kale and cabbage, significantly reduced AGE induced expression of RAGE, ICAM-1, monocyte chemoattractant protein 1 (MCP-1) and vascular cell adhesion molecule 1 (VCAM-1) in HUVECs. It is clear from the literature that whilst AGEs can increase cytokine expression, there are compounds, both natural and synthetic that can offset the inflammatory impacts of AGE generation.

1.7 – Fatty Acids

Fatty acids (FAs) are the basic units of lipids which are stored in adipose tissue. FAs are vital in metabolism; where they serve as a metabolic fuel, a necessary component of the cell membrane they also regulate gene expression [201], they affect cell membrane stability, permeability and fluidity. The hydrophobic hydrocarbon chain is non-polar, while the hydrophilic carboxyl group is polar and readily forms ester links with alcohol groups [202].

1.7.1 – Nomenclature

FAs are a hydrocarbon chain comprising of a carboxyl group at one end which is highly reactive and a methyl group at the other end. The most abundant fatty acids in nature have straight chains and an even number of carbon atoms [203]. Where FAs contain the first double bond on the third, sixth or ninth carbon atom from the methyl end they are referred to as n-3, n-6 and n-9 series respectively.

1.7.2 – Chain length and saturation

Saturated FAs have no double bonds, and are mostly straight hydrocarbon chains containing an even number of carbon atoms [204]. The chain length of all FAs is variable from 2 to 30 carbons and may contain several double bonds dependent on type. Monounsaturated fatty acids (MUFAs) have a single double bond that can occur in different positions, the most common are between 16-22 carbon atoms in length and have a double bond with a *cis* configuration [204]. Two or more double bonds are required for

a fatty acid to be classified as a PUFA [203]. Both linoleic acid (18:2 n-6) and alpha linolenic acid (18:3 n-3) are essential as they cannot be made by mammalian cells. FAs can be classified as short (less than 6 carbons), medium (6-12 carbons), long (more than 12 carbons) and very long (more than 22 carbons) [205].

1.7.3 – Sources

Fatty acids are predominantly obtained from the diet but can also be generated via *de novo* lipogenesis (DNL). DNL primarily occurs in adipose tissue, where circulating carbohydrates are converted into FAs and then further converted into triglycerides and lipids [206]. Certain dietary sources are particularly enriched in certain classes of FAs. Animal meats are generally rich in saturated FAs. Unsaturated fatty acids such as oleic acid (18:1 n-9) is the main FA found in olive oil, whilst corn and sunflower oil are rich in linoleic acid (18:2 n-6), and linseed oil is rich in α-linoleic acid (18:3 n-3) [207]. Arachidonic acid (20:4 n-6) is integral to the cell membrane and for the function of all cells, particularly skeletal muscle, immune system and the nervous system [208]. It is obtained either from food or by desaturation and chain elongation of linoleic acid [209]. Fish oil is particularly rich in eicosapentaenoic acid (EPA) (20:5 n-3) and docosahexaenoic acid (DHA) (22:6 n-3) [210].

1.7.4 – Biological effects and inflammation

The role of n-3 and n-6 PUFAs has been of interest for many years. There are numerous studies describing the benefits of n-3 PUFA intake, particularly involving cardiovascular diseases, mental illnesses, auto-immune diseases and cancer [211-213]. The n-3 PUFAs have been shown to modulate the immune response and have a therapeutic effect on

inflammatory disorders [214]. In contrast high intake of 20:4 n-6 fatty acid has been documented to be pro-inflammatory [215].

Inflammation is the body's pre-programmed response to infection or injury. It is characterized by 5 main signs; redness, swelling, heat, pain and loss of function [140]. FAs have been investigated as potential anti-inflammatory agents via a raft of mechanisms including cell surface and intracellular receptors that control inflammatory cell signaling and also gene expression patterns [216].

The biological effects of FAs are dependent upon many structural characteristics, including chain length, series and degree of unsaturation. Saturated fatty acids tend to have little or no anti-inflammatory activity as compared to PUFAs. Arachidonic acid (20:4 n-6, AA) is the precursor for the formation of the eicosanoids, including prostaglandins, thromboxanes, and leukotrienes [217]. Eicosanoids are essential for platelet aggregation, chemotaxis and cellular growth and modulating the intensity and duration of the inflammatory response and in doing so act in a pro inflammatory way [204, 218]. Fatty acids 20:5 n-3 and 22:6 n-3 can also produce eicosanoids, but they have differing biological effects and, in some cases, can counter the activities of AA derived eicosanoids, for example give rise to newly discovered resolvins which either facilitate or resolve acute inflammation. Resolvins such as prostaglandins and leukotrienes function as pro inflammatory mediators during the onset phase of inflammation, while after injury or trauma, they increase vascular permeability and initiate infiltration of neutrophils [218, 219]. Calder (2006) demonstrated that long chain n-3 PUFA decreased the production of AA derived eicosanoids and also decreased the production of inflammatory cytokines (TNF-α, IL-1 and IL-6) and the expression levels of adhesion molecules (ICAM-1 and VCAM-1) that encompass the inflammatory interaction between leukocytes and endothelial cells [217].

Several studies support the beneficial effects of PUFA on PD and AD [220, 221],their ability to improve cognitive function and demonstrate an inverse association with the risk of developing AD. There are also documented benefits with CVD [222] and inflammation [202, 223]. There is epidemiological evidence that certain long-chain n-3 fatty acids are beneficial for many diseases/disorders including cardiovascular disease [224] by reducing blood pressure and levels of triglycerides along with the ability to influence blood vessel wall characteristics in atherosclerotic patients [225]. Several studies have investigated whether omega-3 fatty acid supplementation can exert beneficial effects in patients with diabetic nephropathy as well as affect the expression of inflammatory cytokines (TNF-α) with differing results [226-230]. However, the discrepancies could be explained by the different population studies, omega-3 fatty acids origins, dosage of used omega-3 fatty acids, and treatment duration [231].

1.7.5 – Fatty acids and AGEs

There are limited studies examining the role of FAs and glycation either *in vitro* or *in vivo*, in particular the role of PUFA on AGE induced cell toxicity and inflammation. There is some evidence that long-chain PUFA modulate RAGE expression in endothelial and smooth muscle cells [70], along with evidence of associations between lipid peroxidation and increased plasma levels of CML [232]. While lipids can also generate AGEs [39] it is unclear whether certain fatty acids have a protective role against AGE formation *in vitro* or *in vivo*. Lipid peroxidation of PUFA can yield carbonyl compounds such as GO and MGO along with MDA and 4-hydroxynonenal (HNE) [180, 233]

Prasanna et al. (2017) [234] determined the inhibitory effects of Oleic acid (18:1 n-9) on AGEs in a glucose-BSA model with a 3-week incubation quantifying fluorescent AGEs. Their docking studies demonstrated that Oleic acid (18:1 n-9) could bind to arginine residues of BSA stabilising the protein structure and preventing it from being glycated. Mirhashemi *et al* (2016) demonstrated that omega 3 supplementation from flaxseed oil significantly reduced serum AGEs in patients with diabetic nephropathy, as compared to healthy controls, whilst no effect was observed when comparing inflammatory cytokine levels [231].

There has been some studies which have investigated the effects of FAs on AGE production, but these are mainly in food models, which are different in comparison to *in vitro* studies, given the vast differences in conditions (temperature etc) with varied results in terms of suppressing AGE formation [24, 45, 231].

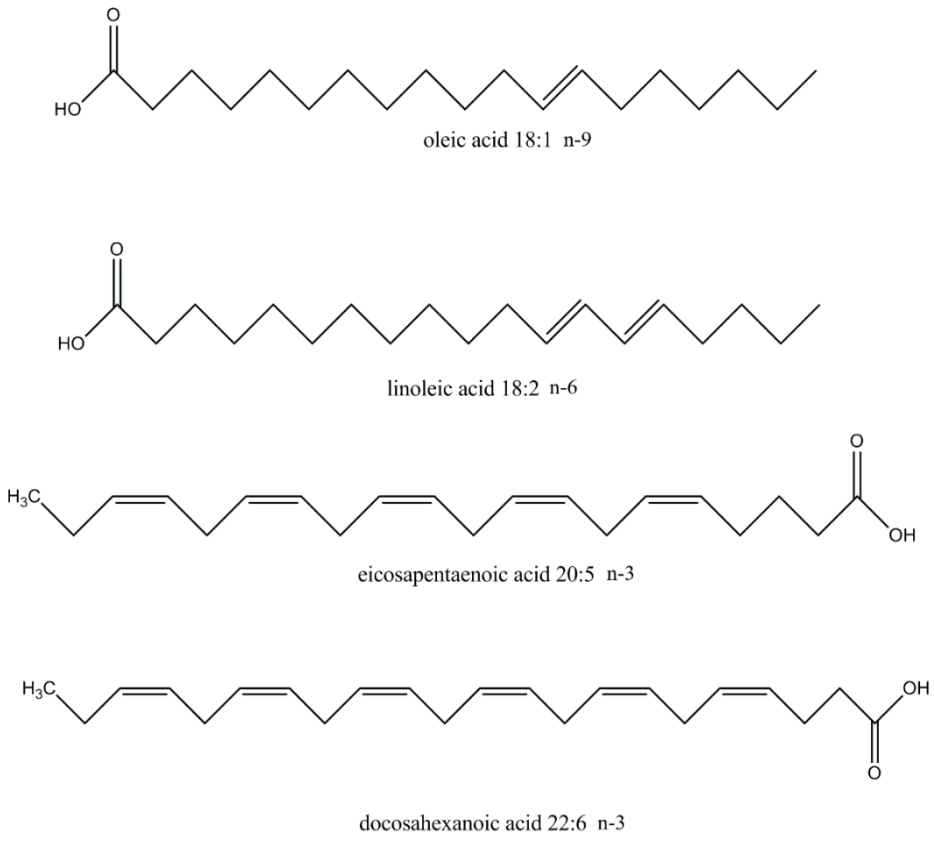


Figure 1.12 - Chemical structure of common fatty acids investigated.
Oleic acid 18:1 n-9; linoleic acid 18:2 n-6; eicosapentaenoic (EPA) 20:5 n-3; and docosahexaenoic acid (DHA) 22:6 n-3.

Table 1.4 - Examples of common saturated fatty acids, structure and formula

FA name	Chemical structure	C:DB
Butyric	$CH_3(CH_2)_2COOH$	4:0
Hexanoic	$CH_3(CH_2)_4COOH$	6:0
Octanoic	$CH_3(CH_2)_6COOH$	8:0
Decanoic	$CH_3(CH_2)_8COOH$	10:0
Lauric	$CH_3(CH_2)_{10}COOH$	12:0
Myristic	$CH_3(CH_2)_{12}COOH$	14:0
Palmitic	$CH_3(CH_2)_{14}COOH$	16:0
Stearic	$CH_3(CH_2)_{16}COOH$	18:0
Arachidic	$CH_3(CH_2)_{18}COOH$	20:0
Behenic	$CH_3(CH_2)_{20}COOH$	22:0
Lignoceric	$CH_3(CH_2)_{22}COOH$	24:0

Examples of common FAs, fatty acids; C, number of carbon atoms; DB, number of double bonds. Adapted from [203].

Table 1.5 – Examples of common unsaturated fatty acids, structure, and formula

FA Name	Chemical Structure	C:DB	series
Palmitoleic	$CH_3(CH_2)_5CH=CH(CH_2)_7COOH$	16:1	n-7
Oleic	$CH_3(CH_2)_7CH=CH(CH_2)_7COOH$	18:1	n-9
Linoleic	$CH_3(CH_2)_4CH=CHCH_2CH=CH(CH_2)_7COOH$	18:2	n-6
α – linolenic	$CH_3CH_2CH=CHCH_2CH=CHCH_2CH=CH(CH_2)_7COOH$	18:3	n-3
Arachidonic	$CH_3(CH_2)_4CH=CHCH_2CH=CHCH_2CH=CHCH_2CH=CH(CH_2)_3COOH$	20:4	n-6
Eicosapentaenoic	$CH_3CH_2CH=CHCH_2CH=CHCH_2CH=CHCH_2CH=CHCH_2CH=CH(CH_2)_3COOH$	20:5	n-3
Docosahexaenoic	$CH_3CH_2CH=CHCH_2CH=CHCH_2CH=CHCH_2CH=CHCH_2CH=CHCH_2CH=CH(CH_2)_2COOH$	22:6	n-3

Examples of common polyunsaturated fatty acids C, number of carbon atoms; DB, number of double bonds. n-x series, the location of the first double bond starting from the omega carbon atom Adapted from [140].

1.8 – Study aims and objectives

1.8.1 – Hypothesis

Fatty acids will demonstrate an ability to reduce both protein-bound fluorescent and non-fluorescent dicarbonyl derived AGE formation in vitro, thus reducing the pro-inflammatory effects of AGEs in endothelial cells by downregulating the RAGE expression and the subsequent expression of inflammatory biomarkers.

1.8.2 – Aims of this study

The overall aim of this project was to develop a physiologically relevant model system to consistently generate dicarbonyl induced AGEs quantifiable by using both fluorometric and liquid chromatography tandem mass spectrometry techniques (LCMS/MS). This would then enable the *in vitro* investigation into the role of fatty acids in AGE formation using an optimised dicarbonyl-BSA model on the receptor for advanced glycation endproducts (RAGE) expression and inflammatory biomarkers in endothelial cells.

1.8.2.1 – Objectives:

- To develop and optimize a BSA-dicarbonyl model system to generate and quantify AGE production.
- To determine the effect of saturated and unsaturated fatty acids on dicarbonyl induced AGE production *in vitro.*

- To investigate the dose and time-dependent effect of dicarbonyl-BSA derived AGEs on the receptor for AGEs (RAGE) expression and markers of inflammation in human umbilical vein endothelial cells (HUVEC).

- To determine the effect of polyunsaturated fatty acids on the AGE-induced expression of the receptor for AGEs (RAGE) and inflammatory biomarkers in human umbilical vein endothelial cells (HUVEC).

Chapter 2 - The Role of saturated and unsaturated fatty acids on dicarbonyl derived advanced glycation end products in vitro

This chapter has been published in *Amino Acids* (https://doi.org/10.1007/s00726-021-03069-6) however is presented in traditional chapter format for consistency of the thesis. Additional information relevant to this chapter is attached as supplementary information (Chapter 5, section 5.1)

2.1 – Introduction

Glycation is a non-enzymatic reaction that occurs between reducing sugars (e.g., glucose and fructose) and amino acids. Lysine and arginine are the most susceptible due to their positively charged amino and guanidino side groups. [1-3, 235]. The main pathway of formation, known as the Maillard reaction involves glucose reacting with a primary amine producing a Schiff base followed by a series of rearrangements and/or fragmentation reactions generating the reversible Amadori product, and ultimately forming a heterogeneous group of compounds, known as advanced glycation end-products (AGEs) [236]. In addition, other glycation pathways include glucose oxidation, lipid oxidation, glycolysis and the polyol pathway[1, 48]. All these pathways lead to the production of dicarbonyl compounds, methylglyoxal (MGO), glyoxal (GO) and 3-deoxyglucosone, with MGO being the most reactive [23, 40].

Dicarbonyls are formed via several pathways intrinsically linked with the glucose derived pathway of AGE formation. The major in vivo source of MGO is the spontaneous degradation of triosephosphates, dihydroxyacetone phosphate and glyceraldehyde 3-phosphate, intermediates of the glycolysis pathway [237]. In addition, MGO can also be derived from fatty acid peroxidation, the Maillard reaction and via the polyol pathway [67, 237]. Formation of GO occurs via metal catalysed fragmentation of glucose, glucose amine adducts such as fructose-lysine and peroxidation of PUFA [44, 238, 239].

Nε-carboxymethyllysine (CML) is the most extensively investigated AGE. It is formed via metal-catalysed oxidative cleavage of Amadori compounds, peroxidation of PUFA,

and GO [56, 67, 68]. MGO reacts with lysine residues to form Nε-carboxyethyllysine (CEL), a homologue of CML [57]. In addition, MGO also reacts with the guanidine group of arginine residues forming hydroimidazolones, primarily MGO-derived hydroimidazolone (MG-H1) [60]. MG-H1 is one of the most abundant and functionally important AGEs in physiological systems and accounts for >90% of glycation adducts, although it has a relatively long half-life (12 days) compared to the majority of cellular proteins (46 h) [97]. Pentosidine, the main fluorescent AGE, is formed via dehydration of a pentose derived Amadori product forming an intermediate that reacts with arginine residues of proteins and often produces protein crosslinks [240].

There are several mechanisms reported for AGE inhibition including, inhibiting sugar attachment to proteins, scavenging reactive carbonyls and free radicals, and also inhibiting Amadori product formation [241]. Aminoguanidine is a known inhibitor of glycation and lipoxidation. It contains hydrazine nitrogen atoms which trap reactive carbonyl compounds in the initial stages of the Maillard reaction, especially Amadori intermediates [233] and prevent their irreversible conversion into AGEs. Pyridoxamine, which is a natural form of vitamin B6 is another known inhibitor of AGEs. In contrast to aminoguanidine, pyridoxamine works in the advanced stages of glycation by forming stable complexes with metal ions which catalyse oxidative reactions [242]. In addition, our and previous studies on natural bioactives have been reported to inhibit AGE formation that correlated with the antioxidant properties [243-246]. One advantage of the use of natural products is their minimal toxicity and relative safety for human consumption [243-245, 247].

There are limited studies investigating the effects of fatty acids and glycation both in vitro and in vivo and the resultant AGE production. Whether certain fatty acids have a

protective role against AGE formation in vitro or in vivo is not documented. Epidemiological evidence suggests that certain long-chain omega-3 fatty acids (EPA 20:5 n-3, DHA 22:6 n-3), are anti-inflammatory in many diseases, including cardiovascular disease [224], reducing blood pressure and levels of triglycerides [225]. It has been established that omega-3 and omega-6 fatty acid supplementation can exert beneficial effects in patients with diabetic nephropathy as well as down-regulate the expression of pro-inflammatory cytokines (IL-6, IL-1β, TNF-α) [218, 226]. Both EPA and DHA have been linked with improved foetal development and cardiovascular function as well as increased brain function in people suffering from mild AD [248].

Indeed fatty acids are vital elements in all cell types as they affect cell membrane stability, permeability and fluidity and are vital in metabolism; where they serve as a metabolic fuel, a necessary component of the cell membrane and also as a gene regulator [201]. The double bonds of fatty acids are a point of attack for free radicals, in a process known as lipid peroxidation where the fatty acid can become a lipid radical with an allylic double bond, which is structurally weak. These lipid radicals combine with oxygen-generating lipid peroxyl radicals, ultimately forming lipid peroxides and ALEs [249]. The cell does have a natural antioxidant defence system, a group of enzymes known as superoxide dismutase (SOD) that allow the cell to cope in high OS environments. However, exposure of the SODs to glucose can lead to their deactivation accompanied by exposure to MGO [250] thus increasing the concentration on damaging radicals within the cell.

To the best of our knowledge, a model system investigating the role of fatty acids on AGE production has not yet been fully explored; therefore, the aim of this study was two-fold. Firstly, to develop a reliable dicarbonyl-BSA model to quantify AGE production, and

secondly, to determine the role of a range of fatty acids on dicarbonyl induced AGE production

2.2 – Materials and Methods.

2.2.1 – Materials

Sodium phosphate dibasic, sodium phosphate monobasic, aminoguanidine, methylglyoxal (MGO), glyoxal (GO), bovine serum albumin (BSA), trichloroacetic acid (TCA), acetonitrile, methanol, ethanol, trifluoroacetic acid (TFA) and formic acid were purchased from Sigma Aldrich, (Sydney, Australia). D_2-CML and D_4-CEL, D_3-MG-H1 and D_4-lysine were purchased from Iris Biotech (Marktredwitz, Germany). Butyric (C4:0), myristic (C14:0), palmitic (C16:0), arachidic (C20:0), oleic (C18:1n-9), linoleic (C18:2n-6), α-linoleic (C18:3n-3), arachidonic (C20:4n-6), eicosapentaenoic (C20:5n-3) and docosahexaenoic acid (C22:6n-3) were purchased from Sapphire Bioscience, (Sydney, Australia).

2.2.2 – Time and concentration-dependent AGE formation

An *in vitro* glycation model was established using MGO and GO to produce protein-bound fluorescent and non-fluorescent AGEs. Both time and concentration-dependent trials were assessed to establish an optimal incubation model. For time-dependent experiments, BSA (10 mg/mL) was dissolved in sodium phosphate buffer (0.2 M, pH 7.4) and either MGO or GO (each at 1 mM) was added into sterile reaction tubes (Sarstedt, Adelaide, Australia). The final volume was adjusted to 4 mL using sodium phosphate buffer (0.2 M, pH 7.4). The reaction tubes were incubated at 37±1^{o}C for 0-288 h in a Ratek shaking incubator (Ratek, Victoria, Australia) at 200 rpm in the dark.

For concentration-dependent experiments, BSA (10 mg/mL final) was dissolved in sodium phosphate buffer (0.2 M, pH 7.4) and added to sterile reaction tubes (Sarstedt, Adelaide, Australia). To each reaction tube, was added either MGO (0.5-2 mM) or GO (0.5-2 mM) and the final volume adjusted to 4 mL using sodium phosphate buffer (0.2 M, pH 7.4). The reaction tubes were incubated at 37±1^{o}C for a period of 72 h in a Ratek shaking incubator (Ratek, , Victoria, Australia) at 200 rpm. Aminoguanidine (30 mM) was used as a positive control, and no treatment was used as the negative control. Each assay was performed in triplicate, and each experiment was repeated at least three times independently.

2.2.3 – Saturated and unsaturated fatty acid treatment

The model system for fatty acid incubation was selected from previously optimised time and concentration-dependent experiments. Briefly, 2 mL of BSA (10 mg/mL), dissolved in sodium phosphate buffer (0.2 M, pH 7.4) was added to sterile reaction tubes (Sarstedt, Adelaide, Australia) and incubated with 400 µL of fatty acid dissolved in ethanol (saturated and unsaturated, 20 µM,) and 1.6 mL of either MGO and GO (1 mM) in a total volume of 4 mL. The samples were incubated at 37 °C for 72 hrs in a Ratek shaking incubator oven at 200 rpm (Ratek, Victoria, Australia). Both positive (aminoguanidine) and negative controls were included in each assay.

2.2.4 – Determination of protein-bound fluorescent AGEs

Following incubation, total protein was isolated as previously described [251-253]. Briefly, 300 µL of cold (4°C) TCA (20% w/v) was added to 250 µL of glycated samples, mixed and incubated on ice for 10 min before centrifugation (8000 x g for 10 min at room

temperature (RT)) using a 5415-R centrifuge (Eppendorf, Hamburg, Germany). The supernatant was discarded, and the pellet dissolved in 1 mL of phosphate buffer (0.2 M, pH 10) and 250 µL aliquoted in triplicate into a black, flat-bottom 96-well plate (ThermoFisher Scientific, Adelaide, Australia). Fluorescence intensity was measured at 370 nm (excitation) and 440 nm (emission) using an Enspire multimode plate reader (Perkin Elmer, Waltham, MA,). Results are expressed as relative fluorescent units (RFU)/mg BSA.

2.2.5 – Preparation of samples for LC-MS/MS

Protein-bound AGEs generated during *in vitro* treatment with MGO, GO, and fatty acids (butyric 4:0, myristic 14:0, palmitic 16:0, arachidic 20:0, oleic 18:1 n-9, linoleic 18:2 n-6, α-linoleic 18:3 n-3, arachidonic 20:4 n-6 (AA), eicosapentaenoic 20:5 n-3 (EPA) and docosahexaenoic acid 22:6 n-3 (DHA)) were analysed to determine the level of CML, CEL, and MG-H1 as previously described [98, 252]. Briefly, 100 µL aliquots were placed into 2 mL Mikio-Schraubröhre microtubes (Sarstedt, Australia). To each sample, 100 µL of borate buffer (0.5 M, pH 9.2) and 20 µL of $NaBH_4$ (1 M in 0.1 M NaOH) were added, mixed and incubated at RT in the dark for 4 hrs. Following incubation, 300 µL of TCA (20% w/v) was added to each tube, mixed, and placed on ice for 10 min. The samples were then centrifuged for 10 min (RT) at 8000 x g and the supernatant discarded. The pellet was dissolved in 1 mL of hydrochloric acid (6 M), and the samples were then incubated at 100°C for 24 h. After incubation, the samples were dried under a stream of nitrogen gas by a dry block heater and nitrogen dryer in preparation for solid-phase extraction.

2.2.6 – Solid Phase Extraction (SPE)

Sep-Pak (RP C_{18} Columns) (Supelco, St Louis, MO, USA) cartridges were used for the purification of samples. Dried samples were reconstituted in 980 µL of Trifluoroacetic acid (TFA) (1% v/v) in H_2O and 5 µL of each heavy labelled (HL) standard (CML, CEL, MG-H1 and Lysine) added at 5 µM final. The Sep-Pak column was conditioned with 3 mL of methanol (100% v/v) followed by equilibration with 3 mL of TFA (1% v/v). The prepared samples were then added to the column, and the eluate discarded. A total of 3 mL of TFA (1% v/v) in methanol (20% v/v) was added to each column, and the eluate was collected and dried under a stream of nitrogen at 40℃ (Ratek) and stored at -20 ℃ until use.

2.2.7 – Liquid chromatography-mass spectrometry

Dried samples were reconstituted in 1 mL of methanol (20% v/v) and then further diluted 1:5 in methanol (20% v/v) for analysis. Aliquots (200 µL) were placed in 2 mL screw-top glass flat bottom inserts (31 x 6mm; ThermoFisher, Adelaide, Australia). Analysis of CML, CEL and MG-H1 in each sample was performed using a Sciex ExionLC coupled to a Sciex 6500 + QTrap (Toronto, Canada), fitted with a TurboSpray IonDrive source (SCIEX, Concord, Ontario, Canada). A Phenomenex Synergi TM 4 mM Hydro-RP 80 Å LC column (150 x 4.6 mm) (Phenomenex, Torrance, CA,) was used with a flow rate of 0.4 mL/min and an injection volume of 1 µL. The run time was 6 min, and the column oven was set to 40°C. The mobile phases used were: 95% ultrapure water (5% acetonitrile; 0.1% formic acid; solvent A) and 95% acetonitrile (5% ultrapure water; 0.1% formic acid; solvent B). A needle wash of acetonitrile: ultrapure water (50:50, 0.1% formic acid) was used to eliminate carryover. The ion source parameters were as

follows: 450°C; curtain gas, 20; collision gas, medium; ion spray voltage, 5500 V; ion source gas 1 and ion source gas 2, 40. Mass spectrometric analyses were performed in positive mode using multiple reaction monitoring (MRM) as described previously [98]. All data were acquired with Analyst 1.7 (SCIEX) and processed using MultiQuant 3.0.2. A standard calibration curve was prepared, and a plot of analyte peak area divided by internal standard peak area (area ratio) against concentration (amount ratio) was generated. This was used to calculate CEL, CML and MG-H1 content in each sample and was expressed as nmol CML, CEL or MG-H1/mg BSA. Quality controls (5, 15 and 30μM) were used to ensure consistency of the instrument.

Table 2.1 - Multiple reaction monitoring (MRM) conditions of LC-MS/MS analysis

Q1 Mass (Da)	Q3 Mass (Da)	Dwell Time (msec)	ID	DP (volts)	EP (volts)	CE (volts)	CXP (volts)
207.1	129.9	50	HL-CML.D2.IS	50	10	16	15
205.1	129.9	50	CML.1	50	10	14	15
205.1	84.0	50	CML.2	50	10	15	15
151.2	87.9	50	HL-Lys.D4.IS	50	10	14	15
147.1	83.9	50	Lysine.1	80	10	17	20
147.1	129.9	50	Lysine.2	80	10	15	20
206.1	130.9	50	CML.3.C13	50	10	14	15
148.1	84.90	50	CML.3.C13	50	10	17	20
219.2	130.0	50	CEL.1	80	10	18	20
219.2	84.1	50	CEL.2	80	10	18	20
222.9	134.2	50	CEL.D4.IS	75	10	19	17
229.2	116.1	50	MGH1.1	40	10	21	17
229.2	166.2	50	MGH1.2	40	10	21	17
232.2	116.1	50	MGH1.D3.IS.1	40	10	21	17

2.2.8 - Statistical Analysis

Data analysis was performed using the statistical software GraphPad Prism (San Diego, CA, Version 7.03). One-way analysis of variance (ANOVA) was used to determine significance in time and concentration-dependent models, followed by Tukey's test. An unpaired *t*-test was used to determine the significance of species-specific AGEs generated in a concentration-dependent model. A p value < 0.05 was considered significant, and results are expressed as mean ± standard deviation (SD) of a minimum of 3 independent experiments performed in triplicate.

2.3 – Results

2.3.1 – Kinetics of protein-bound fluorescent AGE formation

The first aim of this study was to establish an *in vitro* model to analyse the kinetics of AGE formation. For the time-dependent incubation, BSA-MGO showed a gradual and continuous increase in the production of protein-bound fluorescent AGEs up to 288 h while the BSA-GO model demonstrated a linear increase up to 150 h, plateauing to 288 h (Figure 2.1). With both models, protein-bound AGE formation increased over 150 h and then plateaued up to 288 h (Figure 2.1). When comparing the models, BSA-MGO showed significantly higher ($p<0.05$) protein-bound fluorescent AGE levels compared to the BSA-GO models after just 24 hrs (Figure 2.1). As there was no significant increase from 72 h to 150 h, the 72 h time point was chosen for all further work.

For the concentration-dependent experiments, the 72 h BSA-MGO model showed increased protein-bound AGE levels with increasing concentration of MGO (Figure 2.2) with a significant difference above the negative control from 1-2 mM. The BSA-GO

model showed an increasing trend in protein-bound AGE formation, with a significant difference observed between 1-1.5 mM as compared to the negative control; however, it plateaued from 1.5-2 mM. When comparing the two models, BSA-MGO showed higher levels of protein-bound AGE formation when compared with the BSA-GO model. The BSA-MGO model system showed a significant higher protein-bound AGE level at all concentrations when compared with the BSA-GO model.

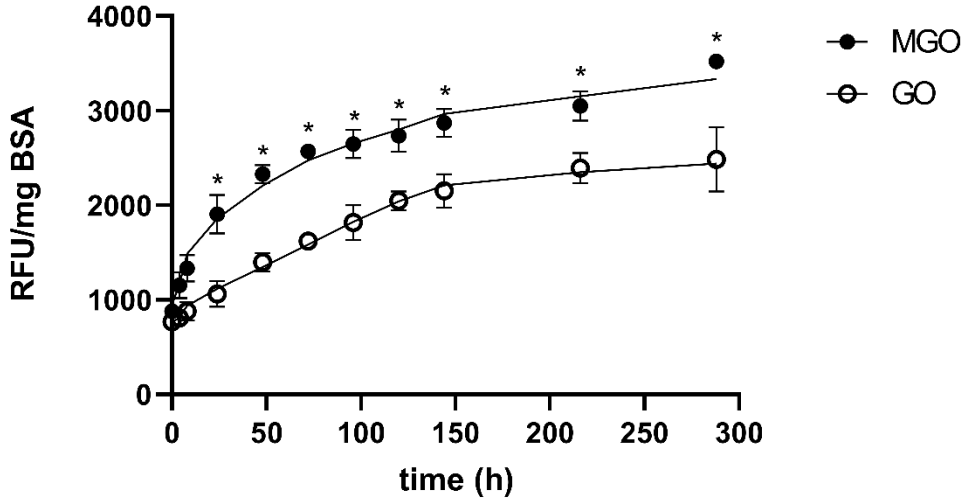


Figure 2.1 - Kinetics of time dependent protein bound fluorescent AGEs quantification

Relative quantification of protein-bound fluorescent AGEs generated in the BSA-MGO (●) and BSA-GO (○) model were quantified in a time-dependent study (0-300 h). Results are normalised with BSA only and expressed as mean ± SD n=3; *represents shows the significant difference (at least $p<0.05$) for the respective time between the two models.

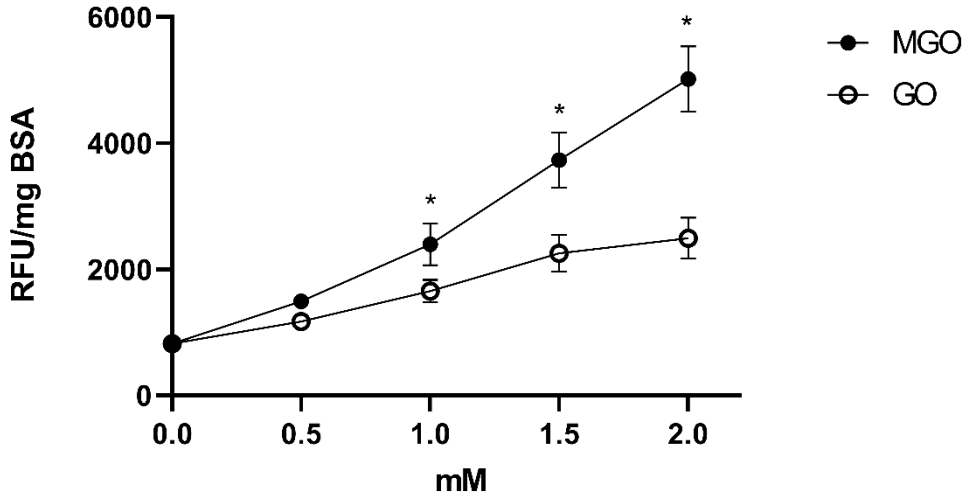


Figure 2.2 - Kinetics of concentration dependent protein bound fluorescent AGEs quantification

Relative quantification of protein-bound fluorescent AGEs generated in the BSA-MGO (●) and BSA-GO (○) model quantified in a concentration-dependent study (0 -2 mM). Results are shown normalized with BSA only and expressed as mean ± SD n=3; * represents shows the significant difference between the two models (of at least $p<0.05$) at the respective concentration.

2.3.2 – Kinetics of CML, CEL and MG-H1 levels.

Non-fluorescent protein-bound AGE quantification was performed using LC-MS/MS to determine if there was any correlation between fluorescent and non-fluorescent AGE production within our model. CML, CEL and MG-H1 were all produced rapidly within the first 24 h with little change in the levels quantified at subsequent time points. CML was detected in the BSA-GO model system, ranging from 3-5 nmol CML/mg BSA (Figure 2.3 A). CEL levels quantified in the BSA-MGO model system were very low and ranged from 0.4-0.5 nmol CEL/mg BSA (Figure 2.3 B). MG-H1 levels quantified in the BSA-MGO model ranged from 50-60 nmol MG-H1/mg BSA (Figure 2.3C).

The effect of dicarbonyl concentration on the generation of species-specific AGEs in different models is shown in Figure 2.4. CML and CEL levels were significantly higher

at 2 mM GO compared to 1 mM GO (Figure 2.4 A, B). However, MG-H1 levels did not show a significant difference between 1 mM and 2 mM MGO (Figure 2.4 C).

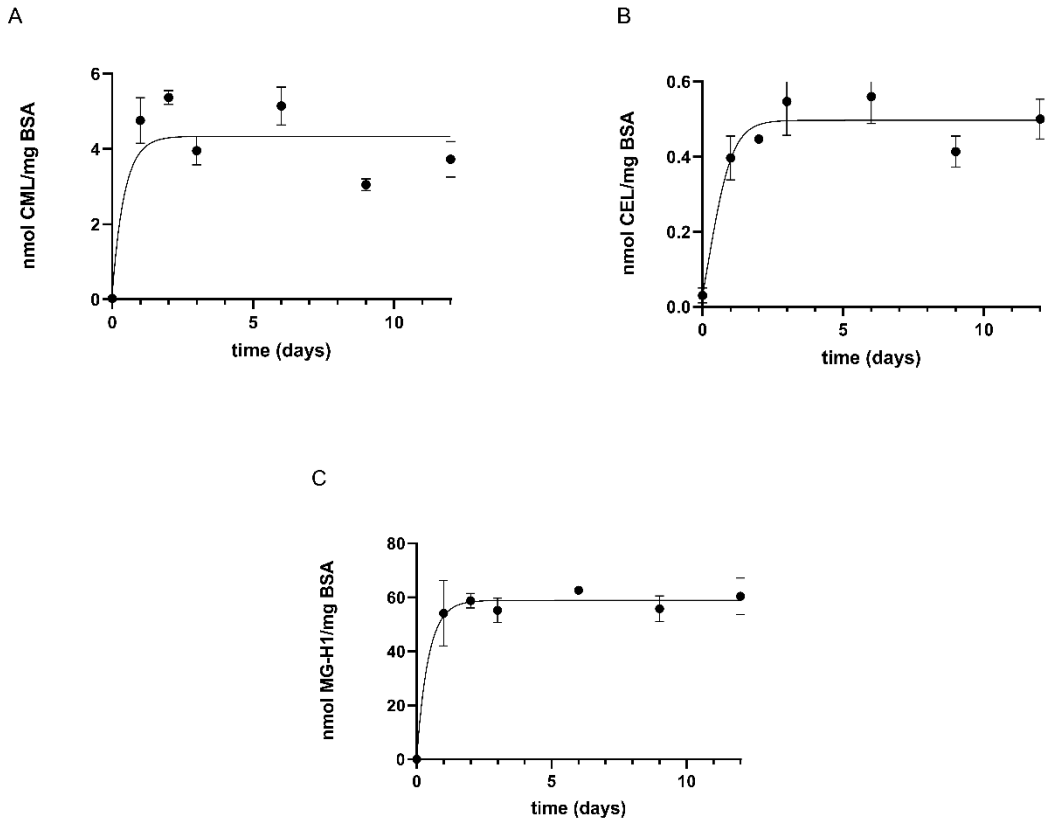


Figure 2.3 - Species specific AGE generation – time dependent study

Species-specific AGE generation in a time-course study. **A.** CML in BSA-GO model; **B.** CEL in BSA-MGO model; **C.** MG-H1 in BSA-MGO model, which is expressed as nmol of analyte/mg of BSA. Results are shown normalised to BSA alone and expressed as mean ± SD n=3.

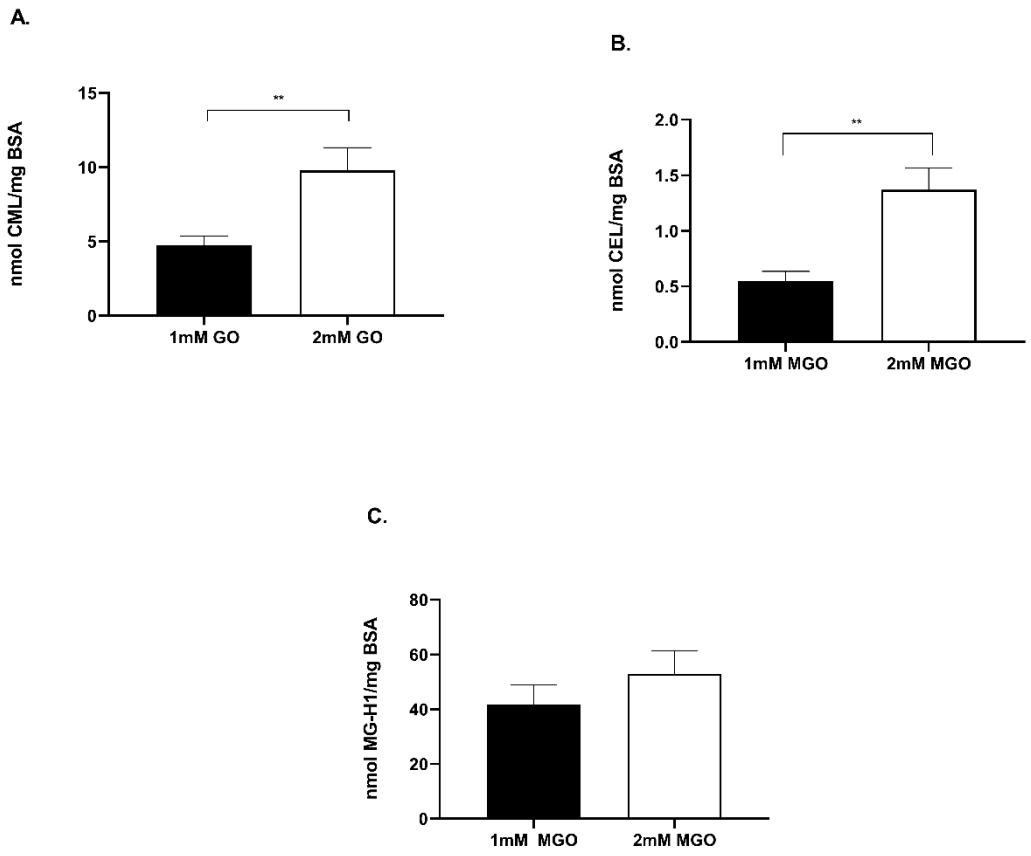


Figure 2.4 - Species-specific AGEs generated in a concentration-dependent study

Species-specific AGEs generated in a concentration-dependent model quantified by tandem LC-MS/MS. 1mM MGO and GO represent normal physiological levels, while 2mM is representative of a diabetic state. Both CML (**A.**) and CEL (**B.**) show a significant difference (**, $p < 0.007$) between normal and diseased states, while MG-H1 (**C.**) shows no significant difference. CML, CEL and MG-H1 expressed as nmol of analyte/mg of BSA, results expressed as mean ± SD n=3,

2.3.3 – The effect of fatty acids on AGE formation.

We next examined a range of fatty acids in our study. BSA-MGO and BSA-GO model systems which included saturated fatty acids ranging from 4:0 to 20:0 showed no effect in the formation of protein-bound fluorescent AGEs when compared to respective

controls (Figure 2.5 A and 2.5 B). When the unsaturated fatty acids 18:1 n-9, 18:2 n-6 and 18:3 n-3 were examined, they too did not show any effect in the formation of protein-

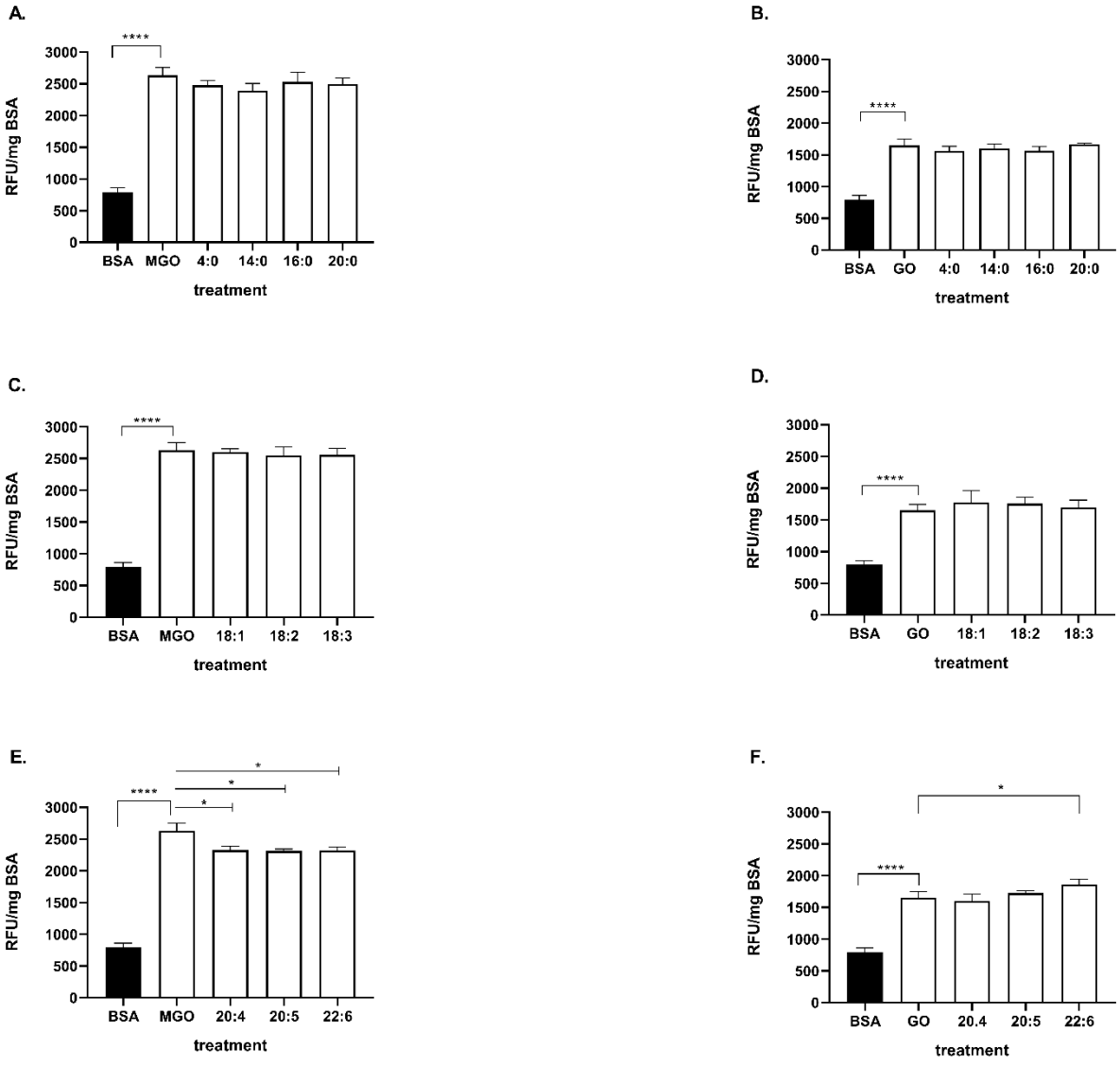


Figure 2.5 - The role of fatty acids on dicarbonyl induced protein-bound fluorescent AGE production.

Protein-bound fluorescent AGEs generated in a BSA + dicarbonyl model system incubated with both short-chain saturated fatty acids and long-chain PUFA. MGO (**A**) and GO (**B**) model systems incubated with 4:0, 14:0, 16:0 and 20:0. MGO (**C**) and GO (**D**) models incubated with 18:1 n-9, 18:2 n-6) and 18:3 n-3). MGO (**E**) and GO (**F**) models incubated with 20:4 n-6, 20:5 n-3 and 22:6 n-3. Results expressed as mean ± SD n=3. * $p<0.05$, **** $p<0.001$.

bound fluorescent AGEs in either the MGO-BSA or GO-BSA model (Fig. 2.5 C and 2.5 D). Interestingly, for the long-chain highly unsaturated fatty acids, a small but significant reduction ($p<0.05$) in the formation of protein-bound fluorescent AGEs was observed with 20:4 (n-6), 20:5 (n-3) and 22:6 (n-3) when compared to BSA-MGO alone (Figure 2.5 E). In contrast, C22:6 showed a significant increase ($p<0.05$) in protein-bound AGE formation when compared with the BSA-GO only model (Figure 2.5 F).

The effect of selected saturated and unsaturated fatty acids on the formation of species-specific AGEs are shown in Figure 2.6. For the saturated fatty acid treatments, a significant reduction in CEL levels was observed with 4:0 ($p<0.001$), 14:0 ($p<0.01$), 16:0 ($p<0.01$) and 20:0 ($p<0.01$) compared to the BSA-MGO only model (Figure 2.6 A). CML levels were also significantly reduced by 4:0, 14:0, 16:0 and 20:0 treatment compared to the BSA-GO only model (Figure 2.6 B). Interestingly, a significant increase was observed in the MG-H1 levels in BSA-MGO when treated with 14:0, 16:0 and 20:0 compared to the negative control (Figure 2.6 C)

For the unsaturated fatty acids, only 18:1(n-9) significantly reduced CEL levels when compared with BSA-MGO only (Figure 2.6 D). A significant reduction of CML level was observed with 18:1 (n-9), 18:2 (n-6) and 18:3 (n-3) treatment when compared with BSA-GO only treatment (Figure 2.6 E). Similar to saturated fatty acids treatment, a significant increase in MG-H1 level was observed with 18:1 (n-9), 18:2 (n-6) and 18:3 (n-3) compared to BSA-MGO only treatment (Figure 2.6 F).

For the highly unsaturated fatty acids, 20:4 (n-6), 20:5 (n-3) and 22:6 (n-3), no effect in either CEL or MG-H1 levels when compared to the control (Figure 2.6 G and 2.6 I) was

observed. However, a significant reduction in the CML was observed compared to BSA-GO only (Figure 2.6 H).

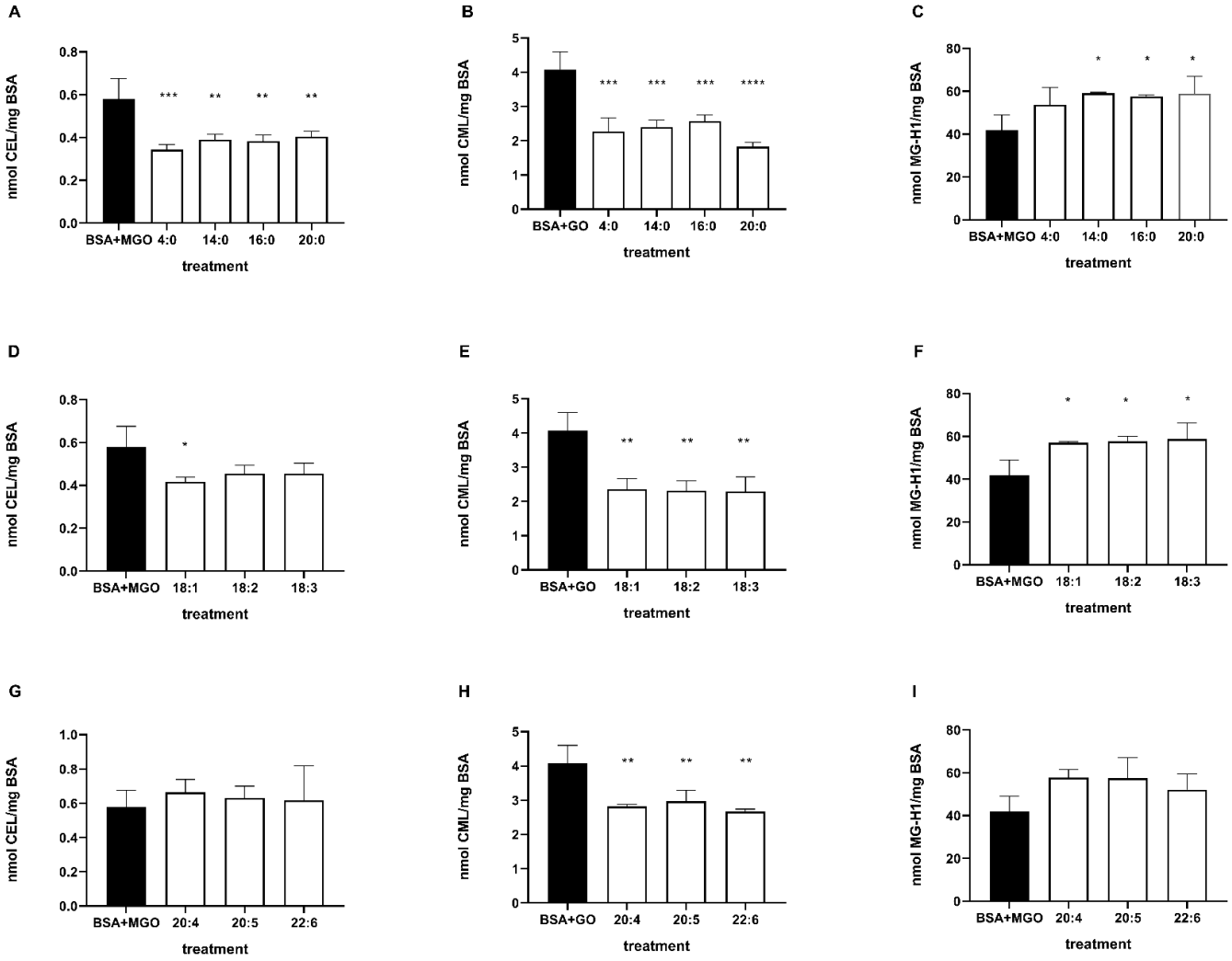


Figure 2.6 - The role of dicarbonyls on CML, CEL and MG-H1 production

Species-specific AGE generation in both MGO and GO models. AGEs were generated as previously described and were quantified using tandem LC-MS/MS. CML, CEL and MG-H1 expressed as nmol of analyte/mg of BSA. (**A.**) CML (**B.**) CEL and (**C.**) MG-H1 quantified in MGO/GO model with 4:0, 14:0, 16:0 and 20:0. (**D.**) CML (**E.**) CEL and (**F.**) MG-H1 quantified in MGO/GO model with 18:1 n-9, 18:2 n-6 and 18:3 n-3). (**G**) CML (**H.**) CEL and (**I.**) MG-H1 quantified in MGO/GO models with 20:4 n-6), 20:5 n-3) and 22:6 n-3. Results expressed as mean ± SD n=3. * $p<0.05$, ** $p<0.005$, *** $P<0.0005$, **** $p<0.0001$.

2.4 – Discussion

Research investigating AGEs and their role in the pathology of diseases such as diabetes and associated complications using *in vitro* and *in vivo* model systems are widely reported [165, 193, 254]. CML, the most widely studied AGE, has long been considered the main AGE produced and involved in the progression and development of disease due to its abundance. Recent studies suggest MG-H1 is a prevalent AGE due to its cellular abundance and elevated serum levels being associated with cardiovascular disease and diabetes [61, 62]. Furthermore, MG-H1 has now been shown to post-translationally affect histones by decreasing acetylation and ubiquitylation, affecting chromatin dynamics, DNA accessibility and transcription [255].

This study presents a BSA-dicarbonyl model system optimised in time and concentration with the determination of the kinetics of protein-bound fluorescent and non-fluorescent AGEs. A 72-hour time point was the optimal time for all work based on fluorometric and LC-MS/MS analysis that demonstrated a significant increase from basal levels of AGEs. The difference in MGO and GO producing protein-bound fluorescent AGEs was significant after 24 h, with the level of the product reaching a plateau after 150 h. Interestingly when compared to non-fluorescent AGE production over the same time period, there was a more rapid production of CML/CEL/MG-H1 within the first 24 h, with all 3 analytes showing little change subsequently. This is likely a result of the highly reactive dicarbonyl compounds (MG and GO) rapidly reacting with BSA generating non-fluorescent AGEs with the dicarbonyl availability becoming exhausted within the first 24 h. MG-H1 levels detected over time were 10-fold higher than CML, representative of its far greater abundance within the model.

Our model demonstrated that concentrations of dicarbonyl (1 and 2 mM) produced relatively low amounts of CML, and CEL over a 72-hour incubation; however, there was a significant difference between the two concentrations. MG-H1, whilst having a significant (10-fold) higher amount of detection over CML, showed no significant difference between 1 and 2 mM. While the concentrations of dicarbonyl are well above cellular levels (typically 1-5 µM) [256], these levels are suitable for *in vitro* modelling in a short incubation period to mimic processes occurring physiologically over weeks to months [113, 257]. Both fluorescent and nonfluorescent AGEs have long been associated with the disease however the extent of implications with species-specific AGEs are not well established. Fluorescent AGEs, including pentosidine, are associated with vascular complications in people with diabetes [258, 259]. Non-fluorescent AGEs however including, CML, CEL and MG-H1 have been associated with people with diabetes, AD, DNA damage and lung cancer [98, 260-262]. Since certain fatty acids have been shown to have protective activities in inflammatory states [203, 216], we investigated whether they could affect AGE formation in our model system. Fatty acids exist in various conformations, varying in chain lengths, series and saturation, which in some cases relate to their biological activity [263, 264]. A wide selection of both saturated and polyunsaturated fatty acids was chosen to investigate the effect of fatty acids on protein-bound fluorescent and non-fluorescent AGE formation. Butyric acid (4:0) is a short-chain fatty acid prevalent in the gut and important for gastrointestinal health [45] . α-Linoleic (18:3), is an essential omega-3 fatty acid that must be sourced from the diet [70]. Highly unsaturated omega 3 fatty acids, 20:5 n-3 and 20:6 n-3, are synthesised in the body from 18:3 n-3 but only in small amounts [248]. Fatty acids, in particular, 20:5 n-3 and 22:6 n-3 have been shown to have a protective role when used *in vitro* and *in vivo* for reducing inflammation and associated cytotoxicity [224, 225, 265]. In addition, the oxidation of lipids is also able to react with proteins to produce

advanced lipoxidation end-products (ALEs). The interaction between AGEs and fatty acids is limited, with knowledge surrounding the abundance of ALEs as compared to AGEs almost non-existent. We hypothesised that there may be a structure/function relationship, the longer the chain length and the higher the degree of unsaturation, the greater the biological activities [266-269].

Saturated fatty acids (SFA) (4:0, 14:0, 16:0, 20:0) when incubated with either MGO or GO, caused no significant difference in protein-bound fluorescent AGE production compared to dicarbonyl-BSA alone. For non-fluorescent AGE formation, these saturated fatty acids (4:0, 14:0, 16:0, 20:0) significantly reduced CML and CEL levels whereas MG-H1 levels were increased. No previous studies have reported on the role of individual SFA on dicarbonyl-BSA induced AGE formation. However, participants on a 22% SFA western diet showed increased levels of serum CML levels compared to the participants on a 10% SFA diet in a 4-week cross-over study [270]. Recently we showed that diets high in red and processed meat consumed for 4 weeks significantly increased plasma CEL and MG-H1 levels however CML level was unaltered in subjects without type 2 diabetes [253].

The 18-carbon unsaturated fatty acids (18:1 n-9,18:2n-6, 18:3 n-3) showed no significant difference in the protein-bound fluorescent AGEs whereas it varied in the non-fluorescent AGEs. These selected, 18 carbon unsaturated fatty acids showed different abilities to reduce CML and CEL levels whereas it significantly increased MG-H1 levels. Prasanna et al. [234] determined the inhibitory effects of 18:1 n-9 on AGEs in a glucose-BSA model with a 3-week incubation quantifying fluorescent AGEs but did not assess CML/CEL or MG-H1 levels. Their docking studies demonstrated that 18:1 n-9 could bind to arginine residues of BSA stabilising the protein structure and preventing it from being glycated. Mirhashimi and colleagues [231] investigated omega 3 fatty acid supplementation from flaxseed oil

(which contains 18:3n-3) and their effect on AGE induced cytokine production and serum AGEs via fluorescent quantification in a randomized double-blind trial. The authors found omega-3 supplementation reduced serum fluorescent AGEs however had no effect on reducing TNF-α [231]. Lima et al. (2010) studied the formation of CML in a casein-glucose-fatty acids model and reported the order of reactivity in CML formation as: 20:4 n-6 >18:3 n3 >18:2 n-6 >18:1 n-9. This study investigated CML at a limited selection of time points in a food model where the samples were subjected to high heating (95°C), in comparison to our model where time and concentration-dependent studies were explored on both fluorescent and non-fluorescent AGEs. Wang *et al.* (2019) used a lysine-glucose model to study the effect of 18:1 n-9, 18:2 n-6 and 18:3 n-3 when exposed to frying temperature on the generation of CML and CEL. The authors showed that both the CML and CEL levels were significantly increased in the models that contained the 18-carbon unsaturated fatty acids. The apparent discrepancies between our study and previous studies may be attributed to different models and heating conditions. In particular, lipid oxidation will occur more rapidly under high temperatures such as 95°C and frying conditions.

Highly unsaturated fatty acids (20:4 n-6, 20:5 n-3) demonstrated a small, yet statistically significant decrease in fluorescent AGEs, in both MGO and GO models. However, 22:6 n-3 showed a significant increase in fluorescent AGEs in the GO-BSA model and a significant decrease in the MGO-BSA model. Furthermore, these highly unsaturated fatty acids proved to be least effective in attenuating CML, CEL and MG-H1 levels compared to SFA and 18 carbon unsaturated fatty acids. Lima and colleagues [24] also reported that 20:4 n-6 increased CML formation compared to 18 carbon saturated fatty acids in a casein-glucose-fatty acids model when subjected to 95°C. In addition, long-chain n-3 PUFA supplementation for 2 months did not reduce AGE concentrations in subjects with type 2 diabetes mellitus [70].

In the present study, either a significant increase or an increasing trend in MG-H1 levels was observed when saturated and unsaturated fatty acids were subjected to the model systems. Saturated and unsaturated fatty acids can attach to lysine residues of proteins, in the protein lipidation process to form lysine fatty acylation products [271] thus making lysine unavailable for other reactions. If this was to occur with our model, MGO/GO may no longer bind to all lysine and may bind to arginine residues, thus increasing MG-H1 levels. In addition, it is possible that lipids might suppress or promote the formation of AGEs since some lipid peroxidation products could react with proteins to form ALEs [45]. Perhaps certain fatty acids can bind MGO and GO and form a new adduct, thus preventing reactions with BSA. This could possibly explain the different dynamics we observed in the formation of protein-bound fluorescent and non-fluorescent AGEs in the model systems.

In the current study, we focussed on measuring the final products in the protein glycation pathways such as fluorescent and species-specific (CML, CEL and MG-H1) AGEs. A limitation of the study is the lack of understanding of the role of peroxidation products of fatty acids. Peroxidation of fatty acids can lead to the generation of dialdehydes (eg., malondialdehyde, aldehyde, 4-hydroxynonenal and GO) and subsequent amino acids modifications leads to the formation of advanced lipoxidation end-products (ALEs). By determining the levels of these dialdehydes in the fatty acid treatment studies would have given a better understanding of CML and CEL levels as these are formed from both carbohydrates and lipids and referred to as AGEs/ALEs. Nevertheless, the fatty acids treatments in our studies do show potential physiological implications as short-term fatty acid supplementation could lead to lower levels of circulating AGEs particularly CML and CEL, hence consequences of using fatty acids supplementation as a potential therapeutic agent. Long term fatty acids supplementation on circulatory AGEs including CML and CEL is yet to be fully elucidated.

2.5 – Conclusion

MG-H1 is the most abundant non-fluorescent AGE generated in this dicarbonyl-BSA model system. In this study, we showed that MG-H1 is produced 15-fold higher than CML and 100-fold higher compared to CEL in the respective models demonstrating its newfound importance and the main AGE generated and linking with its implication in age-related disease. The addition of saturated and unsaturated fatty acids in the dicarbonyl-BSA model reduced the formation of CML and CEL, representative of a protective role in the formation of species-specific AGEs *in vitro,* however, the MG-H1 levels were increased. This increase in MG-H1 may be, at least in part, due to protein lipidation, in particular, lysine fatty acylation formation hence allowing arginine residues to react with respective dicarbonyls to form MG-H1. Thus, fatty acids, both saturated and unsaturated do not appear to attenuate the formation of MG-H1. The evidence produced in this study warrants further studies on the biological implications including the role of fatty acids on dicarbonyl induced activation of the receptor for advanced glycation end products (RAGE), inflammation and DNA damage. Fatty acids that demonstrated an ability to attenuate AGE formation from our BSA-dicarbonyl model could be used in conjunction with endothelial cells to determine if there is a correlation between fatty acids and their ability to reduce AGE-RAGE interactions.

Chapter 3 – The role of fatty acids on dicarbonyl-albumin induced expression of the receptor for advanced glycation end products (RAGE) and inflammatory markers in human endothelial cells

3.1– Introduction

AGEs binding to RAGE in people with diabetes has been implicated in endothelial cell dysfunction, leading to the development of diabetic complications e.g., retinopathy nephropathy and ultimately atherosclerosis [2, 121]. Consistent with observation, people with diabetes have been shown to have higher serum concentrations of CML, CEL and MG-H1 [158]. This is due in part to the fact that human serum albumin (HSA) is glycated at three times the rate of haemoglobin and insulin in a hyperglycaemic environment [20]. It is well documented that the binding of AGEs to the receptor (RAGE) can upregulate expression of the RAGE protein [272-274], leading to an increase in expression of pro inflammatory makers. This is accompanied with the progression of DM, AD, inflammatory conditions and melanogenesis [275], as a result of increased RAGE expression [14, 21, 22]. Once a ligand binds to RAGE, a series of intracellular pathways are triggered (Figure 1.8) .The inhibitor of NF-κB once bound to the p50 and p65 subunits of NF-κB within the cytoplasm, is then linked with ubiquitin and degraded by the proteasome [276]. Subsequent dissociation of the inhibitor initiates translocation of NF-κB to the nucleus where it mediates the expression of inflammatory cytokines such as interleukin-6 (IL-6), interleukin-1β (IL-1β), tumour necrosis factor-alpha (TNF-α), adhesion molecules such as vascular cell adhesion molecule-1 (VCAM-1), intercellular adhesion molecule-1 (ICAM-1) and chemokines such as MCP-1 [277-279].

Fatty acids, particularly PUFA have been shown to be beneficial in reducing inflammation associated with CVD and also improve cognitive function in people with AD and PD [211, 213, 221]. There are limited studies investigating the effects of fatty acids and glycation both *in vitro* and *in vivo*, specifically the role of specific FAs on AGE induced RAGE expression.

There is some evidence that long-chain PUFAs regulate RAGE expression in endothelial and smooth muscle cells [70, 227]. This limitation of the literature provides an opportunity to explore this area further and contribute to the field, whilst following on from our previous work (Chapter 2), where we have shown that FAs can attenuate the formation of both fluorescent and non-fluorescent dicarbonyl induced AGEs. Based on our work from Chapter 2, FAs that showed the greatest ability in attenuating dicarbonyl induced AGE production were selected, which included oleic acid (18:1 n-9), eicosapentaenoic acid (20:5 n-3) and docosahexaenoic acid (22:6 n-3). We hypothesised that these FAs may modulate the AGE-induced expression of RAGE and would also modulate the production of inflammatory cytokine markers IL-1β, IL-8, IL-6, and MCP-1, commonly upregulated by AGE treatment. There have been several previous studies using primary HUVECs as a cell model for investigating AGE related RAGE activation and inflammation [280-282]. An already established model of RAGE expression such as HUVECs, provides an ideal starting point to investigate the role of fatty acids on dicarbonyl-AGE induced RAGE expression *in vitro.*

The aims of this study were two-fold, firstly to optimise a BSA-dicarbonyl model system in endothelial cells to investigate the interaction of dicarbonyl induced AGEs with RAGE and secondly to use the previously optimised model to investigate the role of fatty acids on AGE activated RAGE.

3.2 – Materials

3.2.1 – Chemicals

Acetic acid, bicinchoninic acid, bovine serum albumin (BSA), D-glucose, diethyl pyrocarbonate, ethanol, glyoxal (GO), methylglyoxal (MGO), phenylmethanesulfonyl fluoride, protease inhibitor, RNA*later*™, sodium dodecyl sulfate (SDS), sodium nitrite, sodium phosphate dibasic, sodium phosphate monobasic, trichloroacetic acid, Tris-base, Tween 20, β-mercaptoethanol were purchased from Sigma-Aldrich (Sydney, Australia), 3-(4,5-dimethylthiazol-2-yl)-2,5-diphenyltetrazolium bromide, CellTiter 96® Non-Radioactive Cell Proliferation Assay (MTT) kit was purchased from Promega (Sydney, Australia).

3.2.2 – Fatty Acids

Oleic acid (18:1 n-9), eicosapentaenoic acid (20:5 n-3) and docosahexaenoic acid (22:6 n-3) were purchased from Sapphire Bioscience, (Sydney, Australia).

3.2.3 – Cell culture

Endothelial cell growth media, Hanks balanced salt solution (HBSS), primary human umbilical vein endothelial cells (HUVEC) Dulbecco's phosphate-buffered saline and Trypsin-LE™ express were purchased from Thermo Fisher Scientific (Sydney, Australia).

3.2.4 – Western Blotting

40% Acrylamide, nitrocellulose membrane and luminol were purchased from Bio-Rad Laboratories (Sydney, Australia) (RAGE antibody (A-9) (sc-365154), GAPDH antibody (0411) (sc-47724) and m-IgGκ BP-HRP secondary antibody (sc-516102) were purchased from Santa Cruz Biotechnology (Dallas, USA).

3.2.5 – PCR

Primers (RAGE, NF-κB, 28S and β-actin, Table 3.3) were purchased from Sigma-Aldrich (Sydney, Australia). Aurum™ total RNA mini kit, iScript™ gDNA clear cDNA synthesis kit, SYBR® green, were purchased from Bio-Rad Laboratories (Sydney, Australia).

3.2.6 – ELISA

Separate commercial ELISA kits (IL-1β, IL-8, IL-6, and MCP-1) were purchased from Elisakit.com. (Melbourne, Victoria, Australia)

3.3 - Methods

3.3.1 – Preparation of dicarbonyl derived AGEs for cell culture treatment

An *in vitro* glycation model was prepared as previously described (Section 2.2.2) to determine protein-bound fluorescent and non-fluorescent AGE production with slight modifications. Briefly, 100 mL of BSA (10 mg/mL, final concentration), was added to sterile 250 mL Schott bottles (Schott Duran, Germany). MGO or GO (1 mM and 2 mM, final) was added and the volume adjusted to 250 mL using sodium phosphate buffer (0.2 M pH 7.4). A BSA control was also prepared. The mixtures were incubated at 37 °C in the dark, for 3 days in a Ratek shaking incubator oven at 200 rpm (Ratek, Boronia, VIC, Australia).

3.3.1.1 – Analysis of dicarbonyl derived AGEs for cell culture treatment.

Dicarbonyl derived AGEs generated for cell culture treatment were analysed for protein-bound fluorescent AGEs, CML, CEL and MG-H1 as previously described (Sections 2.2.4 – 2.2.7).

3.3.2 – Ultrafiltration extraction of protein bound AGEs for cell culture experiments

After incubation (37 ^{o}C, 3 days) 250 mL of each model (BSA only, BSA+MGO, BSA+GO ((1 mM and 2 mM)) was filtered through an ultrafiltration column (10 kDa cut off, Merck Millipore, Victoria, Australia.) for 20 min at 5600 x g. The filtrate was collected, and the procedure repeated until the entire 250 mL of glycated model was filtered. The filtrate was then passed through a 0.22 μM filter (Thermofisher Scientific,

Sydney, Australia) into a sterile tube. Filtered protein was then quantified using the Bicinchoninic acid (BCA) protein determination method (Section 3.3.3). Both extracted and remaining glycated sample was stored in aliquots at -80 °C until further analysis with all work conducted in a laminar flow hood.

3.3.3 – Protein concentration determination of glycated models using the BCA method

The BCA protein assay was used to determine the total protein content of the concentrated model systems after ultrafiltration. Briefly a set of BSA standards were made in Milli-Q water in duplicate (0.0, 0.2, 0.4, 0.6, 0.8, 1.0, 1.2 and 1.4 mg/mL) to create a standard curve. A BCA working solution was made by mixing bicinchoninic acid (A) with copper (II) sulfate solution (4% w/v) in a 50:1 ratio (A:B). Aliquots (12.5 µL) of each standard were added to a flat bottom 96 well plate in duplicate (ThermoFisher Scientific, Victoria, Australia). Filtered glycated samples (12.5 µL) were also added into separate wells in duplicate (1:200 and 1:300 dilutions were required). BCA working solution (100 µL) was added to each well and gently mixed for 30 sec. The plate was then incubated for 30 mins at 37 °C. The plate was then removed and allowed to cool for 5 mins and the absorbance measured at 540nm using a Thermofisher Scientific microplate reader (Thermofisher Scientific, Victoria, Australia) and results analysed using GraphPad Prism version 8 (GraphPad Software Inc., CA,) and expressed as mg/mL of each glycated sample.

3.3.4 – HUVEC culture maintenance

HUVECs were purchased from Sigma Aldrich (Product number 200-500N) and stored in liquid nitrogen until use. Cells were cultured in an all-in-one endothelial cell growth medium (Product number 211-500), containing foetal bovine serum purchased from Sigma. Frozen HUVECs were thawed quickly at 37 °C in a bead bath (Thermo Fisher Scientific, Victoria, Australia). After thawing, the cell suspension was transferred into a T-75 flask containing 15 mL of pre-warmed endothelial cell growth media. The cells were placed in an incubator at 37 °C with 5% CO_2 (Sanyo incubator) and allowed to adhere overnight before removing the supernatant and replacing with fresh pre-warmed media. Cells were maintained at 37 °C with 5% CO_2 and the media replaced every 2-3 days. Cells were passaged once they reached near confluency, approximately every 6 days. Media was removed and the cells were rinsed once with 5 mL of pre-warmed HBSS. Tryp-LE™ (3 mL) was added and cells were incubated at RT for up to 5 min until cells detached. The cell suspension was then centrifuged at 120 x g for 10 min at room temperature and the supernatant discarded. The cell pellet was suspended in endothelial cell growth media and divided in a ratio of 1:2 or 1:3. Cells were used for experiments between passage numbers 2-6.

3.3.5 – MTT trials to assess the effect of dicarbonyl induced AGE treatment on HUVEC proliferation

HUVECs were grown until confluent in T75 flasks (37 °C, 5% CO_2) as per section 3.2.4. The CellTiter 96® Non-Radioactive Cell Proliferation

3-(4,5-dimethylthiazol-2-yl)-2,5-diphenyltetrazolium bromide (MTT) based cytotoxicity assay (Promega, Sydney, Australia) was used to determine the effect of the AGE-BSA

models on HUVEC proliferation. Cells were plated at a density of 5 x 10^3 cells per well in 100 µL/well. To control for absorbance due to colour of the AGE-BSA solution, wells containing 100 µL media (no cells) were set up in parallel

The plate was then incubated overnight at 37 °C, 5% CO_2. After incubation 50 µL of media was removed from all wells and 50 µL of AGE treatment (5 mg/mL final) in 100 µL/well was added along with appropriate no treatment controls. All treatments were prepared in triplicate. Plates were then incubated for 24, 48 or 72 h at 37 °C, with 5% CO_2. After incubation 15 µL of MTT dye solution was added to all wells and the plate incubated for 4 h at 37 °C, 5% CO_2 as per manufacturers instruction. After incubation, 100 µL of solubilisation solution was added to each well and left in the dark at RT overnight to ensure complete solubilisation. The following day the wells were gently mixed by hand, and the absorbance was measured at 570 nm (Enspire® Perkin Elmer, MA). The cell viability was determined for AGE-BSA treated cells compared to the cells with no treatment, which was considered 100% viable and expressed as % cell viability (% of control).

3.2.6 – MTT assay to assess the effect of fatty acids on HUVEC proliferation

HUVECs were grown until confluent in T75 flasks (37 °C, 5% CO_2) as per section 3.2.5. with the exception that the cells were treated with 50 µL of FA (18:1 n-9, 20:5 n-3 and 22:6 n-3, at 10, 20 and 30 µM final). FA were dissolved in ethanol with a final concentration of ethanol < 1% per well. The cells were incubated for a further 72 h at 37 °C, 5% CO_2 and the effect on cell viability determined as in 3.2.5.

3.3.7 – Cell Treatments.

3.3.7.1 – AGE-BSA treated HUVECs

HUVECs were grown until confluent in T75 flasks (37 °C, 5% CO_2) as per section 3.2.5. Cells were counted and seeded at a density of 5 x 10^4 cells/ well in a 6 well cell culture plate (ThermoFisher Scientific, Victoria, Australia). The cells were allowed to adhere overnight before adding the AGE treatment and appropriate no treatment control. Briefly 1.5 mL of BSA, BSA-AGE treatment (5mg/mL final concentration) prepared in endothelial cell media (Cell Applications, San Diego, CA,) was added to each well containing 1.5 mL of media (3 mL total volume/well) and left for 24, 48 or 72 h (37 °C, 5% CO_2) before harvesting.

3.3.7.2 – AGE-BSA-FA treated HUVECs

HUVECs were grown until confluent in T75 flasks (37 °C, 5% CO_2). As per section 3.2.5. HUVECs were plated and left to adhere overnight before adding BSA-AGE-FA treatment and appropriate no treatment control. Cells were pretreated with selected FA (20 µM final, either 18:1 n-9, 20:5 n-3 or 22:6 n-3) for 30 min prior to the addition of AGEs. Plates were incubated for 24h (for cytokine quantification) or 72 h (Western blot and qPCR) (37 °C, 5% CO_2) before harvesting. After treatment, the cell supernatant was collected and stored at -80 °C for cytokine analysis, while cells were lysed for protein extraction.

3.3.8 – Cell lysis and protein extraction for western blot analysis

Briefly, 1 mL of HBSS was added to each well and cells were collected using a Corning cell scraper (Corning, New York, NY). The cells were then centrifuged at 8161 x g for 5 min at RT and supernatant discarded. The cells were then lysed in 50 – 100 µL of lysis buffer (50 mM Tris-HCl buffer pH 7.4 containing 150 mM NaCl, 10% glycerol, 1 mM EDTA, 0.05% Triton X-100, 2 mM Na_3VO_4, 10 mM NaF, 10 mM β-glycerophosphate). The lysis buffer was supplemented with 500 µL of protease cocktail inhibitor containing AEBSF at 2 mM, Aprotinin at 0.3 µM, Bestatin at 116 µM, E-64 at 14 µM, Leupeptin at 1 µM and EDTA at 1 mM (1 mM final) (Sigma, Sydney, Australia) and 10 µL of dithiothreitol (DTT) (1 mM final). The cells were sonicated on power setting 3 (Misonix, New York NY,) on ice for 90 sec (15 sec on, 5 sec off). The cells were then centrifuged at 8161 x g for 3 min at RT to pellet the debris. Cell lysates were then subjected to BCA assay to determine the protein concentration.

3.3.9 – RNA extraction

Briefly 1 mL of HBSS was added to treated HUVEC cells and cells disassociated using a Corning cell scraper. Cells were then transferred into a 1.5 mL tube and centrifuged at 8161 x g for 5 min at RT in a microcentrifuge. Following centrifugation, the supernatant was discarded, and the pellet suspended in 100 µL of RT RNA*later*™ (Sigma, Sydney, Australia) and stored at -80 °C until extraction. A lysis solution of guanidine isothiocyanate (350 µL) supplemented with 1% (v/v) β-mercaptoethanol, was added to each tube and the cells were lysed by passing the cells through a pipette tip until fully disassociated. Ethanol (350 µL, 70% v/v), was added and the solution vortexed for 30

sec. The mixture was added to a silica membrane RNA binding column and centrifuged at 8161 x g for 30 sec. The eluate was discarded and 700 µL of low stringency wash solution, diluted with ethanol (95% v/v), added to each tube, and centrifuged at 8161 x g for 30 sec and the eluate discarded. Then, 5 µL of reconstituted DNase I (dissolved in 10 mM Tris pH 7.5), diluted with 75 µL of a DNase dilution solution, was added to each column. The column was incubated at RT for 15 min. After digestion, 700 µL of high stringency wash solution was added to the column and centrifuged for 30 sec at 8161 x g. The wash solution was discarded and a further 700 µL of low stringency wash solution was added and the column centrifuged for 1 min at 8161 x g and the eluate discarded. The column was centrifuged for a further 2 min at 8161 x g to remove any residual wash solution. The column was transferred to a clean collection tube and 40 µL of elution solution was added. After 1 min at RT the tubes were centrifuged for 2 min at 8161 x g to elute the RNA. The RNA content was quantified using a NanoDrop™ lite spectrophotometer (Thermo Scientific, Victoria, Australia) by measuring the absorbance at 260 nm with a purity ratio > 1.80 (ratio of absorbance at 260 nm/280 nm) used for cDNA synthesis.

3.3.10 – gDNA digestion and cDNA synthesis

cDNA synthesis was performed using an iScript™ gDNA clear cDNA synthesis kit (Bio-Rad, Sydney Australia) according to the manufacturer's instructions. Briefly, 2 µL of DNase solution was added to 14 µL of diluted RNA sample (100 ng total RNA per sample) and mixed well by pipetting. The samples were incubated at 25 °C for 5 min using a thermal cycler (SimpliAmp™ Thermal Cycler, Applied Biosystems™, Waltham. MA,). The temperature was increased to 75 °C for 5 min to deactivate the DNase (Table 3.1). Following DNA digestion, the sample was kept on ice and cDNA synthesis was performed by adding 4 µL of iScript™ reverse transcription supermix to each reaction tube. A no reverse transcriptase control was also used for all preparations. The mixtures were incubated in a thermal cycler (Applied Biosystems™) at 25 °C for 5 min and the temperature was increased to 46 °C for 20 min for reverse transcription. The temperature was then increased to 95 °C for 1 min to inactivate the reverse transcriptase and the samples were kept on ice before qPCR preparation (Table 3.2)

Table 3.1 - DNAse reaction protocol and conditions
adapted from the manufacturer's instructions.

Step	Temperature (°C)	Time, min
DNA digestion	25	5
DNase inactivation	75	5
Storage	4; ice (if long term -80 °C)	Until RT step

Table 3.2 - cDNA synthesis reaction table and conditions
adapted from the manufacturer's instructions

Step	Temperature (°C)	Time, min
Priming	25	5
Reverse transcription	46	20
RT inactivation	95	1
Hold (optional)	4	-

.

3.3.11 – Sodium dodecyl sulfate (SDS) Polyacrylamide gel electrophoresis (PAGE) and western blotting.

HUVECs (5 x 10^4 /total) were treated with either BSA, AGEs or AGEs + FAs for 24,48 or 72 h at 37 °C/5% CO_2 in a humidified atmosphere. After treatment, cells were collected by centrifugation (2000 g x 5 min, 4 °C). The supernatant was retained for subsequent cytokine analysis. The cell pellet was suspended in 50 µL of lysis buffer (50 mM Tris-HCl (pH 7.4) containing 150 mM NaCl, 10% v/v glycerol, 1 mM EDTA, 0.05% Triton X-100, 2 mM Na_3VO_4, 10 mM NaF, 10 mM β-glycerophosphate, 1 mM dithiothreitol and protease inhibitor cocktail (AEBSF at 2 mM, Aprotinin at 0.3 µM, Bestatin at 116 µM, E-64 at 14 µM, Leupeptin at 1 µM and EDTA at 1 mM). The cells were sonicated (2 x 20 sec,) (Misonix, New York, NY,), centrifuged (16,000 g x 20 min, 4 °C) and the supernatant collected. Protein concentration was determined as per section 3.2.3. The samples (20µg of protein) plus reducing buffer (20 mM Tris-HCl, pH 6.8, 40% sucrose, 6% sodium dodecyl sulphate (SDS) and 10 mmol/L β -mercaptoethanol, 3:1) were heated at 100 °C or 5 min and then loaded onto by 10% homemade polyacrylamide gels using a BioRad mini gel apparatus from BioRad (Syndey, Australia), run at 160 V for 1 h 20 min. The gel was then soaked in transfer buffer (25 mM Tris base, 20% (v/v) methanol, 125 mM Glycine and MilliQ water) for 20 min and the nitrocellulose membrane (0.2 mm BioRad, Sydney, Australia) equilibrated by being soaked in transfer buffer for 10 min. The separated proteins were transferred to the nitrocellulose membrane at 15 V for 30 min using a semi-dry transfer apparatus (BioRad, Sydney, Australia). Following the transfer, the membrane was washed (3 x 5 min) with tris buffered saline (TBS). The membrane was then blocked for 1 h with blocking buffer (TBS + 0.1 % (v/v) Tween, 5 % (w/v) skim milk - TBST). This was followed by overnight incubation with anti-RAGE

(A9) and anti-GAPDH mouse monoclonal IgG (1:200) (Santa Cruz Biotechnology, Dallas, TX), at 4 °C with rocking. The membrane was then washed (3 x 10 min) with TBST and incubated for 1 h at RT with mouse IgG kappa binding protein (1:10000) (m-IgGκ BP) conjugated to Horseradish Peroxidase (HRP) (Santa Cruz Biotechnology, Dallas, TX). The membrane was then washed (3 x 10 min) with TBST. The immune reactive complex was visualised using a western blotting luminol reagent) (Santa Cruz Biotechnology, Dallas, TX). The membrane was covered for 5 min with a 1:1 mixture of the luminol reagent. The membrane was visualised using an Amersham 680 imager (GE Healthcare Life Sciences Sydney, Australia). Built-in analysis was used to evaluate the relative density of bands after correction for GAPDH loading using the Amersham software (Version 2.0)

3.3.12 – Quantitative real-time polymerase chain reaction (qPCR)

Quantitative real-time polymerase chain reaction (qPCR) was used to quantitate mRNA expression of RAGE, NF-κB and reference genes 28s and β-Actin. The cDNA sequence of the primers, Genbank® accession number, annealing temperature and expected size can be found in table 3.3.

Total RNA was extracted as per section 3.2.9. The RNA content was quantified using a NanoDrop lite spectrophotometer (Thermo Scientific, Victoria, Australia) by measuring absorbance at 260 nm and samples with a purity ratio > 1.80, determined from the ratio of absorbance at 260 nm/280 nm, were used for cDNA synthesis. The cDNA synthesis was performed as per section 3.2.10.

The cDNA samples, 2 µL each, were mixed with 1 µL each of 10 µM sequence specific primers (forward and reverse) and 10 µL of SYBR green and the reaction volume was adjusted to 20 µL with DEPC treated water. The PCR reaction was performed using a magnetic induction cycler (MIC) PCR machine (Bio Molecular Systems, Queensland, Australia). An initial hold step at 95 °C for 2 min was used to activate the reaction. A total of 40 cycles were performed with denaturation at 95 °C for 15 sec, followed by annealing at 65 °C for 30 sec, and elongation at 72 °C for 30 sec. Fluorescence was measured after every elongation stage. A no reverse transcription control and a no template were included in all experiments. After cycling, product melt curves were obtained by slowly increasing the temperature of the reaction from 60 °C to 95 °C in 0.5 °C increments/sec with continuous measurement of fluorescence. Identification of a single peak in the melt curve analysis confirmed the specificity of the PCR product generated. The $2^{-\Delta\Delta CT}$ method [283], was used to represent the normalised expression of the gene of interest relative to the normalised expression of the control sample (BSA only), represented as fold change [284].

Table 3.3 - Primer sequences used in qPCR and accession number

mRNA	Primer sequence 5' → 3'	Product (bp)	T_m	Genbank® accession number
RAGE	F - GCAGTAGTAGGTGCTCAAAAC ATCA R - GGGCCCCCTTACACTTCAG	70	65	NM_001136
NF-κB	F - CAGTAGTAGGTGCTCAAAACATCA R- GGGCCCCCTTACACTTCAG	69	66	NM_001288724.5
28s	F – GACGAGTGTGGTGAGCTTTCTG R – GAGTCTCCATGCCGATCCA	59	66	NM_001101.5
β -Actin	F – GCGCGGCTACAGCTTCA R – TCTCCTTAATGTCACGCACGATT	100	65	X 00525

F; forward, R; reverse. bp; base pairs, T_{m-} primer melting temperature, RAGE; receptor for advanced glycation endproducts, NF- κB – nuclear factor kappa B.

3.3.13 – Quantification of cytokine levels by enzyme linked immunosorbent assay (ELISA)

IL-1β, IL-8, IL-6, and MCP-1 were quantified using sandwich ELISA (Elisakit.com,) as per the manufacturer's protocol. The samples were loaded to antibody captured wells and incubated at RT for 2 h. A standard curve was prepared, and the concentration range was dependent on the kit requirements (IL-1β: 3.125-2000 pg/mL, IL-8 and IL-6: 15.6-1000 pg/mL and MCP-1: 31.25-2000 pg/mL). A biotin labelled detection antibody was added and incubated for 1 h at RT, then followed by a streptavidin-HRP conjugate incubated for 45 min at RT. Colour was developed by the addition of a tetramethylbenzidine substrate, and the reaction was stopped after 15 min by the addition of a stop solution (H_2SO_4). The absorbance was measured at 450 nm (Multiskan™ plate reader, ThermoFisher, Victoria, Australia). The level of each cytokine was calculated by interpolation of the standard curve and expressed as pg/mL.

3.3.14 – Statistical analysis

Data analysis was performed using GraphPad Prism (San Diego, CA, Version 7.03). One-way analysis of variance (ANOVA) was used to determine the significance of fluorescent and non-fluorescent cell culture models , MTT cell proliferation assays, immunoblotting analysis, and qPCR followed by Tukey's test. A p value < 0.05 was considered significant, and results are expressed as mean ± standard error of the mean (SEM) from a minimum of 3 independent experiments performed in triplicate.

3.4 - Results

3.4.1 – Quantification of AGEs in glycated proteins used for cell culture treatment

A separate model system was established for cell culture experiments. This was required as it was essential to obtain sterile samples that could be used in cell culture. Briefly, models were established as described (section 3.2.1) and analysed for the production of protein-bound fluorescent and non-fluorescent AGEs to ensure consistency across all experiments. Levels of both fluorescent AGE production and non-fluorescent AGEs CML/CEL and MG-H1 generated in the separate cell culture model are shown in Tables 3.4 and 3.5 respectively. Both 2 mM models generated significantly more ($p<0.0001$) protein bound fluorescent AGEs than at 1 mM. The 2 mM BSA-MGO model generated the highest with 4083.46 ± 39.43 AU/mg BSA. Both 2 mM models also produced more non-fluorescent AGEs than at 1 mM however only CEL levels generated in the BSA-MGO model were significantly ($p<0.02$) higher (1.14 ± 0.03 nmol CEL/mg BSA). AGE levels produced in all models, both fluorescent and non-fluorescent, were comparable to the initial model established for previous *in vitro* studies where 2 mM BSA-MGO also produced the highest quantity of fluorescent AGEs with 5038 ± 300.6 AU/mg BSA and non-fluorescent MG-H1 48.31 ± 4.83 nmol MG-H1/mg BSA (Figures 2.3 and 2.4).

The concentration of AGEs quantified in the BSA-dicarbonyl model systems is comparable to physiological concentrations of AGEs measured in human plasma. Hanssen et al. (2013) have reported the concentration of protein-bound CML ranges between 26-41 nmol CML/mmol Lysine [158] while van Eupen et al. (2013) report higher concentrations of CML between 92.5-104.6 nmol/mmol Lys [88]. The difference in the

level of protein-bound CML quantified in these studies may be due to different measurement techniques (Hanssen et al (2013) used LC-MS/MS and van Eupen et al. (2013) used HPLC with fluorescence detection). As mentioned in Section 1.3.5, LC-MS/MS is the most sensitive and accurate technique to quantify AGEs in biological samples. Additionally, the AGE concentration was measured by this technique in the present study which enables the direct comparison of the CML/CEL/MG-H1 content of the BSA-dicarbonyl model systems to previously reported levels quantified in human plasma (Table 1.3). When converted to a common unit (nmol CML/mmol Lysine), the protein bound CML content of the BSA-GO model system is 6.94 nmol CML/mmol Lysine at the 2 mM treatment concentration. The concentration of protein bound CEL was below the limit of quantification when expressed as nmol CEL/mmol Lysine at the 2 mM treatment, which is consistent with previous very low levels of CEL generated in this model throughout all experiments compared to other analytes (Figure 2.4). The concentration of protein bound MG-H1 in the BSA-MGO was 93.8 nmol/L at 2 mM. Table 1.3 shows great variation between reported values therefore, the concentration of the BSA-dicarbonyl model system for cell treatment to investigate AGE-induced RAGE expression and inflammatory biomarkers (2 mM final) was chosen to represent a physiological concentration of CML and MG-H1 observed *in vivo*.

Table 3.4 - Quantitation of protein-bound fluorescent AGE production used in cell culture treatments.

Model	Protein bound fluorescent AGEs (AU/mg BSA)
BSA only	753.46 ± 7.12
BSA-MGO 1mM	2797.46 ± 60.40
BSA-MGO 2 mM	4083.46 ± 39.43 ****
BSA-GO 1 mM	1656.93 ± 122.27
BSA-GO 2 mM	2494.80 ± 48.91 ****

Protein-bound fluorescent AGEs generated in a BSA + dicarbonyl model system of protein-bound fluorescent AGEs generated in the BSA, BSA-MGO and BSA-GO cell culture model. Results expressed as AU/mg BSA, mean ± SEM n=3. **** $p<0.0001$ as compared to 1 mM model.

Table 3.5 - Quantitation of species-specific protein-bound AGEs used in cell culture treatments

Model	BSA	BSA-MGO 1 mM	BSA-MGO 2 mM	BSA-GO 1 mM	BSA-GO 2 mM
Protein-bound CML (nmol CML/mg BSA)	1.51 ± 0.05	-	-	4.19 ± 0.29	7.32 ± 1.26
Protein-bound CEL (nmol CEL/mg BSA)	0.26 ± 0.01	0.71 ± 0.01	1.14 ± 0.03 *	-	-
Protein-bound MG-H1 (nmol MG-H1/mg BSA)	< LOQ	57.08 ± 0.27	60.36 ± 1.34	-	-

Species-specific AGE generation in both MGO and GO models. AGEs were generated as previously described and were quantified using tandem LC-MS/MS. CEL, CML and MG-H1. CML, CEL and MG-H1 expressed as nmol of analyte/mg of BSA. Results expressed as mean ± SEM n=3, * p< 0.02 compared to 1 mM model

3.4.2 – 3-(4,5-Dimethylthiazol-2-yl)-2,5-diphenyltetrazolium bromide (MTT) assay

3.4.2.1 – HUVECs treated with the BSA-dicarbonyl model

Primary HUVECs were used between passages 2 and 6 since long term passaging on primary cells can lead to changes in morphology and biological responses [285]. A MTT assay was used to assess the proliferation of HUVECs when exposed to AGEs. In a preliminary study, glycated models of either BSA+MGO or BSA+GO as well as BSA control, were added to HUVECs assess the optimum concentration of the glycated samples for cell treatment studies. Upon data analysis it was evident that the glycated significantly reduced the viability of cells, even the BSA only control (Appendix 5.2.1).

Given the effect noted with the BSA only control, it was determined that the TCA precipitation step was the cause of cell death. It was not possible to remove all TCA from the protein pellet. This was further confirmed by assaying BSA precipitated with TCA compared to BSA dissolved in media only, where there was almost zero cell death (Appendix 5.2.2). As a result, the method was modified to include an ultrafiltration step to separate free MGO and GO from protein bound MGO and GO and any unreacted BSA. BSA only and BSA-dicarbonyl models (both 1mM and 2mM) were then diluted to 5mg/mL final concentration and HUVECs treated as described previously. Both 1 mM and 2 mM BSA-MGO reduced cell viability at 24, 48 and 72 h as compared to the control, with 2 mM, a larger reduction at all 3 timepoints was observed. However, even at 2 mM cell viability remained at 70% of the control for all timepoints. A similar trend was observed in the BSA-GO model where both 1 and 2 mM BSA-GO reduced cell viability across 24, 48 and 72 h, with 2 mM resulting in a larger reduction. Similarly, to BSA-MGO, cell viability remained at 70 % or greater than that of the control. Cell viability on BSA-dicarbonyl models in HUVECs has previously not been reported (Figure 3.1).

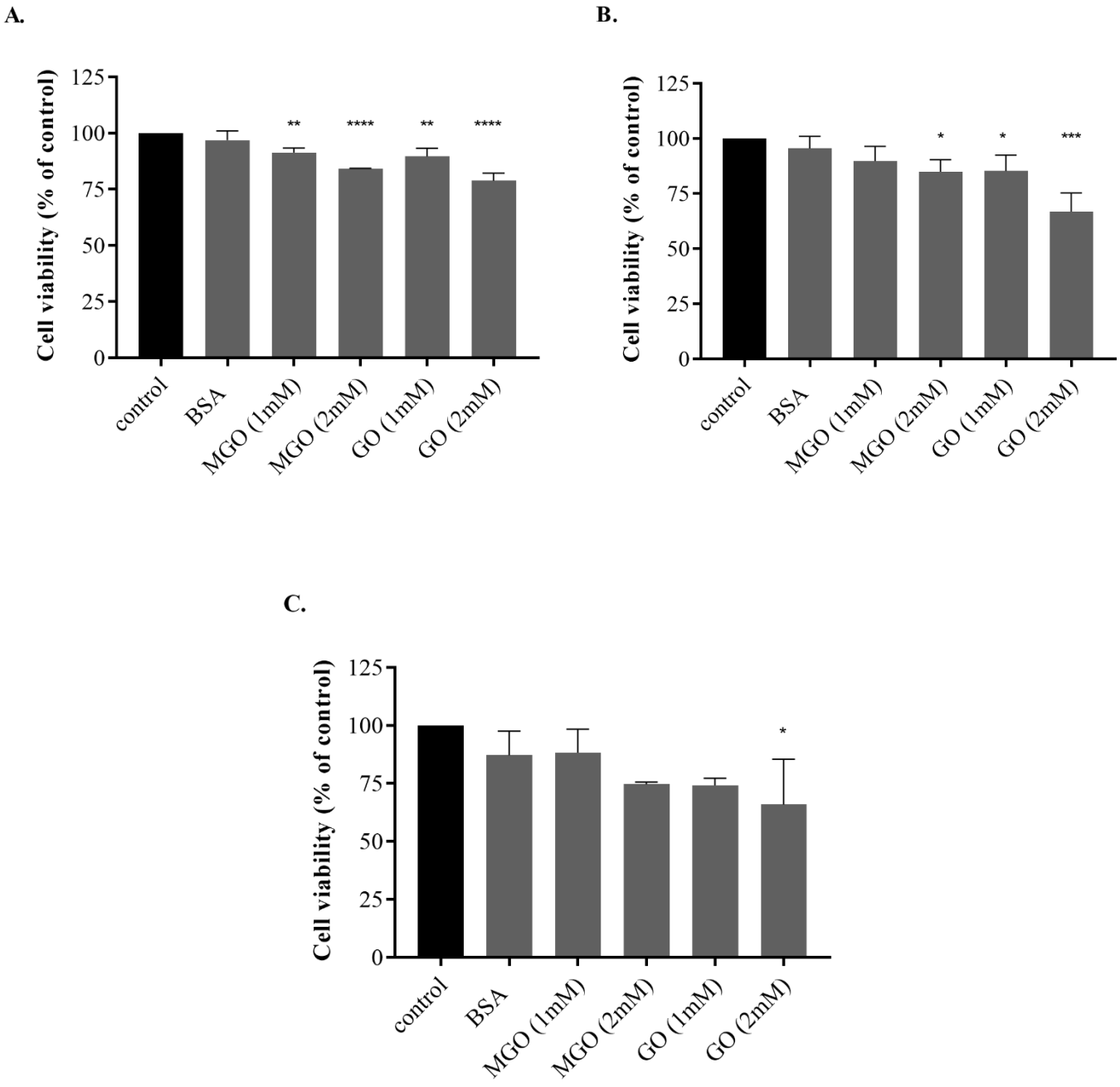


Figure 3.1 - Effect of ultra-filtrated dicarbonyl derived protein-bound AGEs on cell viability in a HUVEC model.

BSA and BSA-AGE models were diluted to a final concentration of 5 mg/mL and cells were treated for a period of 24 (**A**) 48 (**B**) and 72 h (**C**). results normalized to no treatment control, data expressed as mean ± SD, n=3 **** represents $p<0.0001$, *** $p<0.0002$ ** $p<0.003$ and * $p<0.05$ (ANOVA) compared to BSA only treatment control.

3.4.2.2 – Effect of fatty acid treatment on HUVEC viability

HUVECs were treated with FA that showed the most activity in reducing both protein-bound fluorescent and non-fluorescent AGE formation (section 2.3.3) to determine their effect on viability and their suitability for cell treatments. The selected FAs dissolved in ethanol, (<1% v/v final), (18:1 n-9, 20:5 n-3 and 22:6 n-3) were presented to HUVECs at 10, 20 and 30 µM final concentrations for 72 h at 37 °C 5% CO_2 and their changes in cell viability determined. When treated with 10 µM and 20 µM of each fatty acid, cells demonstrated greater than 85% viability compared to the diluent control, whereas at 30 µM, viability significantly reduced to 55% when treated with 18:1 n-9 (Figure 3.2). Given that FA were previously used at 20 µM in the model system (Section 2.3.2) and there were minimal effects on cell viability, this concentration of FA was chosen for all subsequent cell studies.

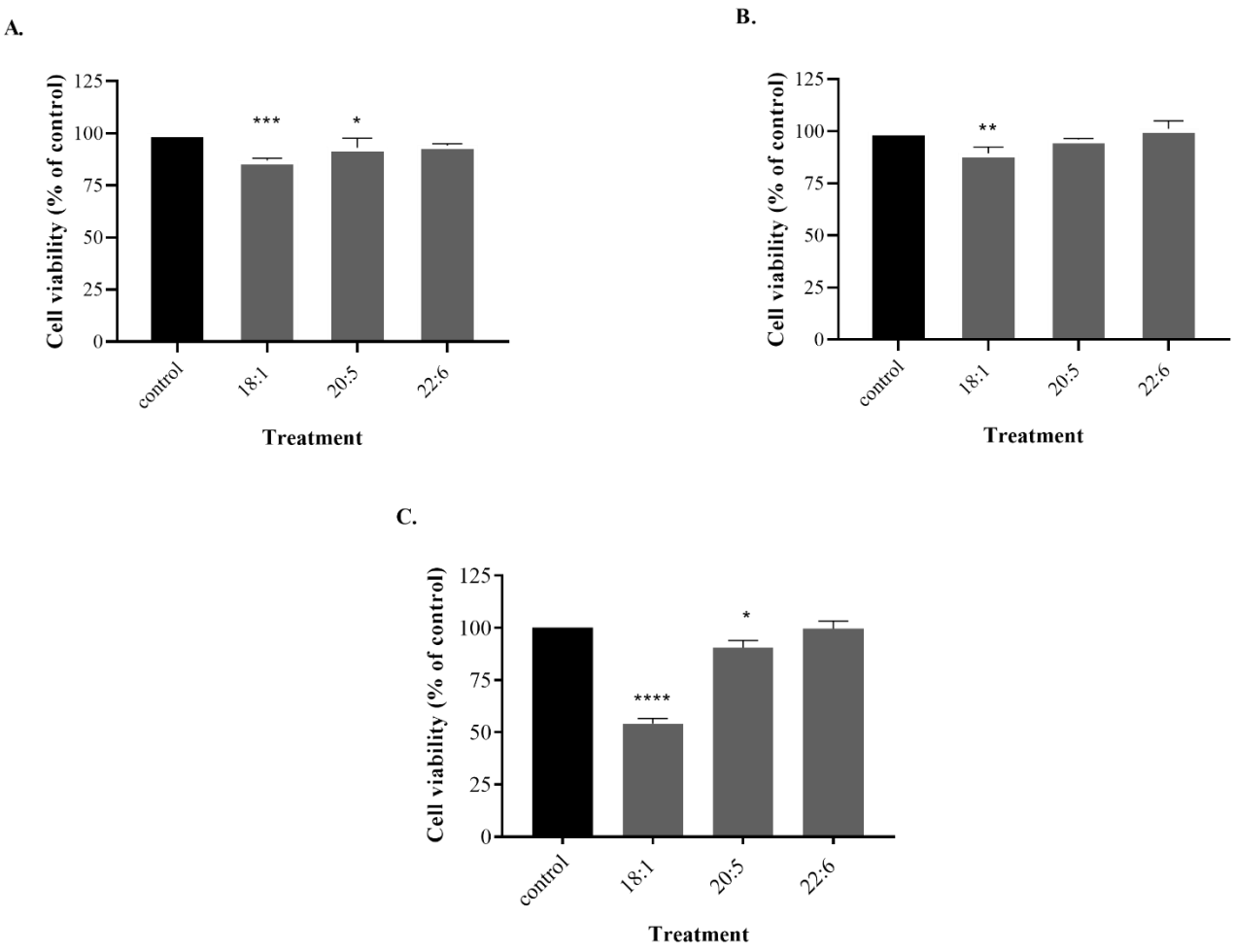


Figure 3.2 - Effect of fatty acids on HUVEC viability.

A selection of fatty acids (18:1 n-9 20:5 n-3 and 22:6 n-3) were added to HUVECs at 10 µM (**A**.), 20 µM (**B**.) and 30 µM (**C**.) for 72 h to assess their suitability for subsequent cell treatments. Results are normalized to the no treatment diluent control, expressed as mean ± SD, n=3. **** $p< 0.0001$, *** $p<0.0008$, ** $p< 0.005$, * $p<0.05$. (ANOVA) compared to no treatment control.

3.4.3 – qPCR analysis for RAGE/NF-κB expression

It was hypothesized that there would be a correlation between RAGE mRNA levels quantified using qPCR and protein expression levels as determined via western blotting. We also sought to determine the extent of NF-κB expression at the mRNA level to later correlate with selected pro-inflammatory cytokines measured via ELISA.

3.4.3.1 – The effect of MGO-BSA and GO-BSA derived AGEs on RAGE and NF-κB mRNA expression.

Initially, the effect of dicarbonyl-derived AGEs on RAGE and NF-κB mRNA expression were assessed for 24, 48 or 72 h. RAGE mRNA expression increased at 24 h (1.51 ± 0.18) decreased at 48 h (0.91 ± 0.12) and increased slightly again at 72 h (1.17 ± 0.24) for MGO-BSA treatments. For GO-BSA treatments the same trend was observed, an increase at 24 h (1.87 ± 0.16) which then decreased at 48 h (0.96 ± 0.17) before again increasing at 72 h (1.22 ± 0.09) demonstrating a nonlinear response between, time and RAGE mRNA expression (Figure 3.3).

Treatment of HUVECs with MGO-BSA showed no significant changes in NF-κB mRNA expression at 24 h (1.23 ± 0.18), 48 h (1.08 ± 0.10), and 72 h (1.14 ± 0.05), when compared to BSA only treatment. A similar non statistically significant trend was observed with GO-BSA 24 h (1.14 ± 0.18), 48 h (1.20 ± 0.20), and 72 h (1.27 ± 0.11) respectively. Since at 72 h treatment there was an increase in RAGE expression with both qPCR and western blotting this timepoint was chosen for all future experimental work involving FA.

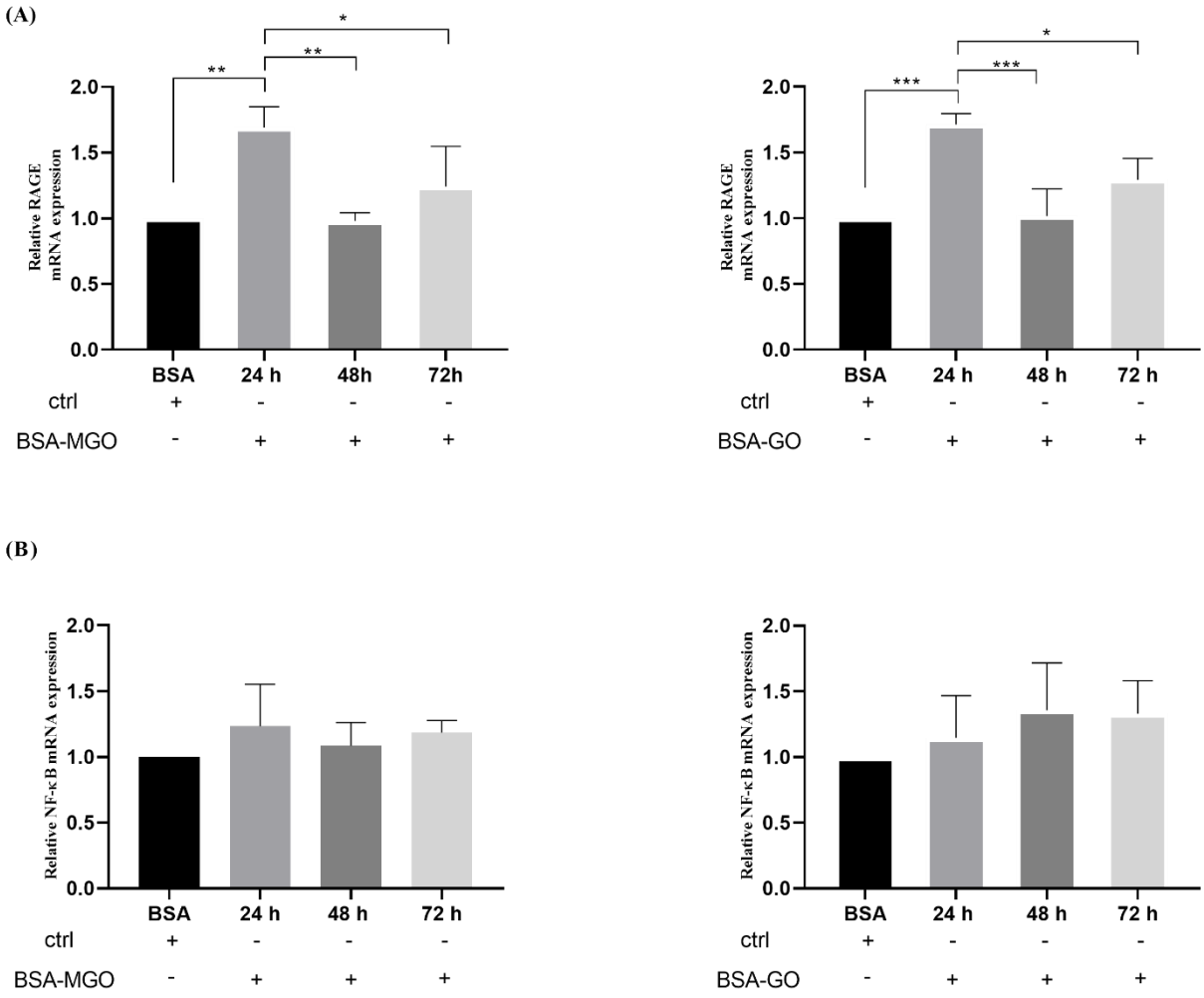


Figure 3.3 - The effect of dicarbonyl derived AGEs on RAGE mRNA expression (A) and NF- κB (B) in HUVECs.

HUVECs were treated with either BSA, MGO-BSA or GO-BSA derived AGEs for 24, 28 and 72 h respectively. Results are expressed as mean ± SEM n=3, relative expression compared to a control (BSA-only).

3.4.3.2 – The effect of FA pretreatment on AGE induced RAGE and NF-κB mRNA expression in HUVECs

HUVECs were pretreated with FA as previously described (section 3.3.7.2) and changes is RAGE expression was assessed by qPCR and immunoblotting. Results from the BSA-MGO-FA treated HUVECs demonstrate that all three FAs reduced relative RAGE mRNA expression. Both 18:1 n-9 (0.42 ± 0.08) and 22:6 n-3 (0.52 ± 0.05) reduced RAGE expression significantly (p<0.002), while 20:5 n-3 reduced RAGE expression slightly (0.22 ± 0.06) as quantified by qPCR (Figure 3.4 (A)). While these results are promising and consistent with the original hypothesis, no similar trend was observed in the BSA-GO-FA model. While 18:1 n-9 and 20:5 n-3 treatment showed no effect in reducing RAGE mRNA expression, 22:6 n-3 (0.15 ± 0.09) showed an increasing trend in RAGE mRNA expression.

Similar to RAGE mRNA expression observed in the MGO-BSA-FA model, NF-κB mRNA expression was significantly reduced by all three FA, 18:1 n-9 (0.45 ± 0.06 p< 0.0009), 20:5 n-3 (0.60 ± 0.03 p<0.0001) and 22:6 n-3(0.41 ± 0.06 p<0.002) (Figure 3.4 (B.)). There was no trend in terms of the degree of saturation and NF-κB reduction, as all three FA showed a similar level of reduction.

In the GO-BSA model, FA pretreatment showed a non-significant trend in decreasing NF-κB mRNA expression. 18:1 n-9 showed no change in NF-κB mRNA expression, while 20:5 n-3 (0.18 ± 0.01) and 22:6 n-3 (0.22 ± 0.05) showed a decreasing trend.

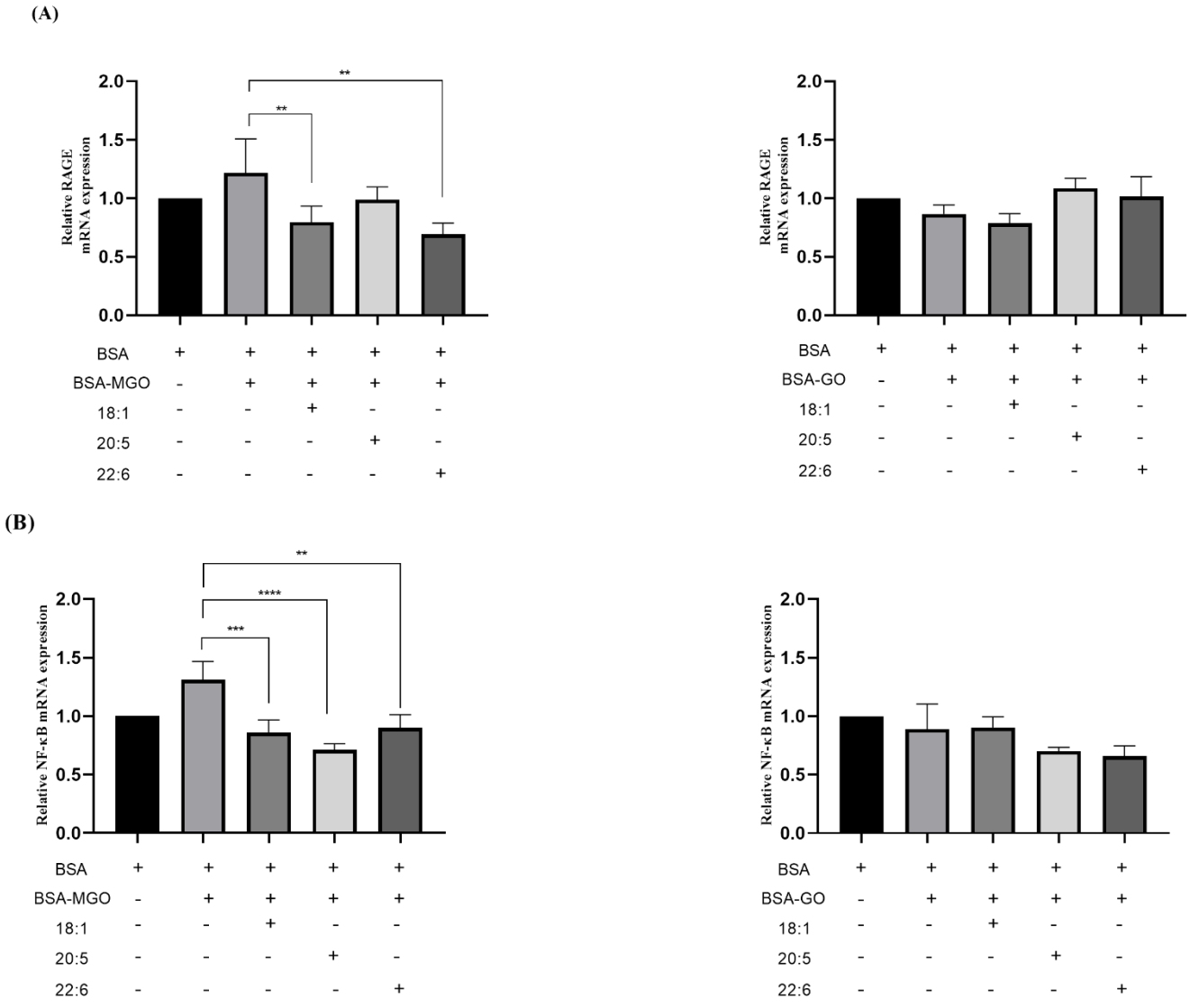


Figure 3.4 - The effect of fatty acid pre-treatment on AGE induced RAGE mRNA expression (A.) and NF- κB mRNA expression (B.) in HUVECs

HUVECs were pre-treated with FA before being exposed to either BSA, MGO-BSA or GO-BSA derived AGEs for 72 h. Results are expressed as mean ± SEM, n=3 relative expression compared to an internal control (BSA-only) *p<0.05, **p<0.002, ***p<0.0009, ****p<0.0001.

3.4.4 – Western Blotting for RAGE expression

HUVECs are known to express RAGE on their cell surface and are activated by AGEs as ligands [281, 286]. Previous studies have reported that RAGE activation triggers inflammatory pathways within the cell and increases NF-κB and pro-inflammatory cytokines production (TNF-α, IL-1β, IL-6) [33, 196, 197, 200]. It was hypothesized that FA pre-treatment may have a role in modulating AGE-induced RAGE expression in HUVECs. Prior to FA studies, the optimal time and concentration for RAGE expression following treatment with BSA-dicarbonyl models was determined in HUVECs.

3.4.4.1 – Time and concentration-dependent studies to establish RAGE expression in HUVECs

HUVECs were seeded into 6 well plates as previously described (section 3.3.7.1). Cells were then treated with 5 mg/mL (final) of BSA or dicarbonyl-derived AGEs for 24 , 48 and 72 h respectively. The results obtained showed no significant change after 24 h, followed by a decrease in RAGE expression at 48 h then by 72 h an increase in RAGE expression (Figure 3.5) demonstrating a similar trend to qPCR experiments. Interestingly there was not a notable difference between concentrations of dicarbonyl and RAGE expression, where 1 and 2 mM showed a similar level of upregulation for both BSA-MGO and BSA-GO treated cells. Given 2 mM produced more AGEs (Table 3.4) and is comparable to the AGE concentrations represented in a disease this was chosen for further experiments involving FA treatments [113].

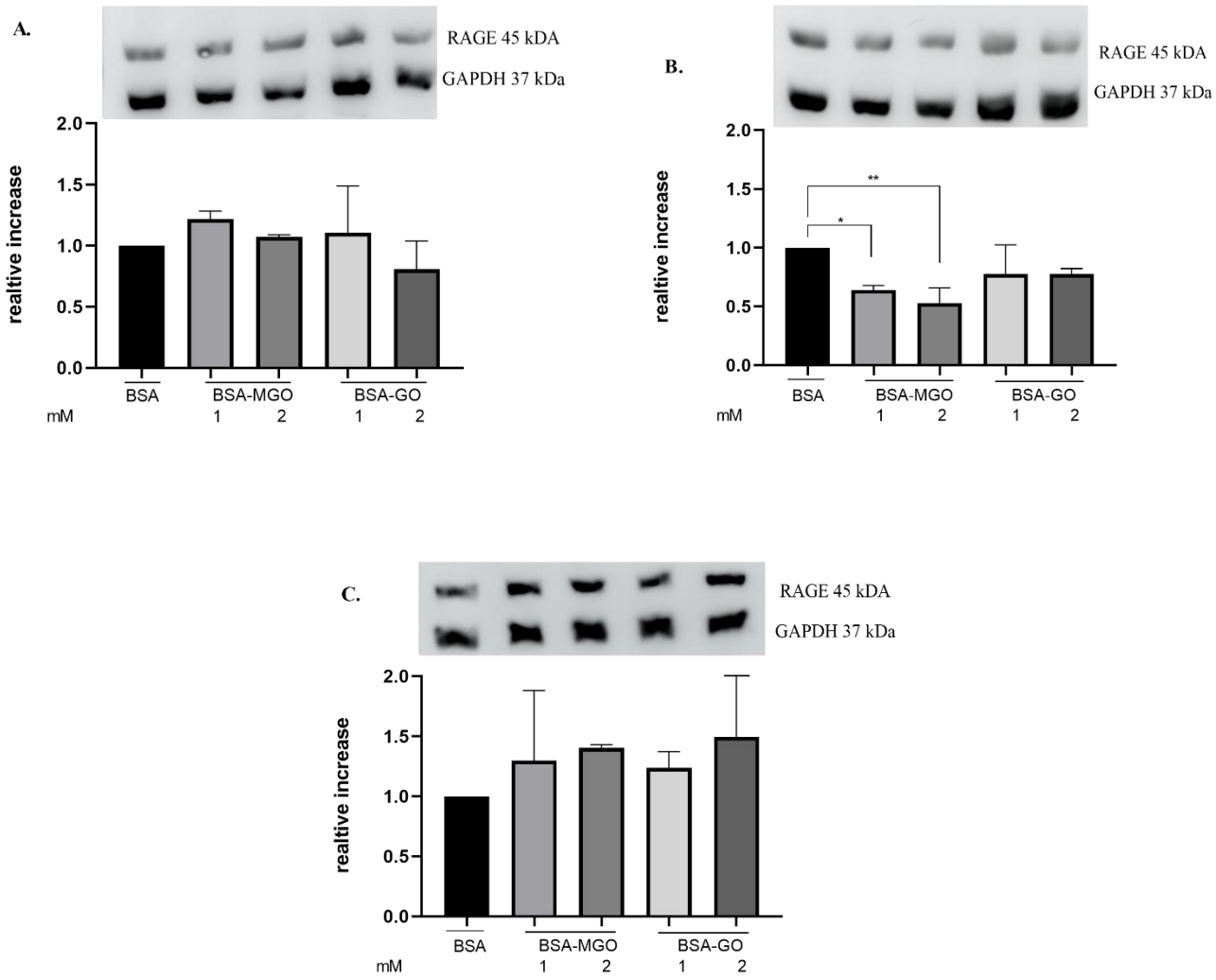


Figure 3.5 - Time and concentration-dependent effect on RAGE expression in HUVECs treated with dicarbonyl-derived AGEs

HUVECs were treated with BSA, BSA-MGO (1 & 2 mM) and BSA-GO (1 & 2 mM) for 24 h (A.), 48 h (B.) and 72 h (C.) and RAGE expression quantified via immunoblotting. Results are expressed as mean ± SEM, n=3, relative expression compared to BSA-only control) * represents $p<0.05$, ** $p<0.005$, (ANOVA) representative blots for each timepoint) RAGE – receptor for advanced glycation endproducts, GAPDH - glyceraldehyde 3 phosphate dehydrogenase, kDa- kilodaltons

3.4.4.2 – The effect of FA pretreatment on AGE induced RAGE protein expression in HUVECs.

Based on previous time and concentration-dependent optimisation studies (section 3.4.4.1), it was determined that 2 mM dicarbonyl derived AGEs for a 72 h treatment was the optimal condition for RAGE expression in HUVECs and subsequent experiments involving FA presentation to cells. FAs chosen were the most active in reducing *in vitro* AGE levels as determined by LC-MS/MS analysis (section 2.3.3)

HUVECs were pre -treated with FA (20 µM) for 30 min and then exposed to 5 mg/mL with either BSA, BSA-MGO (2 mM) or BSA-GO (2 mM) for 72 h. Cells were harvested, lysed and subjected to SDS-PAGE and probed for RAGE via western blotting.

HUVECs treated with BSA-MGO derived AGEs showed an increase in RAGE expression compared to BSA only (0.5-fold). Treatment of HUVECs with FA showed a significant reduction in RAGE expression in the following order: 18:1 n-9 (0.93 ± 0.20, $p< 0.05$), 20:5 n-3 (0.35 ± 0.03, $p<0.001$) and 22:6 n-3 (0.24 ± 0.06, $p<0.001$, (Figure 3.6).

A similar trend in RAGE expression was observed when HUVECs were treated with BSA-GO derived AGEs, however, the increase was approximately 0.25-fold when compared with BSA only treatment. This is not unexpected as previously demonstrated that the BSA-MGO model generated more AGEs compared to BSA-GO (Section 2.3) [287]. In a similar trend to the BSA-MGO treatment of HUVECs with FA, the BSA-GO model showed significant reduction in RAGE expression in the following order: 18:1 n-9 (0.65 ± 0.13, $p<0.03$), 20:5 n-3 (0.50 ± 0.06, $p<0.009$) and 22:6 n-6 (0.59± 0.08, $p<0.009$) (Figure 3.6).

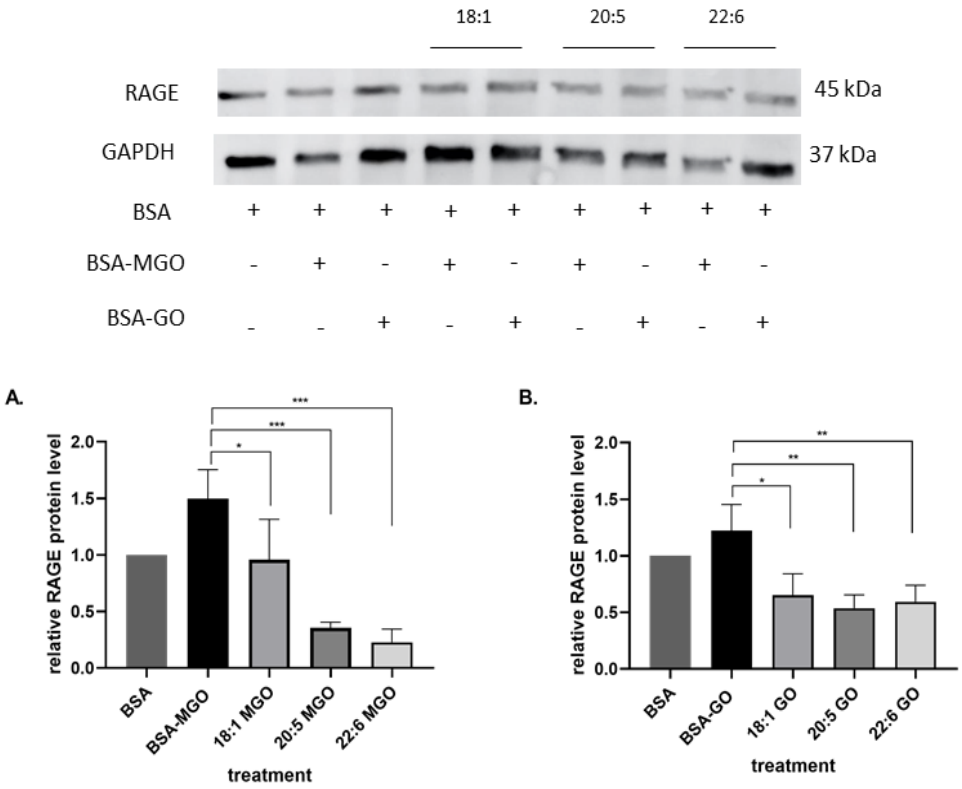


Figure 3.6 - The effect of fatty acids on dicarbonyl derived AGEs on RAGE expression in HUVECs

HUVECs were treated with BSA-MGO and BSA-MGO-FA (a.) and BSA-GO and BSA-MGO-FA (b) for a period of 72 h with relative RAGE expression quantified via immunoblotting. Results are expressed as mean ± SEM n=3, relative expression compared to an internal control (BSA-only) * $p< 0.05$, ** $p<0.009$ and *** $p<0.0009$. (a representative blot) RAGE – receptor for advanced glycation endproducts, GAPDH - glyceraldehyde 3 phosphate dehydrogenase, kDa- kilodaltons

3.4.5 – Inflammatory cytokine production in HUVECs treated with dicarbonyl-BSA derived AGEs with or without fatty acid pre-treatment.

HUVECs were cultured and treated as previously described (sections 3.3.7.1 and 3.3.7.2), to investigate the effect of dicarbonyl derived AGEs with and without FA on the level of inflammatory cytokine and chemokine production. Although 72 h was the timepoint for previous qPCR and western blotting experimentation, due to the kinetics of cytokine production this timepoint would not be suitable as IL-6 and IL-8 are released within 24 h [288-290]. At 72 h, degradation of these biomarkers is likely hence leading to an underestimate of production [291]. Both IL-1β and TNF-α were also assessed by ELISA however they were produced below the limit of quantification (LOQ). These are likely baseline changes and not in response to an agonist (dicarbonyl-derived AGE) stimulation

The data showed no significant change in the production of IL-6 in HUVECs pre-treated with any FA as compared to MGO-BSA control (Figure 3.7). With 18:1 n-9 (58.71 ± 8.13 pg/mL) and 20:5 n-3 (67.89 ± 8.94 pg/mL) treatment resulting in slight but not significant increases in IL-6 production. However 22:6 n-3 showed a decrease in secretion of IL-6 (27.91 ± 3.88 pg/mL), whilst not statistically significant it does fit in line with our hypothesis and previous published data demonstrating the ability of 22:6 n-3 to reduce proinflammatory cytokine production [292, 293]. Comparatively with the GO model, 18:1 n-9 demonstrated no effect, 20:5 n-3 increased IL-6 production (25.23 ± 13.55 pg/mL). Whilst following the same trend as MGO-BSA 22:6 n-3 exhibited a decrease in IL-6 production (6.13 ± 3.83 pg/mL). Whilst these results are not statically significant but still interesting and they would require further investigation into the mechanism of the interaction between the dicarbonyl and fatty acid.

The ELISA data showed a trend of increased IL-8 production in all 3 PUFA treatments as compared to BSA-MGO (Figure 3.8). While not statistically significant the MGO model showed 18:1 n-9 increased IL-8 (616.36 ± 51.95 pg/mL). However, 20:5 n-3 showed a significant increase (1752.77 ± 133.38 pg/mL, $p<0.002$) in IL-8 production, while 22:6 n-3 increased IL-8 production (552.91 ± 17.11 pg/mL) although not significantly. This data is contradictory to the original hypothesis that FA would have anti-inflammatory effects rather than pro-inflammatory. A similar trend was observed in the BSA-GO model, where all 3 FA resulted in an increase in IL-8 production albeit 18:1 n-9 and 22:6 n-3 having little to no effect, however 20:5 n-3 following the trend with the MGO model significantly increasing IL-8 by (1025.29 ± 43.12 pg/mL, $p<0.002$).

MCP-1 is a chemokine, that is secreted in response pro-inflammatory cytokines [294]. The levels of MCP-1 (Figure 3.9) in both the BSA-MGO and BSA-GO models showed no significant change in production when treated with FA as compared to BSA-dicarbonyl. Pre-treatment of HUVECS with 18:1 n-9 resulted in an increase in MCP-1 generation in the BSA-MGO (17.76 ± 5.04 pg/mL) model while in the BSA-GO model no effect was observed. This data while not statically significant is interesting and follows a similar trend to IL-6 and IL-8 data previously described. Contrasting to both IL-6 and IL-8 data, 20:5 n-3 decreased MCP-1 production in both BSA-MGO (2.31 ± 0.90 pg/mL) and BSA-GO (5.16 ± 2.67 pg/mL). Whilst HUVECs pre-treated with 22:6 n-3 also demonstrated an ability to decrease MCP-1 production in both the BSA-MGO model (8.21 ± 1.92 pg/mL) and the BSA-GO model (12.01 ± 0.42 pg/mL). However, whilst not statistically significant, the reduction in production of this pro inflammatory cytokine is interesting and fits with the experimental hypothesis that FA may have an ability to reduce the secretion of pro inflammatory cytokines and chemokines. The data would warrant

further investigation involving different conditions such as concentrations of FA, cell lines and additional chemokines along with kinetic studies for the different cytokines tested.

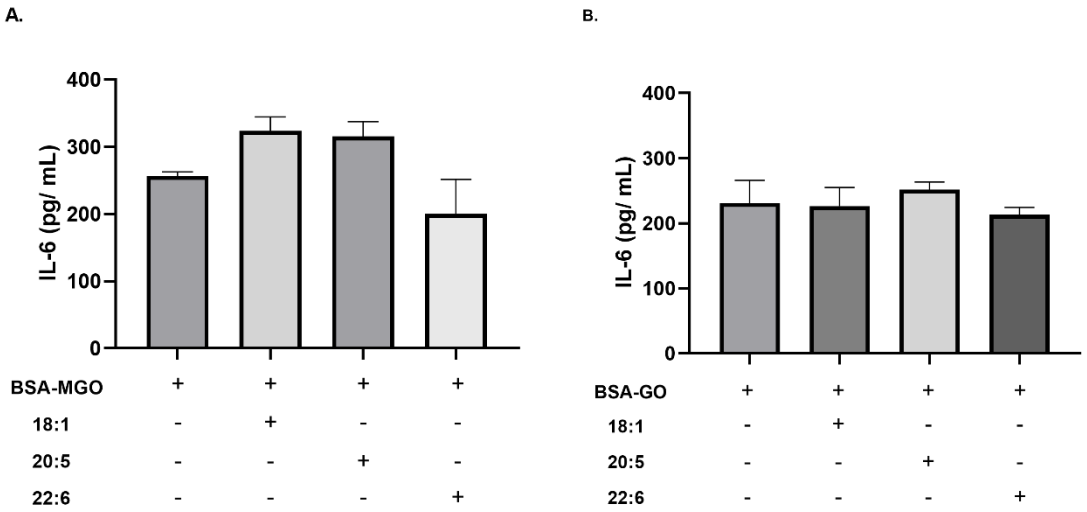


Figure 3.7 - Production of extracellular IL-6 by HUVECs treated with dicarbonyl derived AGEs

HUVECs were treated with BSA-dicarbonyl BSA (2 mM) with or without pre-treatment with fatty acid. **A**. BSA-MGO, **B**. BSA-GO. IL-6: interleukin 6, 18:1 – oleic acid (C18:1 n-9), 20:5 – eicosapentaenoic acid (C20:5 n-3) 22:6 – docosahexaenoic acid (C22:6 n-3). Results are expressed as mean ± SEM, relative expression compared to the internal control (BSA-only) n=3

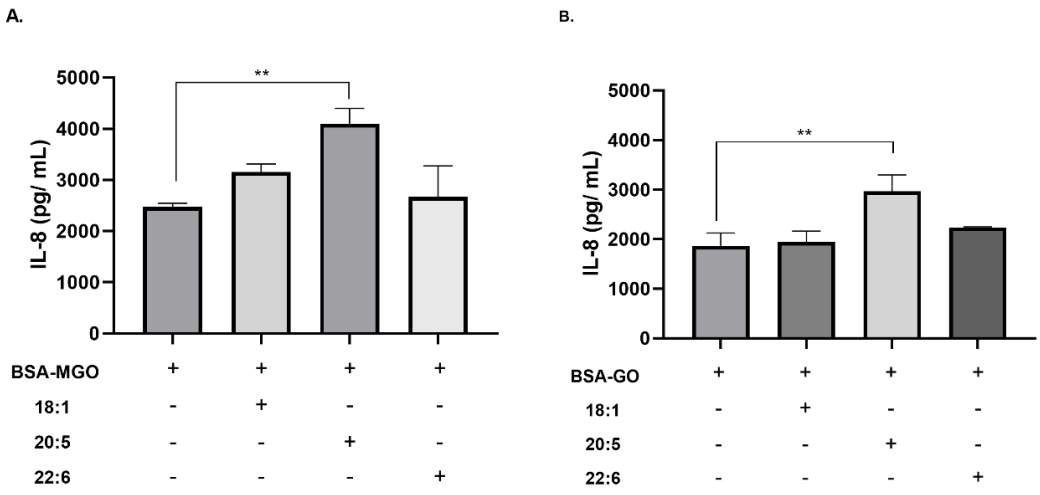


Figure 3.8 - Production of extracellular IL-8 by HUVECs treated with dicarbonyl derived AGEs

HUVECs were treated with BSA-dicarbonyl BSA (2 mM) with or without pre-treatment with fatty acid. **A**. BSA-MGO, **B**. BSA-GO. IL-8: interleukin 8, 18:1 – oleic acid (C18:1 n-9), 20:5 – eicosapentaenoic acid (C20:5 n-3) 22:6 – docosahexaenoic acid (C22:6 n-3) Results are expressed as mean ± SEM, relative expression compared to the internal control (BSA-only) ** represents $p< 0.002$.

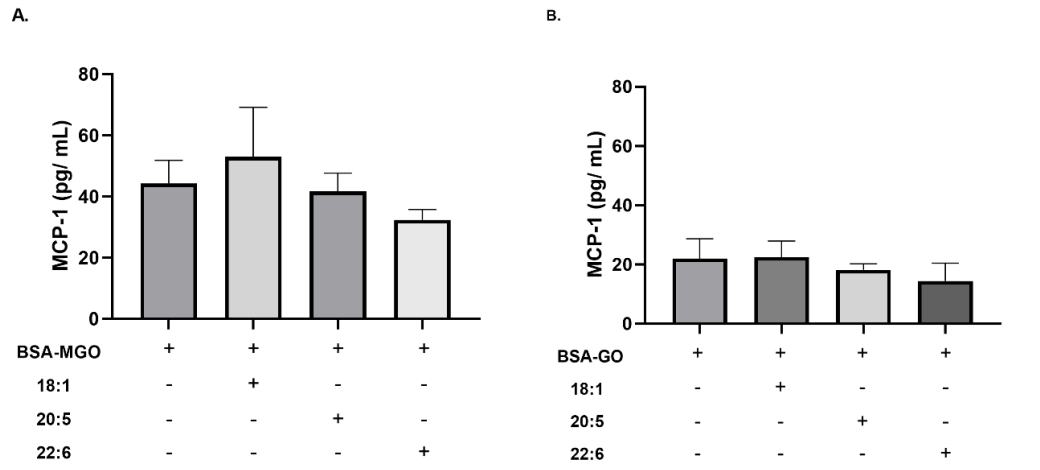


Figure 3.9 - Production of extracellular MCP-1 in HUVECs treated with dicarbonyl derived AGEs

HUVECs were treated with BSA-dicarbonyl BSA (2 mM) with or without pre-treatment with fatty acid. **A**. BSA-MGO, **B**. BSA-GO. MCP-1: monocyte chemoattractant protein 1, 18:1 – oleic acid (C18:1 n-9), 20:5 – eicosapentaenoic acid (C20:5 n-3) 22:6 – docosahexaenoic acid (C22:6 n-3) Results are expressed as mean ± SEM, relative expression compared to an internal control (BSA-only)

3.5 – Discussion

Multiple researchers have shown the binding of AGEs to RAGE can initiate signalling cascades which lead to increased production of pro-inflammatory mediators (IL-1β, IL-6, IL-8 and TNF-α) which are associated with diabetes and CVD, AD and cancer [78, 131, 136, 295-299]. AGEs have also been implicated in the progression of atherosclerosis, both directly and via AGE-RAGE interaction [298]. The importance of this AGE- RAGE interaction has been shown to alter cell signalling, promote gene expression [300], as well as promoting OS in numerous cell types, which all have detrimental effect on the cell [301]. Long chain unsaturated fatty acids have long been reported to be beneficial for general health as well as their reported ability to reduce inflammation [139, 140, 202, 218]. However, the role of specific fatty acids on AGE induced RAGE activation has not been reported.

Several previous studies have used primary HUVECs as a cell model for investigating AGE related RAGE activation and inflammation, since HUVECs express RAGE on their cell surface [280-282]. Although an already established model of RAGE expression in HUVECs exists, previous studies have focused on either glucose or fructose derived AGEs with no kinetic studies on dicarbonyl-derived AGEs on RAGE expression. Thus, in this study, firstly a time and concentration effect of dicarbonyl derived AGEs on RAGE expression in HUVEC was optimised. Following this model optimisation, the role of fatty acids on dicarbonyl-derived AGE induced RAGE expression in HUVECs was investigated.

A BSA-dicarbonyl model previously developed and optimised for quantification of protein-bound fluorescent and non-fluorescent AGE s [302] was required, and it was assessed for its suitability for cell culture treatments. Dicarbonyl-derived AGEs (MGO-BSA and GO-BSA 1 and 2 mM final) as well as an internal control (BSA) were assessed in both time and concentration-dependent manners to confirm AGEs levels were comparable to previous work. Quantification of AGEs both fluorometrically and via LCMS/MS confirmed the level of protein bound fluorescent AGEs and levels of CML, CEL and MG-H1 were comparable to those reported previously. The models were also evaluated for their effect on cell viability. Treatment with MGO-BSA and GO-BSA derived AGEs for 24 h, 48 h and 72 h showed no significant difference between 1 and 2 mM concentrations. All 3 timepoints showed toxicity of dicarbonyl-AGE treatment to a small extent as compared to no treatment control and as expected this toxicity increased with time. As the data suggests, after 72 h, 70% of cells were still viable. Given 2 mM of dicarbonyl is representative of a disease model, based on previous work within our group this concentration was used for the time and concentration dicarbonyl-BSA cell treatments. There is no reported literature involving the role of FA pretreatment on dicarbonyl-derived AGEs in HUVECs. FAs (18:1 n-9, 20:5 n-3, 22:6 n-3) that have previously demonstrated an ability to decrease AGE formation *in vitro* [302] (CML,CEL and MG-H1) were tested for their toxicity to HUVECs to rule out any compounded effect they may have on the cell. Concentrations ranging up to 30 µM were tested with results showing that at all 3 concentrations 18:1 n-9 demonstrated a small amount of toxicity, however 30 µM was too toxic as cell viability was reduced to 50% after 72 h of treatment. Given the lack of difference in cell viability between 10 and 20 µM, 20 µM was chosen as the ideal concentration in line with our previous work [302].

Kinetic studies did not show linear RAGE expression in HUVECs treated with BSA-dicarbonyl derived AGEs. Kinetic studies on dicarbonyl -derived AGE induced RAGE mRNA expression was first investigated to determine the relationship between mRNA and protein expression of RAGE. The data showed an interesting trend in RAGE expression at the mRNA level, with an initial significant increase (p<0.003) in RAGE expression after 24 h in both BSA-MGO and BSA-GO followed by a decrease at 48 h and an increase over basal level by 72h. A theory to explain this is perhaps that we are overserving an initial response in RAGE expression due to dicarbonyl -derived AGE treatment at 24 h, followed by some correction in the cell to limit expression of RAGE at 48 h and ultimately returning to basal levels by 72 h. A similar trend was seen when comparing dicarbonyl-derived AGE induced RAGE expression at the protein level. Indeed, from our data after 24 h of treatment, there is a small increase in RAGE expression when HUVECs were treated with BSA-MGO (1 and 2 mM) and also BSA-GO (1 mM) as determined by western blotting. This increase after 24 h is not dissimilar to work by Subedi *et al* (2020) who showed an increase in RAGE expression after 24h in microglial cells treated with MGO-derived AGEs [12]. However, their model used a much higher concentration of MGO (10 mM) and a significantly longer incubation (8 weeks) and no data quantification of total AGEs produced or any kinetics were presented. Interestingly in our model after 48 h of treatment RAGE expression decreased in all 4 treatments before increasing by approximately 0.25-fold over basal by 72 h. This result is interesting as the relationship between time and RAGE expression both at the mRNA and protein level was not linear. Another theory to explain the differences in expression at the varying timepoints could be resultant of an initial response of the cell to MGO/GO-BSA treatment in the first 24 h generating a state of oxidative or dicarbonyl stress, thus increasing RAGE expression [303]. By 72 h perhaps we are observing some form of chronic effect on the

cell, resulting in the increase of RAGE beyond the basal level. The reason for a decrease in RAGE expression at 48 h is unknown and requires further investigation including kinetic studies to detail RAGE transcription and translation over time. This is the first study that has reported RAGE expression measured by qPCR and WB over time using a protein bound MGO-BSA model of glycation and provides initial evidence for variable RAGE expression over a 72 h period for future studies to consider. Previous studies have shown RAGE expression to increase in HUVECs at a protein level when stimulated with LPS [296], and Zhang *et al* (2007) investigated RAGE expression in HUVECs treated with a highly glycated glucose-BSA model [304], however time and dicarbonyl concentration dependent expression of RAGE expression in HUVECs has not previously been reported. A limitation of our study would be that cell surface expression of RAGE was not measured. This could be measured using flow cytometry [304, 305], and would be interesting in terms of comparing the kinetics of dicarbonyl derived AGE induced RAGE expression data already generated via qPCR and western blotting with flow cytometry. This could further be compared with the role of fatty acids on receptor expression quantified via flow cytometry. However, although outside the scope of this study it is a potential future direction to expand on this work.

Following on from kinetic studies we sought to determine the role of a selection of fatty acids on dicarbonyl-AGE induced RAGE expression at both the mRNA and protein level. In a similar trend to the initial kinetic studies, we investigated the role of fatty acids on RAGE expression at the mRNA level to establish if a correlation exists. Both 18:1 n-9 and 22:6 n-3 significantly reduced RAGE mRNA expression in HUVECs, while 20:5 n-3 partially reduced expression, it did not reach statistical significance. The BSA-GO model showed no significant reduction in RAGE mRNA. These results are encouraging in terms of the ability of FAs to attenuate the expression of RAGE and, would require

further investigation and experimentation to evaluate their suitability as a potential therapeutic agent.

Fatty acids (18:1 n-9, 20:5 n-3 and 22:6 n-3) have previously been shown to reduce AGE formation *in vitro* [232, 302] however their effect on AGE induced RAGE expression is not documented. The identification of an appropriate positive control inhibitor of RAGE expression for use in these assays was a limitation. Aminoguanidine has been used previously as a reference inhibitor of glycation and RAGE expression in a similar study [306] although its understood mechanism of action primarily is through the inhibition of the formation of AGEs and within this study we have treated cells with already formed AGEs. Our group has demonstrated that aminoguanidine and quercetin pre-treatment increased RAGE expression in glucose-BSA induced WIL2-NS cells [179]. Other studies have investigated both natural and drug-based inhibitors for RAGE expression with varying results. Jahan *et al* (2021) showed the ability of an anti-diabetic drug (Gliclazide) to reduce AGE-RAGE induced inflammatory mediators [307]. A study by Chen *et al* (2015) investigating the ability of paeoniflorin, a monoterpene glycoside derived from the medicinal plant *Paeonia* showed that RAGE protein significantly increased by 40% after 6 h of AGE-BSA treatment in HUVECs as compared to a BSA only control and that pre-treatment for 30 min with paeoniflorin increased RAGE protein expression by 75% compared to a BSA only control [281]. Our study establishes a novel finding that 18:1 n-9, 20:5 n-3 and 22:6 n-3 significantly reduce MGO-derived AGE induced RAGE expression in HUVECs at the protein level.

It is important to note that the model system being used is based on a physiological system and to see significant changes in protein expression levels would be surprising and not a true representation of what is occurring in the cell. Large changes in protein expression levels are generally seen where the protein overexpressed or non-physiological levels of

both ligand and/or inhibitor are used. Thus, seeing statistically significant levels of reduction at physiological concentrations within a model system is promising.

This study aimed to further investigate if the anti-inflammatory effects of FA [140] could be observed in endothelial cells stimulated with dicarbonyl derived AGEs, via quantification on NF-κB mRNA. Much like RAGE mRNA levels we observed that HUVECs pre-treated with 18:1 n-9, 20:5 n-3 and 22:6 n-3 prior to MGO derived AGE treatment could significantly attenuate the expression of NF-κB as compared to the respective control. This reduction is consistent with other studies where a significant reduction in NF-κB was observed in HUVECs treated with glucose-derived AGEs and pre-treated with plant-based compounds [308, 309]. However, in the BSA-GO model although NF-κB was reduced it did not reach statistical significance. This is likely to be due to the decreased reactivity of GO, which is evident in our earlier work, where overall levels of GO derived protein bound fluorescent and non-fluorescent AGEs were significantly lower compared to MGO derived AGEs [302]. This decreased abundance of protein-bound AGEs in the GO model potentially binds less RAGE and thus fewer changes in expression of RAGE and NF-κB are seen. This data however is promising and suggests a novel finding that FA have an ability to decrease dicarbonyl induced expression of NF-κB within HUVECs. The exact mechanism within our model is not known but is of interest to further study within our group for future projects.

A possible theory is that FA increases the abundance of sRAGE. As sRAGE lacks the cytosolic tail domain essential for cellular signalling, it does not contribute to inflammatory response. In fact it is known to be a decoy receptor, due to its potential to inhibit FL-RAGE binding to the receptor by binding itself and clearance of circulating ligands [150, 151]. Also, sRAGE and form dimers with FL-RAGE, potentially inhibiting downstream pathway activation involved in RAGE stimulation. sRAGE has also been

reported to inhibit the assembly of RAGE on the cell surface [130]. Levels of sRAGE have been inversely correlated with serum levels of AGEs suggesting its involvement in affecting RAGE binding [310, 311]. However, the theory of FA upregulating sRAGE would require further investigation into quantifying sRAGE levels within the HUVEC model.

The glyoxylase enzymatic system is inbuilt detoxification system within the cytosol of most cells which eliminates AGE precursors and limits the natural accumulation of AGEs in tissues and includes the enzymes glyoxalase 1 (GLO 1) and glyoxalase 2 (GLO 2) [312]. GLO-1 inhibits the formation of methylglyoxal derived AGEs. Overexpression of GLO-1 has been demonstrated to prevent AGE accumulation in endothelial cells in vitro [313] and has also been shown to prevent increases in RAGE, S100A8, S100A12 and HMGB1 expression in vitro [111]. However in this model cells were treated with MGO derived protein-bound AGEs, rather than MGO directly, so there may be no change in the expression of GLO-1. It would still be of future interest to explore GLO-1 levels with in the HUVEC model system as a potential mechanism to decrease in RAGE expression.

Hering (2007) demonstrated that n-3 FAs inhibited NF-κB activation in pancreatic cancer cells [314] while other studies have presented that PUFA can inhibit the NF-κB, p38 MAPK and JNK pathways in microglial cells and HUVECs [315, 316], which are possible mechanisms within our model that could be investigated. It would also be interesting to develop a method to quantify products of polyunsaturated fatty acids decomposition, generated in a response to oxidation/damage of conjugated double bonds.

The production of IL-1β and IL-6 by endothelial cells triggers the upregulation of cell adhesion molecules (VCAM-1 and ICAM-1) aiding leukocyte adhesion to the vessel wall

and infiltration into tissues [278]. Production of IL-8 and MCP-1, chemokines, results in the recruitment of monocytes to the endothelium resulting in atherosclerotic plaque formation [131, 279]. Although we hypothesised that fatty acids would decrease the expression of AGE induced inflammatory cytokines and chemokines, the data did not show this. Indeed all 3 fatty acids showed no significant effect on reducing the production of IL-6, IL-8 or MCP-1 in this model. These results are not dissimilar to those observed by Mirhashemi *et al* (2016) who showed that omega 3 fatty acid supplementation had no effect on inflammatory cytokine production as compared to the placebo control [317]. There are several different pathways for cytokine secretion and perhaps AGE-RAGE induced signalling cascade to upregulate cytokine secretion are imitated by pathways not affected by fatty acids. This is a limitation of this study as different cytokines act on different pathways and are expressed at different timepoints. In this study, only a single timepoint for the collection was used (24 h). A kinetic study of each cytokine to determine the optimal time of secretion after treatment would be needed to optimise the study, however this was not achievable in this project due to time and expense constraints. Also potentially using a positive control such as lipopolysaccharide (LPS) to treat cells to ensure all cytokines being tested are produced within the cell, however this provides an area for us to explore in the future.

3.6 – Conclusion

The interaction of AGEs with RAGE is known to be detrimental to the cell and has been implicated with diseases such as diabetes and CVD by increasing inflammation and atherosclerosis. In this study we have shown previously unreported data demonstrating the kinetics of dicarbonyl induced AGEs and their interaction with RAGE at both protein and mRNA level, as expected there is a correlation between mRNA and protein expression. Although not linear the data from both qPCR and immunoblotting mirror one another. The addition of unsaturated fatty acids (18:1 n-9, 20:5 n-3 and 22:6 n-3) previously shown to reduce AGE induced CML, CEL and MG-H1 levels *in vitro* by our group were able to significantly reduce levels of RAGE expression in an endothelial cell model both at the protein and mRNA level along with the significant reduction of NF-κB. This body of work is previously unreported in the literature and significantly contributes to the field, although levels of inflammatory markers were not reduced significantly The evidence produced in this study warrants further studies into the role of fatty acids on AGE-RAGE induced inflammation, oxidate stress and DNA damage.

Chapter 4 – General discussion and future directions

4.1 – Introduction

The chapter aims to summarise the research outcomes from the studies described in the respective chapters and to explain how these experiments are related to each other. This chapter also explains the importance of developing a sound and physiologically relevant *in vitro* BSA-dicarbonyl model system that enables the investigation of fatty acids as a treatment against AGE-induced, RAGE mediated inflammation. The model system developed and optimised herein could potentially be used in future studies both within our group and within the AGE research field as an investigative tool to identify and determine the effect of a range of pharmaceutical agents/ compounds aimed at attenuating AGE-induced receptor expression, and cellular damage.

4.2 – The role of saturated and unsaturated fatty acids on dicarbonyl derived advanced glycation end products in vitro

4.2.1 – Develop and optimise a dicarbonyl-BSA model system

The literature reports a multitude of model systems to investigate AGEs *in vitro*. Both glucose-BSA and dicarbonyl-BSA (typically MGO) are used extensively. The focus of this study was to use a dicarbonyl-BSA model to generate AGEs. What is striking is that there are no standardized methods that direct researchers to appropriate model systems to generate physiologically relevant glycated albumin samples in vitro. There are large variations in the incubation times (hours to weeks) and the concentration of dicarbonyl used. Furthermore, the critical evaluation and description of the chemical profile of the

model system/s is lacking in studies that employ in vitro cell culture treatment with AGEs. Several studies have used concentrations of dicarbonyl well above physiologically relevance hence the interpretation of results would require caution [12, 318-320]. This thesis used 1 and 2 mM of dicarbonyl, which while higher than the typical cellular levels found (1-5 μM) reflect physiological processes which usually takes weeks to months, in a short period, [113, 257]. Further, the literature suggests minimally glycated albumin better reflects *in vivo* protein glycation [89, 321] while also reporting the inappropriateness of using highly glycated models for investigation [101, 322, 323]. There is great variation in AGE quantification in previous studies using a dicarbonyl model, where only fluorescent AGEs are quantified, or quantifying CML only, using a variety of techniques [320, 324-327]. The models that are used do not provide true levels of AGEs produced or indeed the levels or individual AGEs. This gap in the literature, therefore, required a robust and repeatable model to simultaneously quantify AGEs generated *in vitro* was developed that provided kinetics in both time and concentration-dependent manner.

The results of our study showed that after 3 days incubation, both fluorescent and non-fluorescent AGEs reached a plateau, reaffirming that a dicarbonyl-BSA model system does not require longer than 3 days incubation. These findings using fluorescent quantification accompanied with LCMS/MS provide a robustness, reliability and repeatability of our model system and a complete picture of which AGEs are generated and to what extent. CML has been one of the most common AGEs identified and measured in previous studies, however in this, CML, CEL and MG-H1 levels were quantified simultaneously. This thesis identified that MG-H1 was the AGE generated in most abundance in this model system. This is consistent with reports that MG-H1 accounts for >90% of glycation adducts *in vitro* and *in vivo* and is said to be the most

physiologically relevant MGO-derived AGE [82]. These results are consistent with more recent studies suggesting that MG-H1 has now emerged as the main AGE identified due to its cellular abundance accompanied with elevated serum levels associated with downstream effects of AGE-related disease implications [47, 61, 62, 328]. These results are significant as the data presented within this thesis has previously been unreported, with the quantification of individual AGEs making it a relevant model to investigate further inhibitors of glycation or potential treatments. Future studies into this model could further investigate and quantify more AGEs, for example total levels of, pentosidine, MG-H2 and MG-H3. As highly glycated models are prone to aggregation, measuring crosslinked AGEs (e.g., pentodilysine, GOLD, MOLD) in our minimally glycated model would be of interest, however the availability of deuterated standards may make this difficult.

4.2.2 – The role of fatty acids on dicarbonyl induced AGE production

The production of a reliable model system generating AGEs allowed further investigation into the role of fatty acids on AGE production. The results of this study showed that fatty acids can reduce dicarbonyl induced AGE production *in vitro.* AGEs are known to be pro-inflammatory in their nature [329, 330], and the results shown herein further support the knowledge of fatty acids having the ability to reduce inflammation both *in vitro* and *in vivo*. Whilst the exact mechanism of action is unclear and would require further experimentation, it may due to the FA be able to bind BSA [331, 332] similar to FA binding human serum albumin (HSA) in the blood [333, 334] or perhaps even bind with the dicarbonyl itself, either way preventing a BSA-dicarbonyl interaction and thus the limiting the generation of AGEs. There are still unanswered questions about the involvement of fatty acids and their role in the production of advanced lipoxidation

endproducts (ALEs) and if these have any effect within the model. In addition, our study did not focus on the peroxidation products of FA such as, malondialdehyde, aldehyde, 4-hydroxynonenal where subsequent amino acids modifications lead to the formation of ALEs. By determining the levels of these dialdehydes in the fatty acid treatment studies would have given a better understanding of CML and CEL levels as these are formed from both carbohydrates and lipids and referred to as AGEs/ALEs. However, given that CML and CEL levels generated from both MGO-BSA and GO-BSA models decreased with the addition of FA (Figure 2.6) one could speculate that no further ALEs are generated with the addition of FA. Or FA may be involved in both i.e. in the generation of CML/CEL and also play a role in inhibiting AGE formation. The lack of mechanistic understanding of the interaction of FAs with protein-bound AGEs provides opportunities for further studies and investigations into the dynamics of the relationship.

4.3 – The role of fatty acids on dicarbonyl-albumin induced expression of the receptor for advanced glycation end products and inflammatory markers in human endothelial cells

4.3.1 – Development and optimisation of an endothelial cell model

Previous studies have reported HUVECs as a valid model to investigate the effect of AGEs [304, 306, 308, 335], their role and potential inhibitors/therapeutic agents *in vitro*, however the concentration of reactants, incubation temperatures and purification method varied greatly between the AGE model systems used. Furthermore, the critical evaluation and description of the chemical profile of the model system/s is lacking in studies that employ *in vitro* cell culture treatment with AGEs, especially with respect to dicarbonyl-derived AGEs. Following on from our previous work, the need for an endothelial cell

model that was optimised to investigate changes in RAGE expression and subsequent downstream changes in inflammatory makers was crucial. We initially investigated the effect of dicarbonyl-derived AGEs on RAGE expression in HUVECSs in both time and concentration dependent studies. The model used needed to be reflective of the levels of AGEs produced in our previous work so that we could be certain any change in RAGE expression detected was a result of treatment with the AGEs. In comparison, results obtained from other studies that describe the toxic cellular effects induced by treatment with AGEs are generated in highly glycated model systems are likely to be unsuitable for extrapolation to *in vivo* situations of glycated albumin [318, 320, 336]. Therefore, studies in this thesis were performed to expand and improve on the previous work. The current study showed no difference in toxicity between AGE treated HUVECs in 24, 48 and 72 h time points, however found that dicarbonyl-AGE induced RAGE expression decreased at 48 h confirmed by both qPCR and western blotting. To be consistent with our previously optimised in vitro model (Chapter 2), 72 h was chosen to investigate changes in RAGE expression Future work could investigate the kinetics of dicarbonyl-derived AGEs on the different RAGE isoforms, applying the methodologies from Grossin *et al* (2009) [337] which would contribute to the field by providing details on RAGE isoforms in a time dependent manner.

4.3.2 – The effect of fatty acids on RAGE expression and inflammatory cytokines.

RAGE is a pattern recognition receptor, classified as a signaling receptor which has the ability to endorse both immune and inflammatory events such as cytokine production, immune cell infiltration and chronic inflammation [282, 338, 339]. Activated inflammatory cells can release damage-associated molecular patterns (DAMP) into the

extracellular matrix where they interact with RAGE and to promote immune signaling and inflammation [340]. This study demonstrated the ability of a selection of fatty acids to reduce dicarbonyl induced AGE stimulation of RAGE at both the protein and mRNA level. These results follow what was previously observed in chapter 2 where fatty acids showed an ability to reduce both fluorescent and non-fluorescent AGE levels, hence, we tested the hypothesis that FA would also reduce dicarbonyl-AGE induced RAGE expression. The results also further support the idea of the that fatty acids may have an anti-inflammatory effect *in vitro,* as RAGE has been shown to increase inflammatory makers in the cell previously.

Previous studies investigating a change in the production of inflammatory biomarkers in endothelial cells treated with dicarbonyl derived AGE models are lacking. Of the studies published, endothelial cells were treated with either far higher concentrations of dicabonyl derived AGEs than in our model (10-50 mg/mL BSA and 20-55 mM MGO), or glucose or glyceraldehyde derived AGEs which may elucidate different changes in the cell. The resultant increases in inflammatory makers were determined via qPCR, western blotting or ELISA, however, these studies lacked characterisation to establish the extent of glycation in these model systems, reporting only an observation of an increase in arbitrary fluorescence [197, 308, 335, 341, 342]. This thesis study did not show any significant increase in inflammatory cytokine production in HUVECs -treated with dicarbonyl-derived AGEs. These conflicting results to published literature makes it difficult to interpret our observations. Whether the non-significant increase in the inflammatory biomarkers quantified in this thesis is resultant of less total protein-bound AGEs being formed in the dicarbonyl-derived AGE model system, and/or less suspected albumin aggregation compared to highly glycated model systems used in similar glucose

derived AGE studies [320, 336] requires further investigation. Although an increase in RAGE expression was quantified it was not considerable as originally hypothesised. This lower level of dicarbonyl-derived RAGE induction is likely reflective of the levels of NF-κB and inflammatory cytokines observed in our model.

Whilst the results are not in line with previous studies of fatty acids reducing pro-inflammatory cytokines *in vitro* [343-345], there are several possible explanations for this result. For example, the ability of FA to significantly reduce already low levels of inflammatory markers must be considered. Different cytokines are expressed at different timepoints, not all cell lines express the same cytokines, and cytokines are induced via different pathways. Further progress and investigation into the role of fatty acids on RAGE induced cytokine expression is warranted, including the use of a positive control for stimulation of cytokine within HUVECs, accompanied by appropriate kinetic studies to optimise the time profile for the cytokines of interest to ensure no degradation of samples. Lastly to the investigate mechanism or pathways of cytokine secretion within HUVECs

4.4 – Conclusion

The development of a physiologically relevant, robust and reliable model to investigate AGEs *in vitro* is crucial to the research field to investigate the efficacy of novel compounds or agents targeting the reduction of AGE production or indeed AGE induced RAGE expression the associated downstream complications. The project described in this thesis has developed a model system of dicarbonyl induced AGEs that is more physiologically relevant, using a cell line that has previously been validated for AGE studies. The results from this thesis have shown for the first time that both saturated FA (4:0, 14:0, 16:0 and 20:0) and unsaturated FA (18:1 n-9, 18:2 n-6, 18:3 n-3, 20:4 n-6, 20:5 n-3 and 22:6 n-3) are able reduce dicarbonyl induced CML and CEL production, whilst PUFA (18:1 n-9, 20:5 n-3 and 22:6 n-3) showed a significant reduction in dicarbonyl induced RAGE expression. The outcomes of this thesis advance the field by providing an improved pre-clinical model with enhanced efficiency to identify and determine the effect fatty acids in RAGE mediated inflammation induced by AGEs.

References

1. Singh, R., A. Barden, T. Mori, and L. Beilin.(2001) Advanced glycation end-products: a review. *Diabetologia*. 44(2): p. 129-146.
2. Ono, Y., S. Aoki, K. Ohnishi, T. Yasuda, K. Katsumi, and Y. Tsukada.(1998) Increased serum levels of advanced glycation end-products and diabetic complications. *Diabetes Research and Clinical Practice*. 41(2): p. 131-137.
3. Teerlink, T., R. Barto, H.J. ten Brink, and C.G. Schalkwijk.(2004) Measurement of Nε-(Carboxymethyl)lysine and Nε-(Carboxyethyl)lysine in Human Plasma Protein by Stable-Isotope-Dilution Tandem Mass Spectrometry. *Clinical Chemistry*. 50(7): p. 1222-1228.
4. Matsui, T., N. Nakamura, A. Ojima, Y. Nishino, and S.i. Yamagishi.(2016) Sulforaphane reduces advanced glycation end products (AGEs)-induced inflammation in endothelial cells and rat aorta. *Nutrition, Metabolism and Cardiovascular Diseases*. 26(9): p. 797-807.
5. Sena, C.M., P. Matafome, J. Crisóstomo, L. Rodrigues, R. Fernandes, P. Pereira, and R.M. Seiça.(2012) Methylglyoxal promotes oxidative stress and endothelial dysfunction. *Pharmacological Research*. 65(5): p. 497-506.
6. Thorpe, S.R. and J.W. Baynes.(2003) Maillard reaction products in tissue proteins: New products and new perspectives. *Amino Acids*. 25(3): p. 275-281.
7. Rondeau, P., N.R. Singh, H. Caillens, F. Tallet, and E. Bourdon.(2008) Oxidative stresses induced by glycoxidized human or bovine serum albumin on human monocytes. *Free Radic Biol Med*. 45(6): p. 799-812.
8. N., A. and T.P. J.(2007) Advanced glycation endproducts: what is their relevance to diabetic complications? *Diabetes, Obesity and Metabolism*. 9(3): p. 233-245.
9. Beverly, J.K. and M.J. Budoff.(2020) Atherosclerosis: Pathophysiology of insulin resistance, hyperglycemia, hyperlipidemia, and inflammation. *J Diabetes*. 12(2): p. 102-104.
10. Ruiz, H.H., R. Ramasamy, and A.M. Schmidt.(2020) Advanced Glycation End Products: Building on the Concept of the "Common Soil" in Metabolic Disease. *Endocrinology*. 161(1): p. bqz006.
11. Tessier, F.J. and I. Birlouez-Aragon.(2012) Health effects of dietary Maillard reaction products: the results of ICARE and other studies. *Amino Acids*. 42(4): p. 1119-31.
12. Subedi, L., J.H. Lee, B.P. Gaire, and S.Y. Kim.(2020) Sulforaphane Inhibits MGO-AGE-Mediated Neuroinflammation by Suppressing NF-κB, MAPK, and AGE–RAGE Signaling Pathways in Microglial Cells. 9(9): p. 792.
13. Byun, K., Y. Yoo, M. Son, J. Lee, G.-B. Jeong, Y.M. Park, G.H. Salekdeh, and B. Lee.(2017) Advanced glycation end-products produced systemically and by macrophages: A common contributor to inflammation and degenerative diseases. *Pharmacology & Therapeutics*. 177: p. 44-55.
14. Thornalley, P.J., A. Langborg, and H.S. Minhas.(1999) Formation of glyoxal, methylglyoxal and 3-deoxyglucosone in the glycation of proteins by glucose. *Biochemical Journal*. 344(1): p. 109-116.
15. Younessi, P. and A. Yoonessi.(2011) Advanced glycation end-products and their receptor-mediated roles: Inflammation and oxidative stress. *Iranian Journal of Medical Sciences*. 36(3): p. 154-166.
16. Piperi, C., C. Adamopoulos, and A.G. Papavassiliou.(2017) Potential of glycative stress targeting for cancer prevention. *Cancer Letters*. 390: p. 153-159.

17. Shaikh, S. and L.F. Nicholson.(2008) Advanced glycation end products induce in vitro cross-linking of alpha-synuclein and accelerate the process of intracellular inclusion body formation. *J Neurosci Res*. 86(9): p. 2071-82.
18. Bence, N.F., R.M. Sampat, and R.R. Kopito.(2001) Impairment of the ubiquitin-proteasome system by protein aggregation. *Science*. 292(5521): p. 1552-5.
19. Bruel, A. and H. Oxlund.(1996) Changes in biomechanical properties, composition of collagen and elastin, and advanced glycation endproducts of the rat aorta in relation to age. *Atherosclerosis*. 127(2): p. 155-65.
20. Neelofar, K. and J. Ahmad.(2017) An overview of in vitro and in vivo glycation of albumin: a potential disease marker in diabetes mellitus. *Glycoconjugate Journal*. 34(5): p. 575-584.
21. Bierhaus, A., P.M. Humpert, M. Morcos, T. Wendt, T. Chavakis, B. Arnold, D.M. Stern, and P.P. Nawroth.(2005) Understanding RAGE, the receptor for advanced glycation end products. *Journal of Molecular Medicine*. 83(11): p. 876-886.
22. Davies, J., D. Gonzalez, and R.S. Conlan.(2017) Regulation of the receptor for advanced glycation end products by estrogen receptor ligands in endometrial cancer. *Cancer Research*. 77(13 Supplement): p. 5504-5504.
23. Thornalley, P.J.(2005) Dicarbonyl intermediates in the maillard reaction. *Ann N Y Acad Sci*. 1043(1): p. 111-7.
24. Lima, M., S.H. Assar, and J.M. Ames.(2010) Formation of Nε-(Carboxymethyl)lysine and Loss of Lysine in Casein Glucose−Fatty Acid Model Systems. *Journal of Agricultural and Food Chemistry*. 58(3): p. 1954-1958.
25. Nowotny, K., T. Jung, A. Höhn, D. Weber, and T. Grune.(2015) Advanced Glycation End Products and Oxidative Stress in Type 2 Diabetes Mellitus. *Biomolecules*. 5(1): p. 194.
26. Nigro, C., A. Leone, F. Fiory, I. Prevenzano, A. Nicolò, P. Mirra, F. Beguinot, and C. Miele.(2019) Dicarbonyl Stress at the Crossroads of Healthy and Unhealthy Aging. *Cells*. 8(7): p.
27. Jakus, V. and N. Rietbrock.(2004) Advanced glycation end-products and the progress of diabetic vascular complications. *Physiol Res*. 53(2): p. 131-42.
28. Kiho, T., M. Kato, S. Usui, and K. Hirano.(2005) Effect of buformin and metformin on formation of advanced glycation end products by methylglyoxal. *Clinica Chimica Acta*. 358(1): p. 139-145.
29. Ling, A.R.(1908) Malting. *Journal of the Institute of Brewing*. 14(6): p. 494-521.
30. Rahbar, S.(1968) An abnormal hemoglobin in red cells of diabetics. *Clinica Chimica Acta*. 22(2): p. 296-298.
31. Anet, E.F.L.J., *3-Deoxyglycosuloses (3-Deoxyglycosones) and the Degradation of Carbohydrates*, in *Advances in Carbohydrate Chemistry*, M.L. Wolfrom, Editor. 1964, Academic Press. p. 181-218.
32. Alberts B, J.A., Lewis J, Raff M, Roberts K, and Walter P, *Molecular Biology of the Cell*. 4th ed. 2002, New York: GArland Science.
33. Goldin, A., J.A. Beckman, A.M. Schmidt, and M.A. Creager.(2006) Advanced Glycation End Products. *Sparking the Development of Diabetic Vascular Injury*. 114(6): p. 597-605.
34. Tessier, F.J.(2010) The Maillard reaction in the human body. The main discoveries and factors that affect glycation. *Pathologie Biologie*. 58(3): p. 214-219.

35. Bohlender, J., S. Franke, G. Stein, and G. Wolf, *Advanced glycation end products and the kidney*. Vol. 289. 2005. F645-59.
36. Wolff, S.P. and R.T. Dean.(1987) Glucose autoxidation and protein modification. The potential role of 'autoxidative glycosylation' in diabetes. *Biochemical Journal*. 245(1): p. 243-250.
37. Thornalley, P., S. Wolff, J. Crabbe, and A. Stern.(1984) The autoxidation of glyceraldehyde and other simple monosaccharides under physiological conditions catalysed by buffer ions. *Biochim Biophys Acta*. 797(2): p. 276-87.
38. Miyata, T., K. Kurokawa, and C. Van Ypersele De Strihou.(2000) Advanced Glycation and Lipoxidation End Products: Role of Reactive Carbonyl Compounds Generated during Carbohydrate and Lipid Metabolism. *Journal of the American Society of Nephrology*. 11(9): p. 1744-1752.
39. Vistoli, G., D. De Maddis, A. Cipak, N. Zarkovic, M. Carini, and G. Aldini.(2013) Advanced glycoxidation and lipoxidation end products (AGEs and ALEs): an overview of their mechanisms of formation. *Free Radical Research*. 47(sup1): p. 3-27.
40. Brings, S., T. Fleming, M. Freichel, M.U. Muckenthaler, S. Herzig, and P.P. Nawroth.(2017) Dicarbonyls and Advanced Glycation End-Products in the Development of Diabetic Complications and Targets for Intervention. *Int J Mol Sci*. 18(5): p. 984.
41. O'Brien, P.J., A.G. Siraki, and N. Shangari.(2005) Aldehyde Sources, Metabolism, Molecular Toxicity Mechanisms, and Possible Effects on Human Health. *Critical Reviews in Toxicology*. 35(7): p. 609-662.
42. Yin, H. and N.A. Porter.(2005) New Insights Regarding the Autoxidation of Polyunsaturated Fatty Acids. *Antioxidants & Redox Signaling*. 7(1-2): p. 170-184.
43. Bucala, R., Z. Makita, T. Koschinsky, A. Cerami, and H. Vlassara.(1993) Lipid advanced glycosylation: pathway for lipid oxidation in vivo. *Proceedings of the National Academy of Sciences*. 90(14): p. 6434-6438.
44. Mlakar, A. and G. Spiteller.(1996) Previously unknown aldehydic lipid peroxidation compounds of arachidonic acid. *Chemistry and Physics of Lipids*. 79(1): p. 47-53.
45. Wang, Y., H. Hu, D.J. McClements, S. Nie, M. Shen, C. Li, Y. Huang, J. Chen, M. Zeng, and M. Xie.(2019) Effect of fatty acids and triglycerides on the formation of lysine-derived advanced glycation end-products in model systems exposed to frying temperature. *RSC Advances*. 9(27): p. 15162-15170.
46. Chen, J.-H., X. Lin, C. Bu, and X. Zhang.(2018) Role of advanced glycation end products in mobility and considerations in possible dietary and nutritional intervention strategies. *Nutrition & Metabolism*. 15(1): p. 72.
47. Schalkwijk, C.G. and C.D.A. Stehouwer.(2020) Methylglyoxal, a Highly Reactive Dicarbonyl Compound, in Diabetes, Its Vascular Complications, and Other Age-Related Diseases. *Physiol Rev*. 100(1): p. 407-461.
48. Hamada, Y., N. Araki, N. Koh, J. Nakamura, S. Horiuchi, and N. Hotta.(1996) Rapid Formation of Advanced Glycation End Products by Intermediate Metabolites of Glycolytic Pathway and Polyol Pathway. *Biochemical and Biophysical Research Communications*. 228(2): p. 539-543.
49. Brownlee, M.(2001) Biochemistry and molecular cell biology of diabetic complications. *Nature*. 414: p. 813.

50. Chung, S.S.M., E.C.M. Ho, K.S.L. Lam, and S.K. Chung.(2003) Contribution of Polyol Pathway to Diabetes-Induced Oxidative Stress. *Journal of the American Society of Nephrology*. 14(suppl 3): p. S233-S236.
51. Hamada, Y., N. Araki, S. Horiuchi, and N. Hotta.(1996) Role of polyol pathway in nonenzymatic glycation. *Nephrology Dialysis Transplantation*. 11(supp5): p. 95-98.
52. Grewal, A.S., S. Bhardwaj, D. Pandita, V. Lather, and B.S. Sekhon.(2016) Updates on Aldose Reductase Inhibitors for Management of Diabetic Complications and Non-diabetic Diseases. *Mini Rev Med Chem*. 16(2): p. 120-62.
53. Chalk, C., T.J. Benstead, and F. Moore.(2007) Aldose reductase inhibitors for the treatment of diabetic polyneuropathy. *Cochrane Database Syst Rev*. 2007(4): p. Cd004572.
54. Hamada, Y., J. Nakamura, K. Naruse, T. Komori, K. Kato, Y. Kasuya, R. Nagai, S. Horiuchi, and N. Hotta.(2000) Epalrestat, an aldose reductase ihibitor, reduces the levels of Nepsilon-(carboxymethyl)lysine protein adducts and their precursors in erythrocytes from diabetic patients. *Diabetes Care*. 23(10): p. 1539-1544.
55. Hamada, Y., J. Nakamura, K. Naruse, T. Komori, K. Kato, Y. Kasuya, R. Nagai, S. Horiuchi, and N. Hotta.(2000) Epalrestat, an aldose reductase ihibitor, reduces the levels of Nepsilon-(carboxymethyl) lysine protein adducts and their precursors in erythrocytes from diabetic patients. *Diabetes Care*. 23(10): p. 1539-1544.
56. Oliveira, M.I.A., E.M.d. Souza, F.d.O. Pedrosa, R.R. Réa, A.d.S.C. Alves, G. Picheth, and F.G.d.M. Rego.(2013) RAGE receptor and its soluble isoforms in diabetes mellitus complications. *Jornal Brasileiro de Patologia e Medicina Laboratorial*. 49: p. 97-108.
57. Yu, P., X.-B. Xu, and S.-J. Yu.(2017) Inhibitory effect of sugarcane molasses extract on the formation of Nε-(carboxymethyl)lysine and Nε-(carboxyethyl)lysine. *Food Chemistry*. 221: p. 1145-1150.
58. Wells-Knecht, K.J., E. Brinkmann, M.C. Wells-Knecht, J.E. Litchfield, M.U. Ahmed, S. Reddy, D.V. Zyzak, S.R. Thorpe, and J.W. Baynes.(1996) New biomarkers of Maillard reaction damage to proteins. *Nephrology Dialysis Transplantation*. 11(supp5): p. 41-47.
59. Rabbani, N. and P.J. Thornalley.(2014) Dicarbonyl proteome and genome damage in metabolic and vascular disease. *Biochem Soc Trans*. 42(2): p. 425-32.
60. Marinucci, L., S. Balloni, K. Fettucciari, M. Bodo, V.N. Talesa, and C. Antognelli.(2018) Nicotine induces apoptosis in human osteoblasts via a novel mechanism driven by H2O2 and entailing Glyoxalase 1-dependent MG-H1 accumulation leading to TG2-mediated NF-kB desensitization: Implication for smokers-related osteoporosis. *Free Radical Biology and Medicine*. 117: p. 6-17.
61. Kilhovd, B.K., A. Juutilainen, S. Lehto, T. Ronnemaa, P.A. Torjesen, K.F. Hanssen, and M. Laakso.(2009) Increased serum levels of methylglyoxal-derived hydroimidazolone-AGE are associated with increased cardiovascular disease mortality in nondiabetic women. *Atherosclerosis*. 205(2): p. 590-4.
62. Zhang, W., E.W. Randell, G. Sun, S. Likhodii, M. Liu, A. Furey, and G. Zhai.(2017) Hyperglycemia-related advanced glycation end-products is associated with the altered phosphatidylcholine metabolism in osteoarthritis patients with diabetes. *PLOS ONE*. 12(9): p. e0184105.

63. Bettiga, A., F. Fiorio, F. Di Marco, F. Trevisani, A. Romani, E. Porrini, A. Salonia, F. Montorsi, and R. Vago.(2019) The Modern Western Diet Rich in Advanced Glycation End-Products (AGEs): An Overview of Its Impact on Obesity and Early Progression of Renal Pathology. *Nutrients*. 11(8): p. 1748.
64. Grandhee, S.K. and V.M. Monnier.(1991) Mechanism of formation of the Maillard protein cross-link pentosidine. Glucose, fructose, and ascorbate as pentosidine precursors. *Journal of Biological Chemistry*. 266(18): p. 11649-11653.
65. Sell, D.R., A. Lapolla, P. Odetti, J. Fogarty, and V.M. Monnier.(1992) Pentosidine Formation in Skin Correlates With Severity of Complications in Individuals With Long-Standing IDDM. *Diabetes*. 41(10): p. 1286-1292.
66. Wadman, S.K., P.K. Debree, F.J. Vansprang, J.P. Kamerling, J. Haverkamp, and J.F.G. Vliegenthart.(1975) Ne-(Carboxymethyl)Lysine, a Constituent of Human Urine. *Clinica Chimica Acta*. 59(3): p. 313-320.
67. Fu, M.-X., J.R. Requena, A.J. Jenkins, T.J. Lyons, J.W. Baynes, and S.R. Thorpe.(1996) The Advanced Glycation End Product, N-(Carboxymethyl)lysine, Is a Product of both Lipid Peroxidation and Glycoxidation Reactions. *Journal of Biological Chemistry*. 271(17): p. 9982-9986.
68. Henning, C. and M.A. Glomb.(2016) Pathways of the Maillard reaction under physiological conditions. *Glycoconjugate Journal*. 33(4): p. 499-512.
69. Delgado-Andrade, C.(2016) Carboxymethyl-lysine: thirty years of investigation in the field of AGE formation. *Food & Function*. 7(1): p. 46-57.
70. Kurt, A., G. Andican, Z.O. Siva, A. Andican, and G. Burcak.(2016) The effects of n-3 long-chain polyunsaturated fatty acid supplementation on AGEs and sRAGE in type 2 diabetes mellitus. *Journal of Physiology and Biochemistry*. 72(4): p. 679-687.
71. Deo, P., J.B. Keogh, N.J. Price, and P.M. Clifton.(2017) Effects of Weight Loss on Advanced Glycation End Products in Subjects with and without Diabetes: A Preliminary Report. *International Journal of Environmental Research and Public Health*. 14(12): p. 1553.
72. Boehm, B.O., S. Schilling, S. Rosinger, G.E. Lang, G.K. Lang, R. Kientsch-Engel, and P. Stahl.(2004) Elevated serum levels of N ε-carboxymethyl-lysine, an advanced glycation end product, are associated with proliferative diabetic retinopathy and macular oedema. *Diabetologia*. 47(8): p. 1376-1379.
73. Wautier, M.P., P. Massin, P.J. Guillausseau, M. Huijberts, B. Levy, E. Boulanger, M. Laloi-Michelin, and J.L. Wautier.(2003) N(carboxymethyl)lysine as a biomarker for microvascular complications in type 2 diabetic patients. *Diabetes & Metabolism*. 29(1): p. 44-52.
74. Ahmed, M.U., E.B. Frye, T.P. Degenhardt, S.R. Thorpe, and J.W. Baynes.(1997) Nε-(Carboxyethyl)lysine, a product of the chemical modification of proteins by methylglyoxal, increases with age in human lens proteins. 324(2): p. 565-570.
75. Kuang, L., Z. Jing, J. Wang, L. Ma, X. Liu, and J. Yang.(2014) Quantitative determination of ε-N-carboxymethyl-l-lysine in human plasma by liquid chromatography–tandem mass spectrometry. *Journal of Pharmaceutical and Biomedical Analysis*. 90: p. 1-6.
76. Hanssen, N.M.J., L. Engelen, I. Ferreira, J.L.J.M. Scheijen, M.S. Huijberts, M.M.J. van Greevenbroek, C.J.H. van der Kallen, J.M. Dekker, G. Nijpels, C.D.A. Stehouwer, and C.G. Schalkwijk.(2013) Plasma Levels of Advanced Glycation Endproducts Nϵ-(carboxymethyl)lysine, Nϵ-(carboxyethyl)lysine, and

Pentosidine Are not Independently Associated With Cardiovascular Disease in Individuals With or Without Type 2 Diabetes: The Hoorn and CODAM Studies. *The Journal of Clinical Endocrinology & Metabolism*. 98(8): p. E1369-E1373.
77. Rabbani, N. and P.J.J.A.A. Thornalley.(2012) Methylglyoxal, glyoxalase 1 and the dicarbonyl proteome. 42(4): p. 1133-1142.
78. Fosmark, D.S., P.A. Torjesen, B.K. Kilhovd, T.J. Berg, L. Sandvik, K.F. Hanssen, C.-D. Agardh, and E. Agardh.(2006) Increased serum levels of the specific advanced glycation end product methylglyoxal-derived hydroimidazolone are associated with retinopathy in patients with type 2 diabetes mellitus. *Metabolism - Clinical and Experimental*. 55(2): p. 232-236.
79. Stratmann, B., B. Engelbrecht, B.C. Espelage, N. Klusmeier, J. Tiemann, T. Gawlowski, Y. Mattern, M. Eisenacher, H.E. Meyer, N. Rabbani, P.J. Thornalley, D. Tschoepe, G. Poschmann, and K. Stühler.(2016) Glyoxalase 1-knockdown in human aortic endothelial cells – effect on the proteome and endothelial function estimates. *Scientific Reports*. 6: p. 37737.
80. Thornalley, P.J., S. Battah, N. Ahmed, N. Karachalias, S. Agalou, R. Babaei-Jadidi, and A. Dawnay.(2003) Quantitative screening of advanced glycation endproducts in cellular and extracellular proteins by tandem mass spectrometry. *Biochem J*. 375(Pt 3): p. 581-92.
81. Ahmed, N., P.J. Thornalley, J. Dawczynski, S. Franke, J. Strobel, G.n. Stein, and G.M. Haik.(2003) Methylglyoxal-Derived Hydroimidazolone Advanced Glycation End-Products of Human Lens Proteins. *Investigative Ophthalmology & Visual Science*. 44(12): p. 5287-5292.
82. Schumacher, D., J. Morgenstern, Y. Oguchi, N. Volk, S. Kopf, J.B. Groener, P.P. Nawroth, T. Fleming, and M. Freichel.(2018) Compensatory mechanisms for methylglyoxal detoxification in experimental & clinical diabetes. *Molecular Metabolism*. 18: p. 143-152.
83. Xue, M., M.O. Weickert, S. Qureshi, N.-B. Kandala, A. Anwar, M. Waldron, A. Shafie, D. Messenger, M. Fowler, G. Jenkins, N. Rabbani, and P.J. Thornalley.(2016) Improved Glycemic Control and Vascular Function in Overweight and Obese Subjects by Glyoxalase 1 Inducer Formulation. *Diabetes*. 65(8): p. 2282-2294.
84. Šebeková, K.n., V. Kupčová, R. Schinzel, and A. Heidland.(2002) Markedly elevated levels of plasma advanced glycation end products in patients with liver cirrhosis – amelioration by liver transplantation. *Journal of Hepatology*. 36(1): p. 66-71.
85. Knecht, K.J., J.A. Dunn, K.F. McFarland, D.R. McCance, T.J. Lyons, S.R. Thorpe, and J.W. Baynes.(1991) Effect of Diabetes and Aging on Carboxymethyllysine Levels in Human Urine. *Diabetes*. 40(2): p. 190-196.
86. Gopal, P., N.L. Reynaert, J.L.J.M. Scheijen, L. Engelen, C.G. Schalkwijk, F.M.E. Franssen, E.F.M. Wouters, and E.P.A. Rutten.(2014) Plasma advanced glycation end-products and skin autofluorescence are increased in COPD. *European Respiratory Journal*. 43(2): p. 430-438.
87. Lieuw-A-Fa, M.L.M., V.W.M. van Hinsbergh, T. Teerlink, R. Barto, J. Twisk, C.D.A. Stehouwer, and C.G. Schalkwijk.(2004) Increased levels of Nϵ-(carboxymethyl)lysine and Nϵ-(carboxyethyl)lysine in type 1 diabetic patients with impaired renal function: correlation with markers of endothelial dysfunction. *Nephrology Dialysis Transplantation*. 19(3): p. 631-636.
88. van Eupen, M.G.A., M.T. Schram, H.M. Colhoun, J.L.J.M. Scheijen, C.D.A. Stehouwer, and C.G. Schalkwijk.(2013) Plasma levels of advanced glycation

endproducts are associated with type 1 diabetes and coronary artery calcification. *Cardiovascular Diabetology*. 12(1): p. 149.
89. Ahmed, N., R. Babaei-Jadidi, S.K. Howell, P.J. Beisswenger, and P.J. Thornalley.(2005) Degradation products of proteins damaged by glycation, oxidation and nitration in clinical type 1 diabetes. *Diabetologia*. 48(8): p. 1590-1603.
90. Miyata, S. and V. Monnier.(1992) Immunohistochemical detection of advanced glycosylation end products in diabetic tissues using monoclonal antibody to pyrraline. *The Journal of Clinical Investigation*. 89(4): p. 1102-1112.
91. Aso, Y., K. Takanashi, K. Sekine, N. Yoshida, K. Takebayashi, K. Yoshihara, and T. Inukai.(2004) Dissociation between urinary pyrraline and pentosidine concentrations in diabetic patients with advanced nephropathy. *Journal of Laboratory and Clinical Medicine*. 144(2): p. 92-99.
92. Portero-otín, M., R. Pamplona, M.J. Bellmunt, M. Bergua, R.H. Nagaraj, and J. Prat.(1996) Urinary pyrraline as a biochemical marker of non-oxidative maillard reactions in vivo. *Life Sciences*. 60(4): p. 279-287.
93. Sanaka, T., T. Funaki, T. Tanaka, S. Hoshi, J. Niwayama, T. Taitoh, H. Nishimura, and C. Higuchi.(2002) Plasma Pentosidine Levels Measured by a Newly Developed Method Using ELISA in Patients with Chronic Renal Failure. *Nephron*. 91(1): p. 64-73.
94. Odani, H., Y. Matsumoto, T. Shinzato, J. Usami, and K. Maeda.(1999) Mass spectrometric study on the protein chemical modification of uremic patients in advanced Maillard reaction. *Journal of Chromatography B: Biomedical Sciences and Applications*. 731(1): p. 131-140.
95. Kellow, N.J. and M.T. Coughlan.(2015) Effect of diet-derived advanced glycation end products on inflammation. *Nutrition Reviews*. 73(11): p. 737-759.
96. Rabbani, N., A. Ashour, and P.J. Thornalley.(2016) Mass spectrometric determination of early and advanced glycation in biology. *Glycoconjugate Journal*. 33(4): p. 553-568.
97. Rabbani, N., F. Shaheen, A. Anwar, J. Masania, and Paul J. Thornalley.(2014) Assay of methylglyoxal-derived protein and nucleotide AGEs. *Biochemical Society Transactions*. 42(2): p. 511-517.
98. Deo, P., C.L. McCullough, T. Almond, E.L. Jaunay, L. Donnellan, V.S. Dhillon, and M. Fenech.(2020) Dietary sugars and related endogenous advanced glycation end-products increase chromosomal DNA damage in WIL2-NS cells, measured using cytokinesis-block micronucleus cytome assay. *Mutagenesis*. 35(2): p. 169-177.
99. Thornalley, P.J.(2008) Protein and nucleotide damage by glyoxal and methylglyoxal in physiological systems--role in ageing and disease. *Drug metabolism and drug interactions*. 23(1-2): p. 125-150.
100. Gerrits, E.G., H.L. Lutgers, N. Kleefstra, R. Graaff, K.H. Groenier, A.J. Smit, R.O. Gans, and H.J. Bilo.(2008) Skin autofluorescence: a tool to identify type 2 diabetic patients at risk for developing microvascular complications. *Diabetes Care*. 31(3): p. 517-21.
101. Ahmed, N., O.K. Argirov, H.S. Minhas, C.A. Cordeiro, and P.J. Thornalley.(2002) Assay of advanced glycation endproducts (AGEs): surveying AGEs by chromatographic assay with derivatization by 6-aminoquinolyl-N-hydroxysuccinimidyl-carbamate and application to Nepsilon-carboxymethyl-lysine- and Nepsilon-(1-carboxyethyl)lysine-modified albumin. *Biochem J*. 364(Pt 1): p. 1-14.

102. Badoud, R., L. Fay, U. Richli, and P. Hušek.(1991) Gas chromatographic determination of N-carboxymethyl amino acids, the periodate oxidation products of Amadori compounds. *Journal of Chromatography A*. 552: p. 345-351.
103. Rabbani, N. and P.J. Thornalley.(2014) Measurement of methylglyoxal by stable isotopic dilution analysis LC-MS/MS with corroborative prediction in physiological samples. *Nature Protocols*. 9: p. 1969.
104. Ahmed, N., B. Mirshekar-Syahkal, L. Kennish, N. Karachalias, R. Babaei-Jadidi, and P.J. Thornalley.(2005) Assay of advanced glycation endproducts in selected beverages and food by liquid chromatography with tandem mass spectrometric detection. *Mol Nutr Food Res*. 49(7): p. 691-9.
105. Assar, S.H., C. Moloney, M. Lima, R. Magee, and J.M. Ames.(2009) Determination of N ε-(carboxymethyl)lysine in food systems by ultra performance liquid chromatography-mass spectrometry. *Amino Acids*. 36(2): p. 317-326.
106. Matsui, T., H.D. Joo, J.M. Lee, S.M. Ju, W.H. Tao, Y. Higashimoto, K. Fukami, and S. Yamagishi.(2015) Development of a monoclonal antibody-based ELISA system for glyceraldehyde-derived advanced glycation end products. *Immunol Lett*. 167(2): p. 141-6.
107. Zhao, Z., J. Liu, B. Shi, S. He, X. Yao, and M.D.P. Willcox.(2010) Advanced glycation end product (AGE) modified proteins in tears of diabetic patients. *Molecular vision*. 16: p. 1576-1584.
108. Krishnamoorthy, D., R.C. Hoy, D.M. Natelson, O.M. Torre, D.M. Laudier, J.C. Iatridis, and S. Illien-Jünger.(2018) Dietary advanced glycation end-product consumption leads to mechanical stiffening of murine intervertebral discs. *Dis Model Mech*. 11(12): p.
109. Perrone, A., A. Giovino, J. Benny, and F. Martinelli.(2020) Advanced Glycation End Products (AGEs): Biochemistry, Signaling, Analytical Methods, and Epigenetic Effects. *Oxidative Medicine and Cellular Longevity*. 2020: p. 3818196.
110. Desai, K.M., T. Chang, H. Wang, A. Banigesh, A. Dhar, J. Liu, A. Untereiner, and L. Wu.(2010) Oxidative stress and aging: Is methylglyoxal the hidden enemy?This review is one of a selection of papers published in a Special Issue on Oxidative Stress in Health and Disease. *Canadian Journal of Physiology and Pharmacology*. 88(3): p. 273-284.
111. Yao, D. and M. Brownlee.(2010) Hyperglycemia-Induced Reactive Oxygen Species Increase Expression of the Receptor for Advanced Glycation End Products (RAGE) and RAGE Ligands. 59(1): p. 249-255.
112. Rabbani, N. and Paul J. Thornalley.(2014) Glyoxalase Centennial conference: introduction, history of research on the glyoxalase system and future prospects. *Biochemical Society Transactions*. 42(2): p. 413-418.
113. Sompong, W., H. Cheng, and S. Adisakwattana.(2017) Ferulic acid prevents methylglyoxal-induced protein glycation, DNA damage, and apoptosis in pancreatic β-cells. *Journal of Physiology and Biochemistry*. 73(1): p. 121-131.
114. Frye, E.B., T.P. Degenhardt, S.R. Thorpe, and J.W. Baynes.(1998) Role of the Maillard Reaction in Aging of Tissue Proteins: Advanced Glycation End Product-dependent increase in imidazilome cross linking in human lens protein. *Journal of Biological Chemistry*. 273(30): p. 18714-18719.
115. Yeh, C.-H., L. Sturgis, J. Haidacher, X.-N. Zhang, S.J. Sherwood, R.J. Bjercke, O. Juhasz, M.T. Crow, R.G. Tilton, and L. Denner.(2001) Requirement for p38 and p44/p42 Mitogen-Activated Protein Kinases in RAGE-Mediated Nuclear

Factor-κB Transcriptional Activation and Cytokine Secretion. *Diabetes*. 50(6): p. 1495-1504.
116. Suantawee, T., H. Cheng, and S. Adisakwattana.(2016) Protective effect of cyanidin against glucose- and methylglyoxal-induced protein glycation and oxidative DNA damage. *International Journal of Biological Macromolecules*. 93: p. 814-821.
117. Queisser, M.A., D. Yao, S. Geisler, H.-P. Hammes, G. Lochnit, E.D. Schleicher, M. Brownlee, and K.T. Preissner.(2010) Hyperglycemia Impairs Proteasome Function by Methylglyoxal. *Diabetes*. 59(3): p. 670-678.
118. Park, S.H., M.H. Do, J.H. Lee, M. Jeong, O.K. Lim, and S.Y. Kim.(2017) Inhibitory Effect of Arachis hypogaea (Peanut) and Its Phenolics against Methylglyoxal-Derived Advanced Glycation End Product Toxicity. *Nutrients*. 9(11): p. 1214.
119. Bento, C.F., F. Marques, R. Fernandes, and P. Pereira.(2010) Methylglyoxal Alters the Function and Stability of Critical Components of the Protein Quality Control. *PLOS ONE*. 5(9): p. e13007.
120. Braun, J.D., D.O. Pastene, A. Breedijk, A. Rodriguez, B.B. Hofmann, C. Sticht, E. von Ochsenstein, H. Allgayer, J. van den Born, S. Bakker, S.J. Hauske, B.K. Krämer, B.A. Yard, and T. Albrecht.(2019) Methylglyoxal down-regulates the expression of cell cycle associated genes and activates the p53 pathway in human umbilical vein endothelial cells. *Sci Rep*. 9(1): p. 1152.
121. Irshad, Z., M. Xue, A. Ashour, J.R. Larkin, P.J. Thornalley, and N. Rabbani.(2019) Activation of the unfolded protein response in high glucose treated endothelial cells is mediated by methylglyoxal. *Scientific Reports*. 9(1): p. 7889.
122. Rabbani, N. and P.J. Thornalley.(2015) Dicarbonyl stress in cell and tissue dysfunction contributing to ageing and disease. *Biochemical and Biophysical Research Communications*. 458(2): p. 221-226.
123. Degen, J., M. Vogel, D. Richter, M. Hellwig, and T. Henle.(2013) Metabolic Transit of Dietary Methylglyoxal. *Journal of Agricultural and Food Chemistry*. 61(43): p. 10253-10260.
124. Rabbani, N., M. Xue, and Paul J. Thornalley.(2016) Methylglyoxal-induced dicarbonyl stress in aging and disease: first steps towards glyoxalase 1-based treatments. 130(19): p. 1677-1696.
125. Masania, J., M. Malczewska-Malec, U. Razny, J. Goralska, A. Zdzienicka, B. Kiec-Wilk, A. Gruca, J. Stancel-Mozwillo, A. Dembinska-Kiec, N. Rabbani, and P.J. Thornalley.(2016) Dicarbonyl stress in clinical obesity. *Glycoconjugate Journal*. 33(4): p. 581-589.
126. Neeper, M., A.M. Schmidt, J. Brett, S.D. Yan, F. Wang, Y.C. Pan, K. Elliston, D. Stern, and A. Shaw.(1992) Cloning and expression of a cell surface receptor for advanced glycosylation end products of proteins. *Journal of Biological Chemistry*. 267(21): p. 14998-15004.
127. Lin, J.-A., C.-H. Wu, C.-C. Lu, S.-M. Hsia, and G.-C. Yen.(2016) Glycative stress from advanced glycation end products (AGEs) and dicarbonyls: An emerging biological factor in cancer onset and progression. *Molecular Nutrition & Food Research*. 60(8): p. 1850-1864.
128. Qin, J., R. Goswami, S. Dawson, and G. Dawson.(2008) Expression of the receptor for advanced glycation end products in oligodendrocytes in response to oxidative stress. 86(11): p. 2414-2422.

129. Recabarren-Leiva, D., C.F. Burgos, B. Hernández, F.J. Garcïa-García, R.I. Castro, L. Guzman, E. Fuentes, I. Palomo, and M. Alarcón.(2021) Effects of the age/rage axis in the platelet activation. *International Journal of Biological Macromolecules*. 166: p. 1149-1161.
130. Zong, H., A. Madden, M. Ward, M.H. Mooney, C.T. Elliott, and A.W. Stitt.(2010) Homodimerization Is Essential for the Receptor for Advanced Glycation End Products (RAGE)-mediated Signal Transduction. *Journal of Biological Chemistry*. 285(30): p. 23137-23146.
131. Schmidt, A.M., S.D. Yan, J.L. Wautier, and D. Stern.(1999) Activation of receptor for advanced glycation end products: a mechanism for chronic vascular dysfunction in diabetic vasculopathy and atherosclerosis. *Circ Res*. 84(5): p. 489-97.
132. Schrondinger, L. *The PyMol Molecular Graphics System*. [2.0] 2015.
133. Nabi, R., S.S. Alvi, A. Shah, C.P. Chaturvedi, D. Iqbal, S. Ahmad, and M.S. Khan.(2019) Modulatory role of HMG-CoA reductase inhibitors and ezetimibe on LDL-AGEs-induced ROS generation and RAGE-associated signalling in HEK-293 Cells. *Life Sciences*. p. 116823.
134. Xue, J., R. Ray, D. Singer, D. Böhme, D.S. Burz, V. Rai, R. Hoffmann, and A. Shekhtman.(2014) The Receptor for Advanced Glycation End Products (RAGE) Specifically Recognizes Methylglyoxal-Derived AGEs. *Biochemistry*. 53(20): p. 3327-3335.
135. Fritz, G.(2011) RAGE: a single receptor fits multiple ligands. *Trends in Biochemical Sciences*. 36(12): p. 625-632.
136. Schmidt, A.M. and D.M. Stern.(2001) Receptor for age (RAGE) is a gene within the major histocompatibility class III region: implications for host response mechanisms in homeostasis and chronic disease. *Front Biosci*. 6: p. D1151-60.
137. Baeuerle, P.A.H., T.(1994) 'Function and Activation of NF-kappaB in the Immune System. *Annual Review of Immunology*. 12(1): p.
138. Bierhaus, A., S. Schiekofer, M. Schwaninger, M. Andrassy, P.M. Humpert, J. Chen, M. Hong, T. Luther, T. Henle, I. Klöting, M. Morcos, M. Hofmann, H. Tritschler, B. Weigle, M. Kasper, M. Smith, G. Perry, A.-M. Schmidt, D.M. Stern, H.-U. Häring, E. Schleicher, and P.P. Nawroth.(2001) Diabetes-Associated Sustained Activation of the Transcription Factor Nuclear Factor-κB. *Diabetes*. 50(12): p. 2792-2808.
139. Kunt, T., T. Forst, A. Wilhelm, H. Tritschler, A. Pfuetzner, O. Harzer, M. Engelbach, A. Zschaebitz, E. Stofft, and J. Beyer.(1999) Alpha-lipoic acid reduces expression of vascular cell adhesion molecule-1 and endothelial adhesion of human monocytes after stimulation with advanced glycation end products. *Clin Sci (Lond)*. 96(1): p. 75-82.
140. Calder, P.C.(2001) Polyunsaturated fatty acids, inflammation, and immunity. *Lipids*. 36(9): p. 1007-1024.
141. Soro-Paavonen, A., A.M.D. Watson, J. Li, K. Paavonen, A. Koitka, A.C. Calkin, D. Barit, M.T. Coughlan, B.G. Drew, G.I. Lancaster, M. Thomas, J.M. Forbes, P.P. Nawroth, A. Bierhaus, M.E. Cooper, and K.A. Jandeleit-Dahm.(2008) Receptor for Advanced Glycation End Products (RAGE) Deficiency Attenuates the Development of Atherosclerosis in Diabetes. *Diabetes*. 57(9): p. 2461-2469.
142. Rashid Deane, Z.W., and Berislav V. Zlokovic.(2004) RAGE (Yin) Versus LRP (Yang) Balance Regulates Alzheimer Amyloid β-Peptide Clearance Through Transport Across the Blood–Brain Barrier. *Stroke: A Journal of Cerebral Circulation*. 35(11): p. 2628-2631.

143. Perera, H.K.I. and C.S. Handuwalage.(2015) Analysis of glycation induced protein cross-linking inhibitory effects of some antidiabetic plants and spices. *BMC Complementary and Alternative Medicine*. 15(1): p. 175.
144. Zhao, J., R. Randive, and J.A. Stewart.(2014) Molecular mechanisms of AGE/RAGE-mediated fibrosis in the diabetic heart. *World journal of diabetes*. 5(6): p. 860-867.
145. Yan, S.F., S.D. Yan, R. Ramasamy, and A.M. Schmidt.(2009) Tempering the wrath of RAGE: an emerging therapeutic strategy against diabetic complications, neurodegeneration, and inflammation. *Ann Med*. 41(6): p. 408-22.
146. Ahmed, N.(2005) Advanced glycation endproducts--role in pathology of diabetic complications. *Diabetes Res Clin Pract*. 67(1): p. 3-21.
147. Tan, A.L.Y., J.M. Forbes, and M.E. Cooper.(2007) AGE, RAGE, and ROS in Diabetic Nephropathy. *Seminars in Nephrology*. 27(2): p. 130-143.
148. Raucci, A., S. Cugusi, A. Antonelli, S.M. Barabino, L. Monti, A. Bierhaus, K. Reiss, P. Saftig, and M.E. Bianchi.(2008) A soluble form of the receptor for advanced glycation endproducts (RAGE) is produced by proteolytic cleavage of the membrane-bound form by the sheddase a disintegrin and metalloprotease 10 (ADAM10). *FASEB J*. 22(10): p. 3716-27.
149. Kalea, A.Z., N. Reiniger, H. Yang, M. Arriero, A.M. Schmidt, and B.I. Hudson.(2009) Alternative splicing of the murine receptor for advanced glycation end-products (RAGE) gene. *The FASEB Journal*. 23(6): p. 1766-1774.
150. Yonekura, H., Y. Yamamoto, S. Sakurai, R.G. Petrova, M.J. Abedin, H. Li, K. Yasui, M. Takeuchi, Z. Makita, S. Takasawa, H. Okamoto, T. Watanabe, and H. Yamamoto.(2003) Novel splice variants of the receptor for advanced glycation end-products expressed in human vascular endothelial cells and pericytes, and their putative roles in diabetes-induced vascular injury. *Biochem J*. 370(Pt 3): p. 1097-109.
151. Braley, A., T. Kwak, J. Jules, E. Harja, R. Landgraf, and B.I. Hudson.(2016) Regulation of Receptor for Advanced Glycation End Products (RAGE) Ectodomain Shedding and Its Role in Cell Function *. *Journal of Biological Chemistry*. 291(23): p. 12057-12073.
152. Sharaf, H., S. Matou-Nasri, Q. Wang, Z. Rabhan, H. Al-Eidi, A. Al Abdulrahman, and N. Ahmed.(2015) Advanced glycation endproducts increase proliferation, migration and invasion of the breast cancer cell line MDA-MB-231. *Biochimica et Biophysica Acta (BBA) - Molecular Basis of Disease*. 1852(3): p. 429-441.
153. Omofuma, O.O., D.P. Turner, L.L. Peterson, A.T. Merchant, J. Zhang, and S.E. Steck.(2020) Dietary Advanced Glycation End-products (AGE) and Risk of Breast Cancer in the Prostate, Lung, Colorectal and Ovarian Cancer Screening Trial (PLCO). *Cancer Prevention Research*. 13(7): p. 601-610.
154. Ogurtsova, K., J.D. da Rocha Fernandes, Y. Huang, U. Linnenkamp, L. Guariguata, N.H. Cho, D. Cavan, J.E. Shaw, and L.E. Makaroff.(2017) IDF Diabetes Atlas: Global estimates for the prevalence of diabetes for 2015 and 2040. *Diabetes Res Clin Pract*. 128: p. 40-50.
155. Vallon, V. and R. Komers.(2011) Pathophysiology of the diabetic kidney. *Compr Physiol*. 1(3): p. 1175-232.
156. Kolset, S.O., F.P. Reinholt, and T. Jenssen.(2012) Diabetic nephropathy and extracellular matrix. *J Histochem Cytochem*. 60(12): p. 976-86.

157. Moraru, A., J. Wiederstein, D. Pfaff, T. Fleming, A.K. Miller, P. Nawroth, and A.A. Teleman.(2018) Elevated Levels of the Reactive Metabolite Methylglyoxal Recapitulate Progression of Type 2 Diabetes. *Cell Metabolism*. 27(4): p. 926-934.e8.
158. Hanssen, N.M., L. Engelen, I. Ferreira, J.L. Scheijen, M.S. Huijberts, M.M. van Greevenbroek, C.J. van der Kallen, J.M. Dekker, G. Nijpels, C.D. Stehouwer, and C.G. Schalkwijk.(2013) Plasma levels of advanced glycation endproducts Nε-(carboxymethyl)lysine, Nε-(carboxyethyl)lysine, and pentosidine are not independently associated with cardiovascular disease in individuals with or without type 2 diabetes: the Hoorn and CODAM studies. *J Clin Endocrinol Metab*. 98(8): p. E1369-73.
159. Martinez Fernandez, A., L. Regazzoni, M. Brioschi, E. Gianazza, P. Agostoni, G. Aldini, and C. Banfi.(2019) Pro-oxidant and pro-inflammatory effects of glycated albumin on cardiomyocytes. *Free Radical Biology and Medicine*. 144: p. 245-255.
160. Ghosh, A., L. Gao, A. Thakur, P.M. Siu, and C.W.K. Lai.(2017) Role of free fatty acids in endothelial dysfunction. *Journal of Biomedical Science*. 24(1): p. 50.
161. Ehlermann, P., K. Eggers, A. Bierhaus, P. Most, D. Weichenhan, J. Greten, P.P. Nawroth, H.A. Katus, and A. Remppis.(2006) Increased proinflammatory endothelial response to S100A8/A9 after preactivation through advanced glycation end products. *Cardiovascular Diabetology*. 5(1): p. 6.
162. Ahmad, S., F. Akhter, U. Shahab, Z. Rafi, M.S. Khan, R. Nabi, M.S. Khan, K. Ahmad, J.M. Ashraf, and Moinuddin.(2018) Do all roads lead to the Rome? The glycation perspective! *Seminars in Cancer Biology*. 49: p. 9-19.
163. Bidasee, K.R., K. Nallani, Y. Yu, R.R. Cocklin, Y. Zhang, M. Wang, U.D. Dincer, and H.R. Besch, Jr.(2003) Chronic diabetes increases advanced glycation end products on cardiac ryanodine receptors/calcium-release channels. *Diabetes*. 52(7): p. 1825-36.
164. Bidasee, K.R., Y. Zhang, C.H. Shao, M. Wang, K.P. Patel, U.D. Dincer, and H.R. Besch, Jr.(2004) Diabetes increases formation of advanced glycation end products on Sarco(endo)plasmic reticulum Ca2+-ATPase. *Diabetes*. 53(2): p. 463-73.
165. Sharma, A., D. Weber, J. Raupbach, T.C. Dakal, K. Fließbach, A. Ramirez, T. Grune, and U. Wüllner.(2020) Advanced glycation end products and protein carbonyl levels in plasma reveal sex-specific differences in Parkinson's and Alzheimer's disease. *Redox Biology*. 34: p. 101546.
166. Dalfó, E., M. Portero-Otín, V. Ayala, A. Martínez, R. Pamplona, and I. Ferrer.(2005) Evidence of Oxidative Stress in the Neocortex in Incidental Lewy Body Disease. *Journal of Neuropathology & Experimental Neurology*. 64(9): p. 816-830.
167. Münch, G., S. Mayer, J. Michaelis, A.R. Hipkiss, P. Riederer, R. Müller, A. Neumann, R. Schinzel, and A.M. Cunningham.(1997) Influence of advanced glycation end-products and AGE-inhibitors on nucleation-dependent polymerization of β-amyloid peptide. *Biochimica et Biophysica Acta (BBA) - Molecular Basis of Disease*. 1360(1): p. 17-29.
168. Li, J.J., D. Voisin, A.-L. Quiquerez, and C. Bouras.(1994) Differential expression of advanced glycosylation end-products in neurons of different species. *Brain Research*. 641(2): p. 285-288.

169. Ko, S.-Y., Y.-P. Lin, Y.-S. Lin, and S.-S. Chang.(2010) Advanced glycation end products enhance amyloid precursor protein expression by inducing reactive oxygen species. *Free Radical Biology and Medicine*. 49(3): p. 474-480.
170. Zhou, X., N. Lin, M. Zhang, X. Wang, Y. An, Q. Su, P. Du, B. Li, and H. Chen.(2020) Circulating soluble receptor for advanced glycation end products and other factors in type 2 diabetes patients with colorectal cancer. *BMC Endocrine Disorders*. 20(1): p. 170.
171. Denis, U., M. Lecomte, C. Paget, D. Ruggiero, N. Wiernsperger, and M. Lagarde.(2002) Advanced glycation end-products induce apoptosis of bovine retinal pericytes in culture: involvement of diacylglycerol/ceramide production and oxidative stress induction. *Free Radical Biology and Medicine*. 33(2): p. 236-247.
172. Kaji, Y., S. Amano, T. Usui, T. Oshika, K. Yamashiro, S. Ishida, K. Suzuki, S. Tanaka, A.P. Adamis, R. Nagai, and S. Horiuchi.(2003) Expression and Function of Receptors for Advanced Glycation End Products in Bovine Corneal Endothelial Cells. *Investigative Ophthalmology & Visual Science*. 44(2): p. 521-528.
173. Kasper, M., C. Roehlecke, M. Witt, H. Fehrenbach, A. Hofer, T. Miyata, C. Weigert, R.H.W. Funk, and E.D. Schleicher.(2000) Induction of Apoptosis by Glyoxal in Human Embryonic Lung Epithelial Cell Line L132. 23(4): p. 485-491.
174. Hung, L.-F., K.-Y. Huang, D.-H. Yang, D.-M. Chang, J.-H. Lai, and L.-J. Ho.(2010) Advanced glycation end products induce T cell apoptosis: Involvement of oxidative stress, caspase and the mitochondrial pathway. *Mechanisms of Ageing and Development*. 131(11): p. 682-691.
175. Loske, C., A. Neumann, A.M. Cunningham, K. Nichol, R. Schinzel, P. Riederer, and G. Münch.(1998) Cytotoxicity of advanced glycation endproducts is mediated by oxidative stress. *Journal of Neural Transmission*. 105(8): p. 1005-1015.
176. Antognelli, C., L. Mezzasoma, K. Fettucciari, and V.N. Talesa.(2013) A novel mechanism of methylglyoxal cytotoxicity in prostate cancer cells. *The International Journal of Biochemistry & Cell Biology*. 45(4): p. 836-844.
177. Ghosh, A., S. Bera, S. Ray, T. Banerjee, and M. Ray.(2011) Methylglyoxal induces mitochondria-dependent apoptosis in sarcoma. *Biochemistry (Moscow)*. 76(10): p. 1164.
178. Deo, P., V.S. Dhillon, W.M. Lim, E.L. Jaunay, L. Donnellan, B. Peake, C. McCullough, and M. Fenech.(2020) Advanced glycation end-products accelerate telomere attrition and increase pro-inflammatory mediators in human WIL2-NS cells. *Mutagenesis*. p.
179. Jaunay, E.L., *Advanced glycation end-product induced genotoxicity and receptor expression in human cells.*, in *Clinical and Health Sciences*. 2022, University of South Australia.
180. Wetzels, S., T. Vanmierlo, J.L.J.M. Scheijen, J. van Horssen, S. Amor, V. Somers, C.G. Schalkwijk, J.J.A. Hendriks, and K. Wouters.(2019) Methylglyoxal-Derived Advanced Glycation Endproducts Accumulate in Multiple Sclerosis Lesions. *Frontiers in immunology*. 10: p. 855-855.
181. Kang, Q. and C. Yang.(2020) Oxidative stress and diabetic retinopathy: Molecular mechanisms, pathogenetic role and therapeutic implications. *Redox Biology*. p. 101799.

182. Brownlee, M.(2005) The Pathobiology of Diabetic Complications. *A Unifying Mechanism*. 54(6): p. 1615-1625.
183. Wautier, M.-P., O. Chappey, S. Corda, D.M. Stern, A.M. Schmidt, and J.-L. Wautier.(2001) Activation of NADPH oxidase by AGE links oxidant stress to altered gene expression via RAGE. *American Journal of Physiology-Endocrinology and Metabolism*. 280(5): p. E685-E694.
184. Suzuki, D., T. Miyata, N. Saotome, K. Horie, R. Inagi, Y. Yasuda, K. Uchida, Y. Izuhara, M. Yagame, H. Sakai, and K. Kurokawa.(1999) Immunohistochemical evidence for an increased oxidative stress and carbonyl modification of proteins in diabetic glomerular lesions. *J Am Soc Nephrol*. 10(4): p. 822-32.
185. Wolff, S.P., Z.Y. Jiang, and J.V. Hunt.(1991) Protein glycation and oxidative stress in diabetes mellitus and ageing. *Free Radical Biology and Medicine*. 10(5): p. 339-352.
186. Kang, J.H.(2003) Oxidative damage of DNA induced by methylglyoxal in vitro. *Toxicology Letters*. 145(2): p. 181-187.
187. Yamagishi, S.-i., S. Maeda, T. Matsui, S. Ueda, K. Fukami, and S. Okuda.(2012) Role of advanced glycation end products (AGEs) and oxidative stress in vascular complications in diabetes. *Biochimica et Biophysica Acta (BBA) - General Subjects*. 1820(5): p. 663-671.
188. Zhang, J.-M. and J. An.(2007) Cytokines, inflammation, and pain. *International anesthesiology clinics*. 45(2): p. 27-37.
189. Nathan, C. and M. Sporn.(1991) Cytokines in context. *The Journal of cell biology*. 113(5): p. 981-986.
190. Dinarello, C.A.(2007) Historical insights into cytokines. *European Journal of Immunology*. 37(S1): p. S34-S45.
191. Blackwell, T.S. and J.W. Christman.(1997) The Role of Nuclear Factor- κ B in Cytokine Gene Regulation. *American Journal of Respiratory Cell and Molecular Biology*. 17(1): p. 3-9.
192. Berbaum, K., K. Shanmugam, G. Stuchbury, F. Wiede, H. Körner, and G. Münch.(2008) Induction of novel cytokines and chemokines by advanced glycation endproducts determined with a cytometric bead array. *Cytokine*. 41(3): p. 198-203.
193. Dariya, B. and G.P. Nagaraju.(2020) Advanced glycation end products in diabetes, cancer and phytochemical therapy. *Drug Discovery Today*. 25(9): p. 1614-1623.
194. Wang, H., Q.H. Meng, J.R. Gordon, H. Khandwala, and L. Wu.(2007) Proinflammatory and proapoptotic effects of methylglyoxal on neutrophils from patients with type 2 diabetes mellitus. *Clinical Biochemistry*. 40(16): p. 1232-1239.
195. Berlanga, J., D. Cibrian, I. Guillen, F. Freyre, J.S. Alba, P. Lopez-Saura, N. Merino, A. Aldama, A.M. Quintela, M.E. Triana, J.F. Montequin, H. Ajamieh, D. Urquiza, N. Ahmed, and P.J. Thornalley.(2005) Methylglyoxal administration induces diabetes-like microvascular changes and perturbs the healing process of cutaneous wounds. *Clin Sci (Lond)*. 109(1): p. 83-95.
196. Simm, A., G. Münch, F. Seif, O. Schenk, A. Heidland, H. Richter, S. Vamvakas, and R. Schinzel.(1997) Advanced glycation endproducts stimulate the MAP-kinase pathway in tubulus cell line LLC-PK1. *FEBS Letters*. 410(2): p. 481-484.
197. Fan, X., R. Subramaniam, M.F. Weiss, and V.M. Monnier.(2003) Methylglyoxal–bovine serum albumin stimulates tumor necrosis factor alpha

secretion in RAW 264.7 cells through activation of mitogen-activating protein kinase, nuclear factor κB and intracellular reactive oxygen species formation. *Archives of Biochemistry and Biophysics*. 409(2): p. 274-286.
198. Du, J., H. Suzuki, F. Nagase, A.A. Akhand, X.-Y. Ma, T. Yokoyama, T. Miyata, and I. Nakashima.(2001) Superoxide-mediated early oxidation and activation of ASK1 are important for initiating methylglyoxal-induced apoptosis process. *Free Radical Biology and Medicine*. 31(4): p. 469-478.
199. Wu, L., G.F. Davies, W.J. Roesler, and B.H.J. Juurlink.(2002) Regulation of the Glyoxalase Pathway in Human Brain Microvascular Endothelium: Effects of Troglitazone and Tertiary Butylhydroperoxide. *Endothelium*. 9(4): p. 273-278.
200. Nonaka, K., Y. Kajiura, M. Bando, E. Sakamoto, Y. Inagaki, J.H. Lew, K. Naruishi, T. Ikuta, K. Yoshida, T. Kobayashi, H. Yoshie, T. Nagata, and J. Kido.(2018) Advanced glycation end-products increase IL-6 and ICAM-1 expression via RAGE, MAPK and NF-κB pathways in human gingival fibroblasts. *Journal of Periodontal Research*. 53(3): p. 334-344.
201. Rustan, A.C. and C.A. Drevon, *Fatty Acids: Structures and Properties*, in *Encyclopedia of Life Sciences*. 2001.
202. Calder, P.C.(2006) n−3 Polyunsaturated fatty acids, inflammation, and inflammatory diseases. *The American Journal of Clinical Nutrition*. 83(6): p. 1505S-1519S.
203. Calder, P.C.(2008) Polyunsaturated fatty acids, inflammatory processes and inflammatory bowel diseases. *Molecular Nutrition & Food Research*. 52(8): p. 885-897.
204. Rustan, A.C. and C.A. Drevon, *Fatty Acids: Structures and Properties*, in *eLS*.
205. Sanders, R.J., R. Ofman, M. Duran, S. Kemp, and R.J.A. Wanders.(2006) Omega-oxidation of very long-chain fatty acids in human liver microsomes. Implications for X-linked adrenoleukodystrophy. *J Biol Chem*. 281(19): p. 13180-13187.
206. Ameer, F., L. Scandiuzzi, S. Hasnain, H. Kalbacher, and N. Zaidi.(2014) De novo lipogenesis in health and disease. *Metabolism*. 63(7): p. 895-902.
207. Calder, P.C. and E.A. Newsholme.(1993) Influence of antioxidant vitamins on fatty acid inhibition of lymphocyte proliferation. *Biochemistry and molecular biology international*. 29(1): p. 175-183.
208. Tallima, H. and R. El Ridi.(2018) Arachidonic acid: Physiological roles and potential health benefits – A review. *Journal of Advanced Research*. 11: p. 33-41.
209. Tallima, H. and R. El Ridi.(2017) Arachidonic acid: Physiological roles and potential health benefits - A review. *Journal of advanced research*. 11: p. 33-41.
210. Simopoulos, A.P.(1999) Essential fatty acids in health and chronic disease. *The American Journal of Clinical Nutrition*. 70(3): p. 560s-569s.
211. Dyall, S.C. and A.T. Michael-titus.(2008) Neurological Benefits of Omega-3 Fatty Acids. *Neuromolecular Medicine*. 10(4): p. 219-35.
212. Ruxton, C.H.S., S.C. Reed, M.J.A. Simpson, and K.J. Millington.(2004) The health benefits of omega-3 polyunsaturated fatty acids: a review of the evidence. *Journal of Human Nutrition and Dietetics*. 17(5): p. 449-459.
213. von Schacky, C. and W.S. Harris.(2007) Cardiovascular benefits of omega-3 fatty acids. *Cardiovascular Research*. 73(2): p. 310-315.
214. Draper, E., C.M. Reynolds, M. Canavan, K.H. Mills, C.E. Loscher, and H.M. Roche.(2011) Omega-3 fatty acids attenuate dendritic cell function via NF-κB

independent of PPARγ. *The Journal of Nutritional Biochemistry*. 22(8): p. 784-790.
215. Innes, J.K. and P.C. Calder.(2018) Omega-6 fatty acids and inflammation. *Prostaglandins, Leukotrienes and Essential Fatty Acids*. 132: p. 41-48.
216. Calder, P.C.(2011) Fatty acids and inflammation: The cutting edge between food and pharma. *European Journal of Pharmacology*. 668: p. S50-S58.
217. Calder, P.C.(2006) Polyunsaturated fatty acids and inflammation. *Prostaglandins, Leukotrienes and Essential Fatty Acids*. 75(3): p. 197-202.
218. Calder, P.C.(2010) Omega-3 fatty acids and inflammatory processes. *Nutrients*. 2(3): p. 355-374.
219. Moro, K., M. Nagahashi, R. Ramanathan, K. Takabe, and T. Wakai.(2016) Resolvins and omega three polyunsaturated fatty acids: Clinical implications in inflammatory diseases and cancer. *World journal of clinical cases*. 4(7): p. 155-164.
220. Kalmijn, S., L.J. Launer, A. Ott, J.C. Witteman, A. Hofman, and M.M. Breteler.(1997) Dietary fat intake and the risk of incident dementia in the Rotterdam Study. *Ann Neurol*. 42(5): p. 776-82.
221. Morris, M.C., D.A. Evans, J.L. Bienias, C.C. Tangney, D.A. Bennett, R.S. Wilson, N. Aggarwal, and J. Schneider.(2003) Consumption of fish and n-3 fatty acids and risk of incident Alzheimer disease. *Arch Neurol*. 60(7): p. 940-6.
222. Kris-Etherton, P.M., C.K. Richter, K.J. Bowen, A.C. Skulas-Ray, K.H. Jackson, K.S. Petersen, and W.S. Harris.(2019) Recent Clinical Trials Shed New Light on the Cardiovascular Benefits of Omega-3 Fatty Acids. *Methodist DeBakey cardiovascular journal*. 15(3): p. 171-178.
223. Calder, P.C.(2012) Long-chain fatty acids and inflammation. *Proceedings of the Nutrition Society*. 71(2): p. 284-289.
224. Siddiqui, R.A., S.R. Shaikh, L.A. Sech, H.R. Yount, W. Stillwell, and G.P. Zaloga.(2004) Omega 3-Fatty Acids: Health Benefits and Cellular Mechanisms of Action. *Mini Reviews in Medicinal Chemistry*. 4(8): p. 859-871.
225. Schmidt, E.B. and J. Dyerberg.(1994) Omega-3 Fatty Acids. *Drugs*. 47(3): p. 405-424.
226. Soleimani, A., M. Taghizadeh, F. Bahmani, N. Badroj, and Z. Asemi.(2017) Metabolic response to omega-3 fatty acid supplementation in patients with diabetic nephropathy: A randomized, double-blind, placebo-controlled trial. *Clinical Nutrition*. 36(1): p. 79-84.
227. Wei, W., M. Chen, Y. Zhu, J. Wang, P. Zhu, Y. Li, and J. Li.(2012) Down-regulation of vascular HMGB1 and RAGE expression by n-3 polyunsaturated fatty acids is accompanied by amelioration of chronic vasculopathy of small bowel allografts. *The Journal of Nutritional Biochemistry*. 23(10): p. 1333-1340.
228. Lee, S.M., S.H. Chung, Y. Park, M.K. Park, Y.K. Son, S.E. Kim, and W.S. An.(2015) Effect of Omega-3 Fatty Acid on the Fatty Acid Content of the Erythrocyte Membrane and Proteinuria in Patients with Diabetic Nephropathy. *Int J Endocrinol*. 2015: p. 208121.
229. Derosa, G., A.F. Cicero, E. Fogari, A. D'Angelo, A. Bonaventura, D. Romano, and P. Maffioli.(2012) Effects of n-3 PUFAs on postprandial variation of metalloproteinases, and inflammatory and insulin resistance parameters in dyslipidemic patients: evaluation with euglycemic clamp and oral fat load. *J Clin Lipidol*. 6(6): p. 553-64.
230. Soleimani, A., M. Taghizadeh, F. Bahmani, N. Badroj, and Z. Asemi.(2017) Metabolic response to omega-3 fatty acid supplementation in patients with

diabetic nephropathy: A randomized, double-blind, placebo-controlled trial. *Clin Nutr*. 36(1): p. 79-84.
231. Mirhashemi, S.M., F. Rahimi, A. Soleimani, and Z. Asemi.(2016) Effects of Omega-3 Fatty Acid Supplementation on Inflammatory Cytokines and Advanced Glycation End Products in Patients With Diabetic Nephropathy: A Randomized Controlled Trial. *Iranian Journal of Kidney Diseases*. 10(4): p. 197-204.
232. Deo, P., V.S. Dhillon, P. Thomas, and M. Fenech.(2021) The association of N ε-Carboxymethyllysine with polyunsaturated and saturated fatty acids in healthy individuals. *J Gerontol A Biol Sci Med Sci*. p.
233. Miyata, T., R. Inagi, K. Asahi, Y. Yamada, K. Horie, H. Sakai, K. Uchida, and K. Kurokawa.(1998) Generation of protein carbonyls by glycoxidation and lipoxidation reactions with autoxidation products of ascorbic acid and polyunsaturated fatty acids. *FEBS Letters*. 437(1-2): p. 24-28.
234. Prasanna, G. and N.T. Saraswathi.(2017) Linolenic acid prevents early and advanced glycation end-products (AGEs) modification of albumin. *International Journal of Biological Macromolecules*. 95: p. 121-125.
235. Armstrong, C.T., P.E. Mason, J.L.R. Anderson, and C.E. Dempsey.(2016) Arginine side chain interactions and the role of arginine as a gating charge carrier in voltage sensitive ion channels. *Scientific Reports*. 6(1): p. 21759.
236. Zhang, Q., J.M. Ames, R.D. Smith, J.W. Baynes, and T.O. Metz.(2009) A perspective on the Maillard reaction and the analysis of protein glycation by mass spectrometry: probing the pathogenesis of chronic disease. *Journal of proteome research*. 8(2): p. 754-769.
237. Phillips, S.A. and P.J. Thornalley.(1993) The formation of methylglyoxal from triose phosphates. Investigation using a specific assay for methylglyoxal. *Eur J Biochem*. 212(1): p. 101-5.
238. Wells-Knecht, K.J., D.V. Zyzak, J.E. Litchfield, S.R. Thorpe, and J.W. Baynes.(1995) Mechanism of Autoxidative Glycosylation: Identification of Glyoxal and Arabinose as Intermediates in the Autoxidative Modifaction of Proteins by Glucose. *Biochemistry*. 34(11): p. 3702-3709.
239. Glomb, M.A. and V.M. Monnier.(1995) Mechanism of Protein Modification by Glyoxal and Glycolaldehyde, Reactive Intermediates of the Maillard Reaction. *Journal of Biological Chemistry*. 270(17): p. 10017-10026.
240. Sell, D.R., R.H. Nagaraj, S.K. Grandhee, P. Odetti, A. Lapolla, J. Fogarty, and V.M. Monnier.(1991) Pentosidine: a molecular marker for the cumulative damage to proteins in diabetes, aging, and uremia. *Diabetes/metabolism reviews*. 7(4): p. 239-251.
241. Anwar, S., S. A. Almatroodi, A. Almatroudi, K.S. Allemailem, R.J. Joseph, A.A. Khan, F. Alrumaihi, M.A. Alsahli, and A. Husain Rahmani.(2021) Biosynthesis of silver nanoparticles using Tamarix articulata leaf extract: an effective approach for attenuation of oxidative stress mediated diseases. *International Journal of Food Properties*. 24(1): p. 677-701.
242. Ramis, R., J. Ortega-Castro, C. Caballero, R. Casasnovas, A. Cerrillo, B. Vilanova, M. Adrover, and J. Frau.(2019) How Does Pyridoxamine Inhibit the Formation of Advanced Glycation End Products? The Role of Its Primary Antioxidant Activity. *Antioxidants (Basel)*. 8(9): p.
243. Anwar, A., P.M. Abruzzo, S. Pasha, K. Rajpoot, A. Bolotta, A. Ghezzo, M. Marini, A. Posar, P. Visconti, P.J. Thornalley, and N. Rabbani.(2018) Advanced

glycation endproducts, dityrosine and arginine transporter dysfunction in autism - a source of biomarkers for clinical diagnosis. *Molecular Autism*. 9(1): p. 3.
244. Anwar, S. and H. Younus.(2017) Antiglycating potential of ellagic acids against glucose and methylglyoxal - induced glycation of superoxide dismutase. *Journal of Proteins & Proteomics*. 8: p.
245. Deo, P., E. Hewawasam, A. Karakoulakis, D.J. Claudie, R. Nelson, B.S. Simpson, N.M. Smith, and S.J. Semple.(2016) In vitro inhibitory activities of selected Australian medicinal plant extracts against protein glycation, angiotensin converting enzyme (ACE) and digestive enzymes linked to type II diabetes. *BMC Complement Altern Med*. 16(1): p. 435.
246. Kim, S., S.J. Semple, B.S. Simpson, and P. Deo.(2020) Antioxidant and Antiglycation Activities of Syzygium paniculatum Gaertn and Inhibition of Digestive Enzymes Relevant to Type 2 Diabetes Mellitus. *Plant Foods Hum Nutr*. 75(4): p. 621-627.
247. Younus, H. and S. Anwar.(2016) Prevention of non-enzymatic glycosylation (glycation): Implication in the treatment of diabetic complication. *International journal of health sciences*. 10(2): p. 261-277.
248. Swanson, D., R. Block, and S.A. Mousa.(2012) Omega-3 Fatty Acids EPA and DHA: Health Benefits Throughout Life1. *Advances in Nutrition*. 3(1): p. 1-7.
249. Desai, S.N., F.F. Farris, and S.D. Ray, *Lipid Peroxidation*, in *Encyclopedia of Toxicology (Third Edition)*, P. Wexler, Editor. 2014, Academic Press: Oxford. p. 89-93.
250. Khan, M.A., S. Anwar, A.N. Aljarbou, M. Al-Orainy, Y.H. Aldebasi, S. Islam, and H. Younus.(2014) Protective effect of thymoquinone on glucose or methylglyoxal-induced glycation of superoxide dismutase. *International Journal of Biological Macromolecules*. 65: p. 16-20.
251. Koch, E.R. and P. Deo.(2016) Nutritional supplements modulate fluorescent protein-bound advanced glycation endproducts and digestive enzymes related to type 2 diabetes mellitus. *BMC Complementary and Alternative Medicine*. 16(1): p. 338.
252. Deo, P., C. Chern, B. Peake, and S.Y. Tan.(2020) Non-nutritive sweeteners are in concomitant with the formation of endogenous and exogenous advanced glycation end-products. *Int J Food Sci Nutr*. 71(6): p. 706-714.
253. Kim, Y., J.B. Keogh, P. Deo, and P.M. Clifton.(2020) Differential Effects of Dietary Patterns on Advanced Glycation end Products: A Randomized Crossover Study. *Nutrients*. 12(6): p. 1767.
254. van der Lugt, T., A.R. Weseler, W.A. Gebbink, M.F. Vrolijk, A. Opperhuizen, and A. Bast.(2018) Dietary Advanced Glycation Endproducts Induce an Inflammatory Response in Human Macrophages in Vitro. *Nutrients*. 10(12): p. 1868.
255. Galligan, J.J., J.A. Wepy, M.D. Streeter, P.J. Kingsley, M.M. Mitchener, O.R. Wauchope, W.N. Beavers, K.L. Rose, T. Wang, D.A. Spiegel, and L.J. Marnett.(2018) Methylglyoxal-derived posttranslational arginine modifications are abundant histone marks. *Proceedings of the National Academy of Sciences*. 115(37): p. 9228-9233.
256. Lee, D.-Y. and G.-D. Chang.(2014) Methylglyoxal in cells elicits a negative feedback loop entailing transglutaminase 2 and glyoxalase 1. *Redox Biology*. 2: p. 196-205.

257. Sadowska-Bartosz, I., S. Galiniak, and G. Bartosz.(2014) Kinetics of Glycoxidation of Bovine Serum Albumin by Methylglyoxal and Glyoxal and its Prevention by Various Compounds. *Molecules*. 19(4): p. 4880-4896.
258. Guerin-Dubourg, A., M. Cournot, C. Planesse, X. Debussche, O. Meilhac, P. Rondeau, and E. Bourdon.(2017) Association between Fluorescent Advanced Glycation End-Products and Vascular Complications in Type 2 Diabetic Patients. *BioMed Research International*. 2017: p. 7989180.
259. Indyk, D., A. Bronowicka-Szydełko, A. Gamian, and A. Kuzan.(2021) Advanced glycation end products and their receptors in serum of patients with type 2 diabetes. *Scientific Reports*. 11(1): p. 13264.
260. Khan, H., M.S. Khan, and S. Ahmad.(2018) The in vivo and in vitro approaches for establishing a link between advanced glycation end products and lung cancer. *Journal of Cellular Biochemistry*. 119(11): p. 9099-9109.
261. Takeuchi, M. and S.-i. Yamagishi.(2008) Possible Involvement of Advanced Glycation End-Products (AGEs) in the Pathogenesis of Alzheimer's Disease. *Current Pharmaceutical Design*. 14(10): p. 973-978.
262. Donnellan, L., B. Simpson, V.S. Dhillon, M. Costabile, M. Fenech, and P. Deo.(2021) Methylglyoxal induces chromosomal instability and mitotic dysfunction in lymphocytes. *Mutagenesis*. p.
263. Calder, P.C.(2008) The relationship between the fatty acid composition of immune cells and their function. *Prostaglandins, Leukotrienes and Essential Fatty Acids*. 79(3): p. 101-108.
264. Bates, E.J., A. Ferrante, L. Smithers, A. Poulos, and B.S. Robinson.(1995) Effect of fatty acid structure on neutrophil adhesion, degranulation and damage to endothelial cells. *Atherosclerosis*. 116(2): p. 247-259.
265. Weaver, K.L., P. Ivester, M. Seeds, L.D. Case, J.P. Arm, and F.H. Chilton.(2009) Effect of Dietary Fatty Acids on Inflammatory Gene Expression in Healthy Humans*. *Journal of Biological Chemistry*. 284(23): p. 15400-15407.
266. Zárate, R., N. El Jaber-Vazdekis, N. Tejera, J.A. Pérez, and C. Rodríguez.(2017) Significance of long chain polyunsaturated fatty acids in human health. *Clinical and translational medicine*. 6(1): p. 25-25.
267. Zhang, H., L. Zhang, L.-j. Peng, X.-w. Dong, D. Wu, V.C.-H. Wu, and F.-Q. Feng.(2012) Quantitative structure-activity relationships of antimicrobial fatty acids and derivatives against Staphylococcus aureus. *Journal of Zhejiang University. Science. B*. 13(2): p. 83-93.
268. Kabara, J.J., D.M. Swieczkowski, A.J. Conley, and J.P. Truant.(1972) Fatty acids and derivatives as antimicrobial agents. *Antimicrobial agents and chemotherapy*. 2(1): p. 23-28.
269. Costabile, M., C.S.T. Hii, M. Melino, C. Easton, and A. Ferrante.(2005) The Immunomodulatory Effects of Novel β-Oxa, β-Thia, and γ-Thia Polyunsaturated Fatty Acids on Human T Lymphocyte Proliferation, Cytokine Production, and Activation of Protein Kinase C and MAPKs. *The Journal of Immunology*. 174(1): p. 233-243.
270. Lopez-Moreno, J., G.M. Quintana-Navarro, J. Delgado-Lista, A. Garcia-Rios, J.F. Alcala-Diaz, F. Gomez-Delgado, A. Camargo, P. Perez-Martinez, F.J. Tinahones, G.E. Striker, F. Perez-Jimenez, J.M. Villalba, J. Lopez-Miranda, and E.M. Yubero-Serrano.(2016) Mediterranean Diet Supplemented With Coenzyme Q10 Modulates the Postprandial Metabolism of Advanced Glycation End

Products in Elderly Men and Women. *The Journals of Gerontology: Series A*. 73(3): p. 340-346.
271. Chen, B., Y. Sun, J. Niu, G.K. Jarugumilli, and X. Wu.(2018) Protein Lipidation in Cell Signaling and Diseases: Function, Regulation, and Therapeutic Opportunities. *Cell chemical biology*. 25(7): p. 817-831.
272. Rabbani, N. and P.J. Thornalley.(2018) Advanced glycation end products in the pathogenesis of chronic kidney disease. *Kidney international*. 93(4): p. 803-813.
273. Thornalley, P.J.(2007) Dietary AGEs and ALEs and risk to human health by their interaction with the receptor for advanced glycation endproducts (RAGE) – an introduction. *Molecular Nutrition & Food Research*. 51(9): p. 1107-1110.
274. Abe, R. and S.-i. Yamagishi.(2008) AGE-RAGE System and Carcinogenesis. *Current Pharmaceutical Design*. 14(10): p. 940-945.
275. Lee, E.J., J.Y. Kim, and S.H. Oh.(2016) Advanced glycation end products (AGEs) promote melanogenesis through receptor for AGEs. *Scientific Reports*. 6: p. 27848.
276. Herrmann, J., S.M. Soares, L.O. Lerman, and A. Lerman.(2008) Potential role of the ubiquitin-proteasome system in atherosclerosis: aspects of a protein quality disease. *J Am Coll Cardiol*. 51(21): p. 2003-10.
277. Tanaka, N., H. Yonekura, S. Yamagishi, H. Fujimori, Y. Yamamoto, and H. Yamamoto.(2000) The receptor for advanced glycation end products is induced by the glycation products themselves and tumor necrosis factor-alpha through nuclear factor-kappa B, and by 17beta-estradiol through Sp-1 in human vascular endothelial cells. *J Biol Chem*. 275(33): p. 25781-90.
278. Basta, G., G. Lazzerini, S. Del Turco, G.M. Ratto, A.M. Schmidt, and R. De Caterina.(2005) At least 2 distinct pathways generating reactive oxygen species mediate vascular cell adhesion molecule-1 induction by advanced glycation end products. *Arterioscler Thromb Vasc Biol*. 25(7): p. 1401-7.
279. Basta, G., G. Lazzerini, M. Massaro, T. Simoncini, P. Tanganelli, C. Fu, T. Kislinger, D.M. Stern, A.M. Schmidt, and R. De Caterina.(2002) Advanced glycation end products activate endothelium through signal-transduction receptor RAGE: a mechanism for amplification of inflammatory responses. *Circulation*. 105(7): p. 816-22.
280. Sang, H.-q., J.-f. Gu, J.-r. Yuan, M.-h. Zhang, X.-b. Jia, and L. Feng.(2014) The protective effect of smilax glabra extract on advanced glycation end products-induced endothelial dysfunction in HUVECs via RAGE-ERK1/2-NF-κB pathway. *Journal of Ethnopharmacology*. 155(1): p. 785-795.
281. Chen, Y., X. Du, Y. Zhou, Y. Zhang, Y. Yang, Z. Liu, C. Liu, and Y. Xie.(2015) Paeoniflorin protects HUVECs from AGE-BSA-induced injury via an autophagic pathway by acting on the RAGE. *Int J Clin Exp Pathol*. 8(1): p. 53-62.
282. Luan, Z.-G., H. Zhang, P.-T. Yang, X.-C. Ma, C. Zhang, and R.-X. Guo.(2010) HMGB1 activates nuclear factor-κB signaling by RAGE and increases the production of TNF-α in human umbilical vein endothelial cells. *Immunobiology*. 215(12): p. 956-962.
283. Livak, K.J. and T.D. Schmittgen.(2001) Analysis of Relative Gene Expression Data Using Real-Time Quantitative PCR and the 2−ΔΔCT Method. *Methods*. 25(4): p. 402-408.
284. Livak, K.J. and T.D. Schmittgen.(2001) Analysis of relative gene expression data using real-time quantitative PCR and the 2(-Delta Delta C(T)) Method. *Methods*. 25(4): p. 402-8.

285. Liao, H., H. He, Y. Chen, F. Zeng, J. Huang, L. Wu, and Y. Chen.(2014) Effects of long-term serial cell passaging on cell spreading, migration, and cell-surface ultrastructures of cultured vascular endothelial cells. *Cytotechnology*. 66(2): p. 229-238.
286. Zhang, X., Y. Song, X. Han, L. Feng, R. Wang, M. Zhang, M. Zhu, X. Jia, and S. Hu.(2013) Liquiritin attenuates advanced glycation end products-induced endothelial dysfunction via RAGE/NF-κB pathway in human umbilical vein endothelial cells. *Molecular and Cellular Biochemistry*. 374(1): p. 191-201.
287. Michel, M., C. Hess, L. Kaps, W.M. Kremer, M. Hilscher, P.R. Galle, M. Moehler, J.M. Schattenberg, M.-A. Wörns, C. Labenz, and M. Nagel.(2021) Elevated serum levels of methylglyoxal are associated with impaired liver function in patients with liver cirrhosis. *Scientific Reports*. 11(1): p. 20506.
288. Brauner, A., M. Söderhäll, S. Jacobson, J. Lundahl, U. Andersson, and J. Andersson.(2001) Escherichia coli-induced expression of IL-1 α, IL-1 β, IL-6 and IL-8 in normal human renal tubular epithelial cells. *Clinical & Experimental Immunology*. 124(3): p. 423-428.
289. DeForge, L.E. and D.G. Remick.(1991) Kinetics of TNF, IL-6, and IL-8 gene expression in LPS-stimulated human whole blood. *Biochemical and Biophysical Research Communications*. 174(1): p. 18-24.
290. Kumolosasi, E., E. Salim, I. Jantan, and W. Ahmad.(2014) Kinetics of intracellular, extracellular and production of pro-inflammatory cytokines in lipopolysaccharide-stimulated human peripheral blood mononuclear cells. *Tropical Journal of Pharmaceutical Research*. 13(4): p. 536-543.
291. Niwa, Y., H. Akamatsu, H. Sumi, Y. Ozaki, and A. Abe.(2000) Evidence for degradation of cytokines in the serum of patients with atopic dermatitis by calcium-dependent protease. *Archives of Dermatological Research*. 292(8): p. 391-396.
292. Khalfoun, B., F. Thibault, H. Watier, P. Bardos, and Y. Lebranchu.(1997) Docosahexaenoic and eicosapentaenoic acids inhibit in vitro human endothelial cell production of interleukin-6. *Advances in experimental medicine and biology*. 400B: p. 589-597.
293. Song, E.A., J.W. Lim, and H. Kim.(2017) Docosahexaenoic acid inhibits IL-6 expression via PPARγ-mediated expression of catalase in cerulein-stimulated pancreatic acinar cells. *The International Journal of Biochemistry & Cell Biology*. 88: p. 60-68.
294. Deshmane, S.L., S. Kremlev, S. Amini, and B.E. Sawaya.(2009) Monocyte chemoattractant protein-1 (MCP-1): an overview. *Journal of interferon & cytokine research : the official journal of the International Society for Interferon and Cytokine Research*. 29(6): p. 313-326.
295. Bierhaus, A., D.M. Stern, and P.P. Nawroth.(2006) RAGE in inflammation: a new therapeutic target? *Current opinion in investigational drugs (London, England : 2000)*. 7(11): p. 985-991.
296. Wang, L., J. Wu, X. Guo, X. Huang, and Q. Huang.(2017) RAGE Plays a Role in LPS-Induced NF-κB Activation and Endothelial Hyperpermeability. *Sensors (Basel, Switzerland)*. 17(4): p. 722.
297. Yan, S.F., R. Ramasamy, and A.M. Schmidt.(2009) The receptor for advanced glycation endproducts (RAGE) and cardiovascular disease. *Expert Reviews in Molecular Medicine*. 11: p. e9.

298. Barlovic, Drazenka P., A. Soro-Paavonen, and Karin A.M. Jandeleit-Dahm.(2011) RAGE biology, atherosclerosis and diabetes. *Clinical Science*. 121(2): p. 43-55.
299. Waghela, B.N., F.U. Vaidya, K. Ranjan, A.S. Chhipa, B.S. Tiwari, and C. Pathak.(2021) AGE-RAGE synergy influences programmed cell death signaling to promote cancer. *Molecular and Cellular Biochemistry*. 476(2): p. 585-598.
300. Zhang, C.(2008) The role of inflammatory cytokines in endothelial dysfunction. *Basic Research in Cardiology*. 103(5): p. 398-406.
301. Tobon-Velasco, J.C., E. Cuevas, and M.A. Torres-Ramos.(2014) Receptor for AGEs (RAGE) as mediator of NF-kB pathway activation in neuroinflammation and oxidative stress. *CNS Neurol Disord Drug Targets*. 13(9): p. 1615-26.
302. Peake, B., M. Ghetia, C. Gerber, M. Costabile, and P. Deo.(2021) Role of saturated and unsaturated fatty acids on dicarbonyl–albumin derived advanced glycation end products in vitro. *Amino Acids*. p.
303. Muniyappa, R. and P.R. Srinivas.(2014) Dicarbonyl Stress and Atherosclerosis: Is It All RAGE? *Diabetes*. 63(11): p. 3587-3589.
304. Zhang, F.-L., H.-Q. Gao, and L. Shen.(2007) Inhibitory Effect of GSPE on RAGE Expression Induced by Advanced Glycation End Products in Endothelial Cells. *Journal of Cardiovascular Pharmacology*. 50(4): p. 434-440.
305. Ponath, G., C. Schettler, F. Kaestner, B. Voigt, D. Wentker, V. Arolt, and M. Rothermundt.(2007) Autocrine S100B effects on astrocytes are mediated via RAGE. *Journal of Neuroimmunology*. 184(1): p. 214-222.
306. Feng, L., M.-m. Zhu, M.-h. Zhang, R.-s. Wang, X.-b. Tan, J. Song, S.-m. Ding, X.-b. Jia, and S.-y. Hu.(2013) Protection of glycyrrhizic acid against AGEs-induced endothelial dysfunction through inhibiting RAGE/NF-κB pathway activation in human umbilical vein endothelial cells. *Journal of Ethnopharmacology*. 148(1): p. 27-36.
307. Jahan, H. and M.I. Choudhary.(2021) Gliclazide alters macrophages polarization state in diabetic atherosclerosis in vitro via blocking AGE-RAGE/TLR4-reactive oxygen species-activated NF-kβ nexus. *European Journal of Pharmacology*. 894: p. 173874.
308. Liu, Q., A.-M. Qiao, L.-T. Yi, Z.-L. Liu, and S.-M. Sheng.(2016) Protection of kinsenoside against AGEs-induced endothelial dysfunction in human umbilical vein endothelial cells. *Life Sciences*. 162: p. 102-107.
309. Zhang, X., Y. Song, X. Han, L. Feng, R. Wang, M. Zhang, M. Zhu, X. Jia, and S. Hu.(2013) Liquiritin attenuates advanced glycation end products-induced endothelial dysfunction via RAGE/NF-κB pathway in human umbilical vein endothelial cells. *Mol Cell Biochem*. 374(1-2): p. 191-201.
310. Yamagishi, S., H. Adachi, K. Nakamura, T. Matsui, Y. Jinnouchi, K. Takenaka, M. Takeuchi, M. Enomoto, K. Furuki, A. Hino, Y. Shigeto, and T. Imaizumi.(2006) Positive association between serum levels of advanced glycation end products and the soluble form of receptor for advanced glycation end products in nondiabetic subjects. *Metabolism-Clinical and Experimental*. 55(9): p. 1227-1231.
311. Nakamura, K., S.I. Yamagishi, T. Matsui, H. Adachi, M. Takeuchi, and T. Imaizumi.(2007) Serum levels of soluble form of receptor for advanced glycation end products (sRAGE) are correlated with AGEs in both diabetic and non-diabetic subjects. *Clin Exp Med*. 7(4): p. 188-90.
312. Trellu, S., A. Courties, S. Jaisson, L. Gorisse, P. Gillery, S. Kerdine-Römer, C. Vaamonde-Garcia, X. Houard, F.-P. Ekhirch, A. Sautet, B. Friguet, C. Jacques,

F. Berenbaum, and J. Sellam.(2019) Impairment of glyoxalase-1, an advanced glycation end-product detoxifying enzyme, induced by inflammation in age-related osteoarthritis. *Arthritis Research & Therapy*. 21(1): p. 18.
313. Shinohara, M., P.J. Thornalley, I. Giardino, P. Beisswenger, S.R. Thorpe, J. Onorato, and M. Brownlee.(1998) Overexpression of glyoxalase-I in bovine endothelial cells inhibits intracellular advanced glycation endproduct formation and prevents hyperglycemia-induced increases in macromolecular endocytosis. *The Journal of Clinical Investigation*. 101(5): p. 1142-1147.
314. Hering, J., S. Garrean, T.R. Dekoj, A. Razzak, A. Saied, J. Trevino, T.A. Babcock, and N.J. Espat.(2007) Inhibition of Proliferation by Omega-3 Fatty Acids in Chemoresistant Pancreatic Cancer Cells. *Annals of Surgical Oncology*. 14(12): p. 3620-3628.
315. Youssef, M., A. Ibrahim, K. Akashi, and M.S. Hossain.(2019) PUFA-Plasmalogens Attenuate the LPS-Induced Nitric Oxide Production by Inhibiting the NF-kB, p38 MAPK and JNK Pathways in Microglial Cells. *Neuroscience*. 397: p. 18-30.
316. Massaro, M., M.A. Carluccio, C. Bonfrate, L. Siculella, G. Lazzerini, W. Bernini, G. Basta, and R. De Caterina.(1999) The double bond in unsaturated fatty acids is the necessary and sufficient requirement for the inhibition of expression of endothelial leukocyte adhesion molecules through interference with nuclear factor-κB activation. *Lipids*. 34(S1Part2): p. S213-S214.
317. Mirhashemi, S.M., F. Rahimi, A. Soleimani, and Z. Asemi.(2016) Effects of Omega-3 Fatty Acid Supplementation on Inflammatory Cytokines and Advanced Glycation End Products in Patients With Diabetic Nephropathy: a Randomized Controlled Trial. *Iran J Kidney Dis*. 10(4): p. 197-204.
318. Syed, A., Q. Zhu, and E.A. Smith.(2016) Ligand binding affinity and changes in the lateral diffusion of receptor for advanced glycation endproducts (RAGE). *Biochimica et Biophysica Acta (BBA) - Biomembranes*. 1858(12): p. 3141-3149.
319. Yu, W., X. Hu, and M. Wang.(2018) Pterostilbene inhibited advanced glycation end products (AGEs)-induced oxidative stress and inflammation by regulation of RAGE/MAPK/NF-κB in RAW264.7 cells. *Journal of Functional Foods*. 40: p. 272-279.
320. Schupp, N., R. Schinzel, A. Heidland, and H. Stopper.(2005) Genotoxicity of Advanced Glycation End Products: Involvement of Oxidative Stress and of Angiotensin II Type 1 Receptors. *Annals of the New York Academy of Sciences*. 1043(1): p. 685-695.
321. Thornalley, P.J., S. Battah, N. Ahmed, N. Karachalias, S. Agalou, R. Babaei-Jadidi, and A. Dawnay.(2003) Quantitative screening of advanced glycation endproducts in cellular and extracellular proteins by tandem mass spectrometry. *Biochemical Journal*. 375(3): p. 581-592.
322. Rabbani, N. and P.J. Thornalley.(2021) Protein glycation–biomarkers of metabolic dysfunction and early-stage decline in health in the era of precision medicine. *Redox Biology*. 42: p. 101920.
323. Rabbani, N., M. Xue, and P.J. Thornalley.(2021) Dicarbonyl stress, protein glycation and the unfolded protein response. *Glycoconjugate Journal*. 38(3): p. 331-340.
324. Sun, Z., X. Peng, J. Liu, K.-W. Fan, M. Wang, and F. Chen.(2010) Inhibitory effects of microalgal extracts on the formation of advanced glycation endproducts (AGEs). *Food chemistry*. 120(1): p. 261-267.

325. Yu, W., M. Tao, Y. Zhao, X. Hu, and M. Wang.(2018) 4′-Methoxyresveratrol Alleviated AGE-Induced Inflammation via RAGE-Mediated NF-κB and NLRP3 Inflammasome Pathway. *Molecules*. 23(6): p. 1447.
326. Jahan, H., N.N. Siddiqui, S. Iqbal, F.Z. Basha, M.A. Khan, T. Aslam, and M.I. Choudhary.(2022) Indole-linked 1,2,3-triazole derivatives efficiently modulate COX-2 protein and PGE2 levels in human THP-1 monocytes by suppressing AGE-ROS-NF-kβ nexus. *Life Sciences*. 291: p. 120282.
327. Nagai, R., K. Matsumoto, X. Ling, H. Suzuki, T. Araki, and S. Horiuchi.(2000) Glycolaldehyde, a reactive intermediate for advanced glycation end products, plays an important role in the generation of an active ligand for the macrophage scavenger receptor. *Diabetes*. 49(10): p. 1714-1723.
328. Ishibashi, Y., T. Matsui, N. Nakamura, A. Sotokawauchi, Y. Higashimoto, and S.-i. Yamagishi.(2017) Methylglyoxal-derived hydroimidazolone-1 evokes inflammatory reactions in endothelial cells via an interaction with receptor for advanced glycation end products. 14(5): p. 450-453.
329. Vlassara, H. and J. Uribarri.(2014) Advanced glycation end products (AGE) and diabetes: cause, effect, or both? *Current diabetes reports*. 14(1): p. 1-10.
330. Ahmed, N. and P.J. Thornalley.(2007) Advanced glycation endproducts: what is their relevance to diabetic complications? *Diabetes, Obesity and Metabolism*. 9(3): p. 233-245.
331. Spector, A.A., K. John, and J.E. Fletcher.(1969) Binding of long-chain fatty acids to bovine serum albumin. *J Lipid Res*. 10(1): p. 56-67.
332. Oliveira, A.F., D.A. Cunha, L. Ladriere, M. Igoillo-Esteve, M. Bugliani, P. Marchetti, and M. Cnop.(2015) In vitro use of free fatty acids bound to albumin: A comparison of protocols. *BioTechniques*. 58(5): p. 228-233.
333. Haeri, H.H., B. Schunk, J. Tomaszewski, H. Schimm, M.J. Gelos, and D. Hinderberger.(2019) Fatty Acid Binding to Human Serum Albumin in Blood Serum Characterized by EPR Spectroscopy. *ChemistryOpen*. 8(5): p. 650-656.
334. Guo, C. and H.X. Zhou.(2019) Fatty Acids Compete with Aβ in Binding to Serum Albumin by Quenching Its Conformational Flexibility. *Biophys J*. 116(2): p. 248-257.
335. Talmor, Y., E. Golan, S. Benchetrit, J. Bernheim, O. Klein, J. Green, and G. Rashid.(2008) Calcitriol blunts the deleterious impact of advanced glycation end products on endothelial cells. *American Journal of Physiology-Renal Physiology*. 294(5): p. F1059-F1064.
336. Stopper, H., R. Schinzel, K. Sebekova, and A. Heidland.(2003) Genotoxicity of advanced glycation end products in mammalian cells. *Cancer Letters*. 190(2): p. 151-156.
337. Grossin, N., M.P.S. Wautier, J. Picot, D.M. Stern, and J.L.T. Wautier.(2009) Differential effect of plasma or erythrocyte AGE-ligands of RAGE on expression of transcripts for receptor isoforms. *Diabetes & Metabolism*. 35(5): p. 410-417.
338. Schmidt, A.M., S. Du Yan, S.F. Yan, and D.M. Stern.(2001) The multiligand receptor RAGE as a progression factor amplifying immune and inflammatory responses. *The Journal of clinical investigation*. 108(7): p. 949-955.
339. Hofmann, M.A., S. Drury, C. Fu, W. Qu, A. Taguchi, Y. Lu, C. Avila, N. Kambham, A. Bierhaus, and P. Nawroth.(1999) RAGE mediates a novel proinflammatory axis: a central cell surface receptor for S100/calgranulin polypeptides. *Cell*. 97(7): p. 889-901.

340. Akirav, E.M., P. Preston-Hurlburt, J. Garyu, O. Henegariu, R. Clynes, A.M. Schmidt, and K.C. Herold.(2012) RAGE expression in human T cells: a link between environmental factors and adaptive immune responses. *PLoS One*. 7(4): p. e34698.
341. Son, W.-r., M.-H. Nam, C.-O. Hong, Y. Kim, and K.-W. Lee.(2017) Plantamajoside from Plantago asiatica modulates human umbilical vein endothelial cell dysfunction by glyceraldehyde-induced AGEs via MAPK/NF-κB. *BMC complementary and alternative medicine*. 17(1): p. 1-12.
342. Zhou, Q., K.-W. Cheng, J. Gong, E.T.S. Li, and M. Wang.(2019) Apigenin and its methylglyoxal-adduct inhibit advanced glycation end products-induced oxidative stress and inflammation in endothelial cells. *Biochemical Pharmacology*. 166: p. 231-241.
343. Whiting, C.V., P.W. Bland, and J.F. Tarlton.(2005) Dietary N-3 Polyunsaturated Fatty Acids Reduce Disease and Colonic Proinflammatory Cytokines in a Mouse Model of Colitis. *Inflammatory Bowel Diseases*. 11(4): p. 340-349.
344. Akerele, O. and S. Cheema.(2018) A diet enriched in longer chain omega-3 fatty acids reduced placental inflammatory cytokines and improved fetal sustainability of C57BL/6 mice. *Prostaglandins, Leukotrienes and Essential Fatty Acids*. 137: p. 43-51.
345. Liu, T., J. Li, Y. Liu, N. Xiao, H. Suo, K. Xie, C. Yang, and C. Wu.(2012) Short-chain fatty acids suppress lipopolysaccharide-induced production of nitric oxide and proinflammatory cytokines through inhibition of NF-κB pathway in RAW264. 7 cells. *Inflammation*. 35(5): p. 1676-1684.

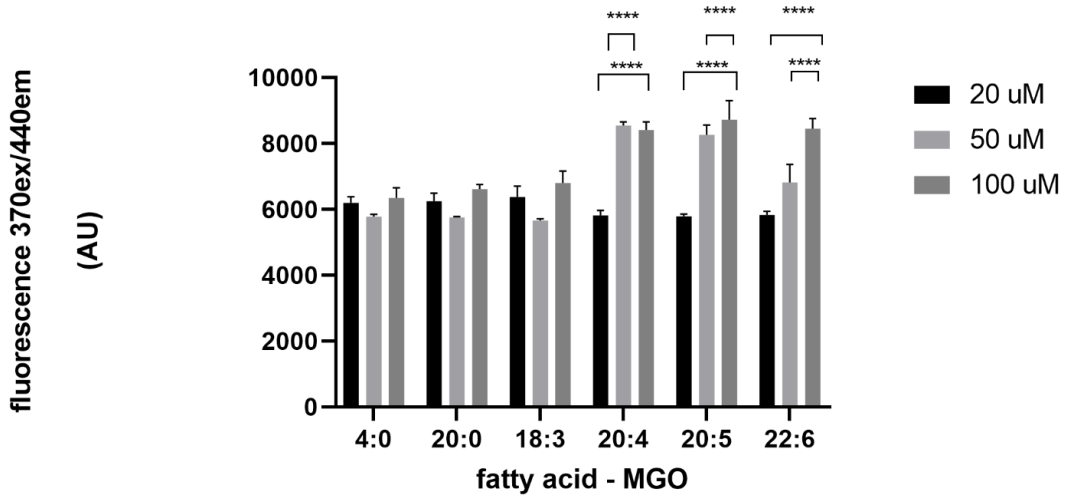
Chapter 5 – Appendix and supplementary information

5.1 – supplementary information for chapter 2.

5.1.1 – Comparison of 20μM, 50μM and 100μM fatty acid models

In previous experiments involving fatty acids in our group, a physiologically relevant concentration of 20 μM of fatty acid was used. Due to there appearing to be no structure/function relationship between degree of unsaturation and the effect on AGE production, we next wanted to see what effect increasing the concentration on fatty acids may have in our model system. It was of interest to investigate whether there would be a structure/concentration effect correlating to chain length and degree of unsaturation. For these experiments, a selection of fatty acids was chosen based on their activity in previous experiments. 4:0, 20:0, 18:3 n-3, 20:4 n-6, 20:5 n-3 and 22:6 n-3 were chosen to be quantified by both fluorescent screening as well as LC/MS/MS analysis. Consistent with previous results, the unsaturated fatty acids produced a significant increase in protein bound fluorescent AGEs production in both the MGO and GO models at 50 and 100 μM as compared to 20 μM.

A.



B.

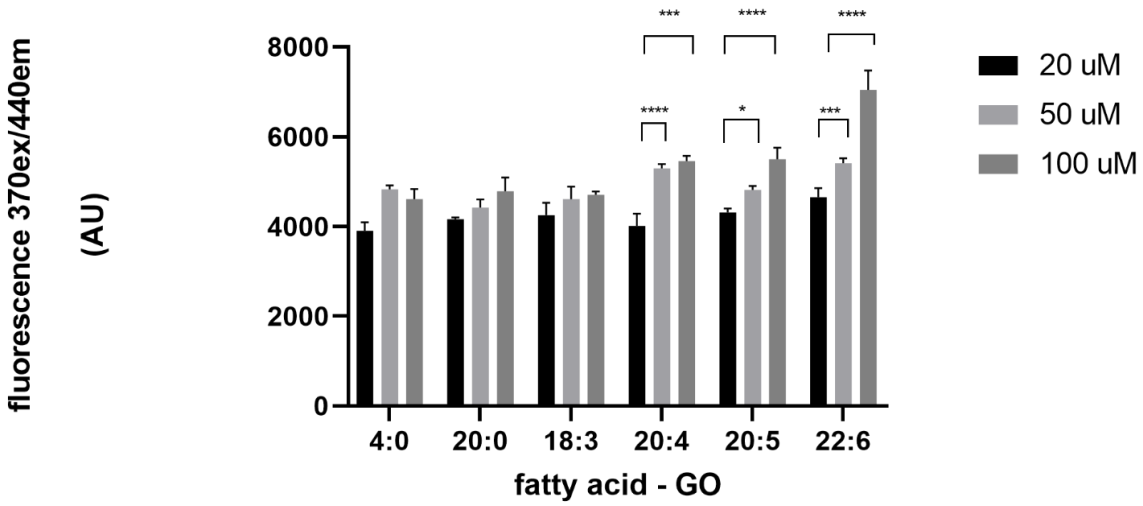


Figure 5.1 - The effect of different concentration of fatty acids on the production of protein-bound fluorescent AGEs.

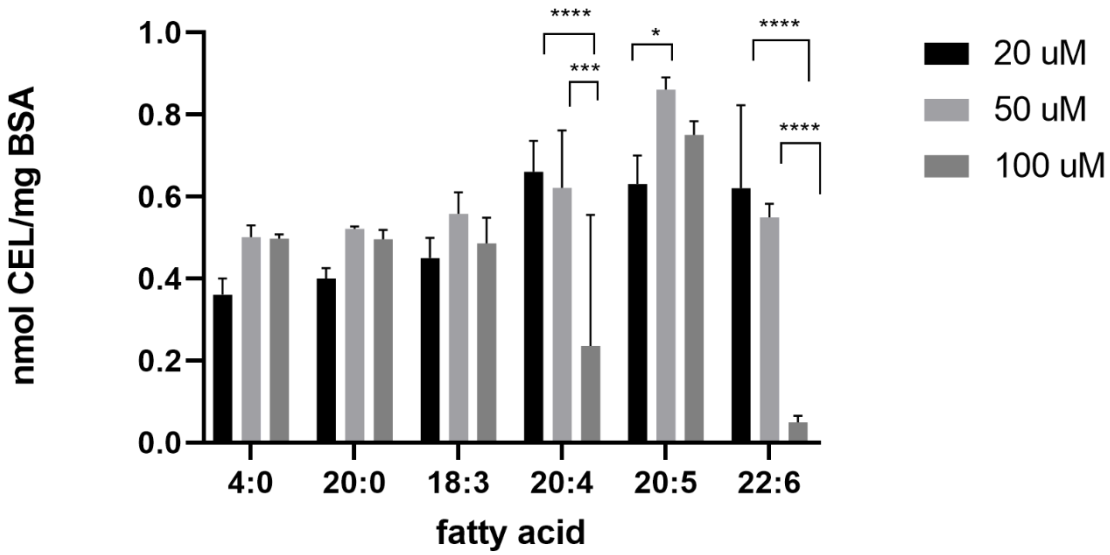
A. BSA-MGO-FA model, **B.** BSA-GO-FA model. Results expressed as mean ±SD n=3. ****p<0.0001, ***p<0004, *p<0.02.

5.1.2 – Concentration dependent quantitation of CML/CEL and MG-H1 production in a BSA-dicarbonyl model using LC-MS/MS.

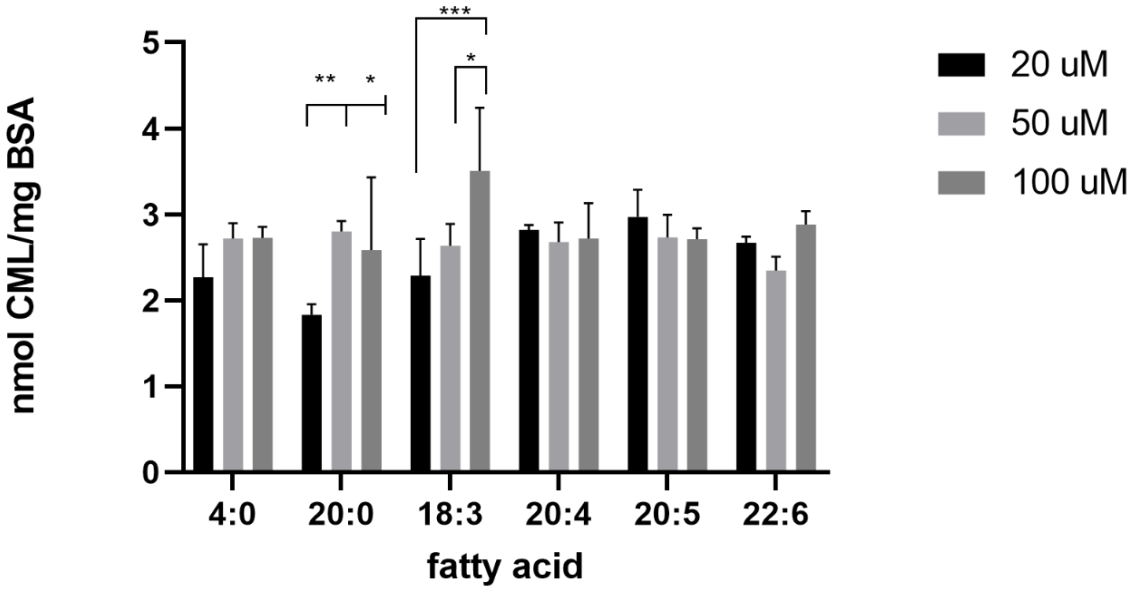
The unsaturated fatty acids were the only fatty acids that induced significant changes in protein-bound CEL production in our model system. It should be noted that it is hard to gauge whether these results are in fact of significance when CEL production itself in in such a low quantity ((a)) (<1nmol/mg BSA), however this is still above both the limit of detection (LOD) and lower limit of quantitation (LLOQ). CML production only showed significant change with 20:0 and 18:3

n-6 fatty acids, whereas with MG-H1 there was no significant difference irrespective of the concentration of fatty acid.

A.


nmol CEL/mg BSA
1.0
0.8
0.6
0.4
0.2
0.0
4:0
20:0
18:3
20:4
20:5
22:6
fatty acid
****
***
*
****
****
20 uM
50 uM
100 uM

B.


nmol CML/mg BSA
5
4
3
2
1
0
4:0
20:0
18:3
20:4
20:5
22:6
fatty acid
**
*
***
*
20 uM
50 uM
100 uM

C.

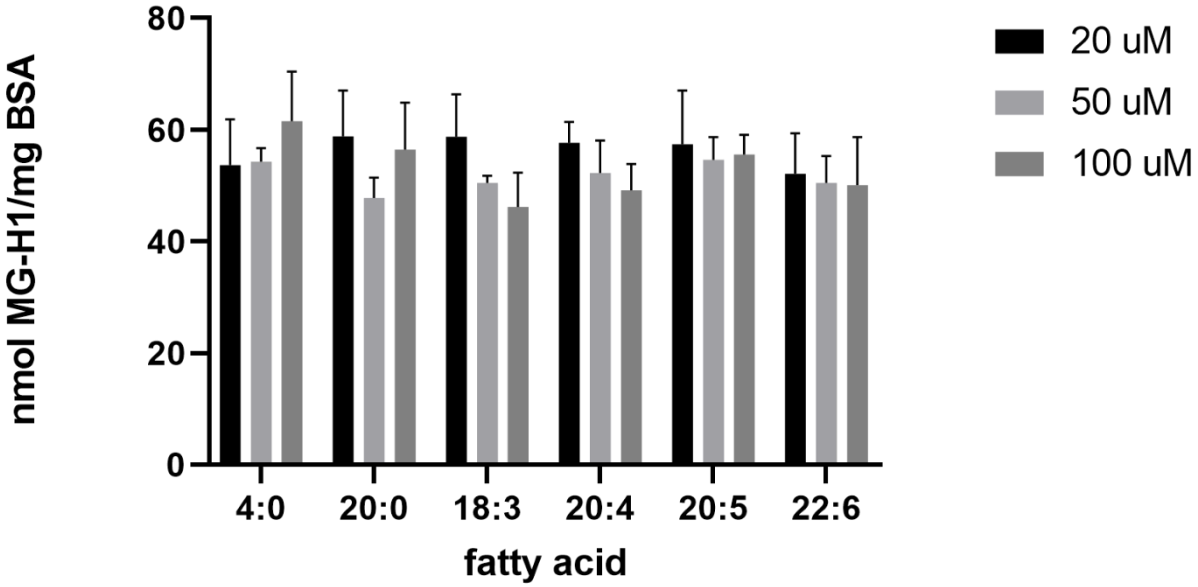


Figure 5.2 - Concentration dependent quantitation of protein bound non-fluorescent AGE production
Dicarbonyl derived AGE model system quantified using LC-MS/MS. a. CEL quantitation, b. CML quantitation and c. MG-H1 quantitation. Results are blank adjusted and expressed as mean ±SD n=3. ****p<0.0001, ***p<0.002, **p<0.005, *p<0.04.

Table 5.1 – Limit of quantitation for liquid chromatography mass spectrometry analysis of AGEs

Analyte	Signal to noise ratio	pmol/mL
CML	**12.3**	**15**
CEL	**18.2**	**3**
MG-H1	**10.1**	**10**
Lysine	**10.6**	**100**

Signal to noise ratio > 10; CML: *N*ε-carboxymethyllysine (CML); CEL: *N*ε-carboxyethyllysine (CEL); MG-H1: methylglyoxal derived hydroimidazolone 1.

Table 5.2 – limit of detection for liquid chromatography mass spectrometry analysis of AGEs

Analyte	Signal to noise ratio	pmol/mL
CML	**4.3**	**5**
CEL	**3.6**	**1.5**
MG-H1	**6.1**	**3**
Lysine	**3.4**	**10**

Signal to noise ratio > 3; CML: *N*ε-carboxymethyllysine (CML); CEL: *Nε-carboxyethyllysine (CEL); MG-H1:* methylglyoxal derived hydroimidazolone 1

5.2 – Supplementary information for chapter 3

5.2.1 – MTT Trials using TCA

Initial MTT trials using TCA precipitation for protein proved problematic as TCA could not be completely removed from cell pellet resulting in cell death (figure 30). This was further confirmed by comparing BSA in media only versus BSA precipitated in TCA (figure 31), leading to the use of ultrafiltration columns to concentrate protein.

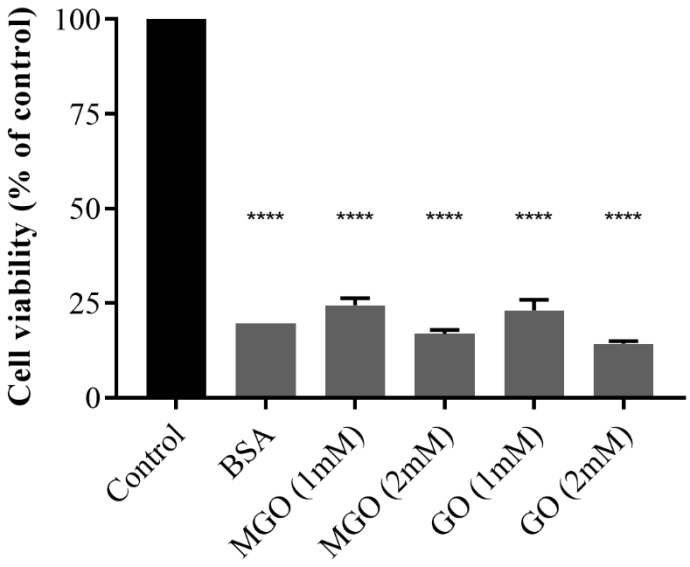


Figure 5.3 - TCA protein precipitation trials on cell culture model system

TCA precipitation testing of protein extraction in a cell culture model system. HUVECs treated with BSA/BSA-MGO and BSA-GO for 24 h and subjected to MTT cell proliferation assay. TCA was determined to be to too toxic with viability significantly reduced by approximately 75% in all treatments. Results expressed as mean n=3. **** represents p< 0001, (ANOVA)

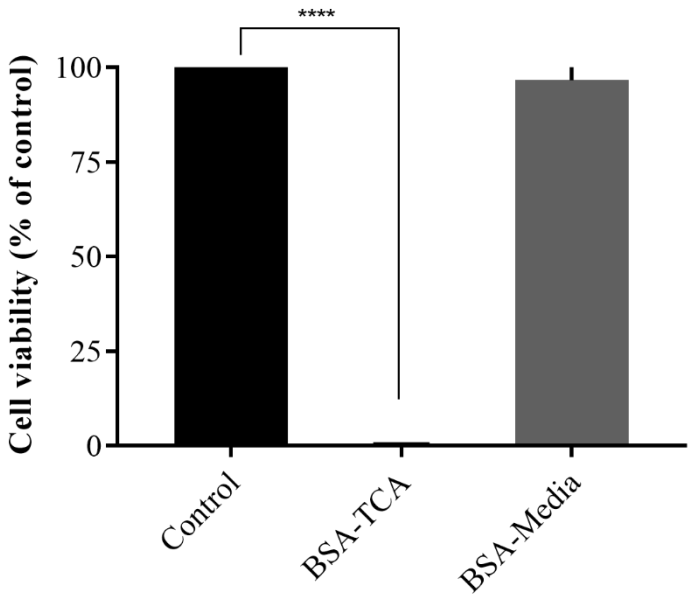


Figure 5.4 - TCA precipitation vs Media only testing for optimisation of protein extraction.
TCA precipitation testing of protein extraction in a cell culture model system. HUVECs treated with TCA extracted BSA only and BSA only dissolved in endothelial cell growth media for 24 h and subjected to MTT cell proliferation assay. TCA was determined to be to too toxic with viability significantly reduced by approximately 95% in all treatments compared to media only. Results expressed as mean n=3. **** represents p< 0001, (ANOVA)